U.S. DEPARTMENT OF THE INTERIOR

GEOLOGICAL SURVEY

Geology of Contaminants in Coal:

Phase I Report of Investigations

By C. B. Cecil, R. W. Stanton, and F. T. Dulong

Open-File Report 81-953-A

This report was prepared under Interagency Agreement EPA-IAG-D8-E685-FR between the U.S. Geological Survey and the U.S. Environmental Protection Agency, Research Triangle Park, NC 32711. This report is preliminary and has not been reviewed for conformity with USGS editorial standards and stratigraphic nomenclature.

CONTENTS

	Page
Abstract	1a-1b
Acknowledgements	1c
Introduction	1d
Geologic Setting of the Homer City Study Area	2
General Geology	2
Stratigraphy	2
Field Studies	5
Sampling	5
Coal Stratigraphy	5
Depositional History	9
Laboratory Studies	11
Sample Handling	11
Coal Petrography	11
Maceral Composition	11
Vitrinite Reflectance	20
Analyses of Sulfur in Coal	28
Megascopic Iron Disulfide Occurrences	35
Scanning Electron Microscopy of Minerals	35
Low Temperature Ash Mineralogy	41
Methodology and Experimental Studies with Mineral Standards	41
Mineral Composition	50

Laboratory Studies Continued — Page

Chemical Analyses..... 53

Elemental Analyses..... 53

Electron Microprobe Analyses..... 67

Statistical Analysis of Analytical Data..... 68

Interpretations and Conclusions..... 73

Sedimentation and Peat Accumulation..... 73

Origin of Mineral Matter in the Coal..... 76

Technical Applications..... 81

Summary..... 85

References Cited..... 87

Appendices*

*Appendices are USGS Open-File Report 81-953-B.

Figures

Page

1. Index map of the Homer City, PA, study area and Conemaugh-Allegheny contact..... 3

2. Generalized stratigraphic column of rocks in Homer City study area..... 4

3. Sample numbers and map locations of complete- and bench-channel samples from Lucerne #6 and Homer City #1 mines..... 6

4. Fence diagram of Upper Freeport coal facies/Lucerne #6 and Homer City #1 mines..... 7

5. Generalized stratigraphy of the Upper Freeport coal bed/Lucerne #6 and Homer City #1 mines..... 8

6. Analyses performed on coal samples..... 12

7. Petrographic and mineralogic analyses performed on coal samples.. 13

8. Maceral compositions of bench-channel samples/Upper Freeport coal, Homer City, Pennsylvania..... 19

9. Maceral variety compositions of bench-channel samples/Upper Freeport coal, Homer City, Pennsylvania..... 21

10. Isopleth map of vitrinite reflectances Upper Freeport coal bed, Homer City, Pennsylvania..... 22

11. Vitrinite reflectances, fixed-carbon contents, and low-temperature-ash contents of 22 selected bench-channel samples Upper Freeport coal bed, Homer City, Pennsylvania..... 25

12. Vitrinite reflectances versus ash contents of 22 bench-channel samples from the Upper Freeport coal bed, Homer City, Pennsylvania 26

13. Vitrinite reflectances versus fixed-carbon contents of 21 complete-channel samples of the Upper Freeport coal bed, Homer City, Pennsylvania..... 27

14. Iron disulfide forms, associations, and grain sizes in samples from LUC-NM and H2-5/3L, Upper Freeport coal/Homer City, Pa..... 33

15. Iron disulfide forms, associations, and grain sizes in samples from HEL-2R and H2-42P, Upper Freeport coal/Homer City, Pa..... 34

16. SEM photographs of two common forms of pyrite (P) in Upper Freeport coal..... 38

17. SEM photographs of clay minerals (C) in fusinite..... 38

18. XRD intensity percent calculation..... 44

19. Generalized major-oxide and corresponding mineral data by coal facies..... 55

20. Concentration of arsenic (As) in complete- and bench-channel samples from Lucerne #6 and Homer City #1 mines..... 57

21. Concentration of cadmium (Cd) in complete- and bench-channel samples from Lucerne #6 and Homer City #1 Mines..... 58

22. Concentration of zinc (Zn) in complete- and bench-channel samples from Lucerne #6 and Homer City #1 mines..... 59

23. Concentration of iron (Fe) in complete- and bench-channel samples from Lucerne #6 and Homer City #1 mines..... 60

24. Concentration of pyritic sulfur(S) in complete- and bench-channel samples from Lucerne #6 and Homer City #1 mines..... 61

25. Concentration of total sulfur(S) in complete- and bench-channel samples from Lucerne #6 and Homer City #1 mines..... 62

26. Concentration of lead (Pb) in complete- and bench-channel samples from Lucerne #6 and Homer City #1 mines..... 63

27. Concentration of selenium (Se) in complete- and bench-channel samples from Lucerne #6 and Homer City #1 mines..... 64

28. Concentration of manganese (Mn) in complete- and bench-channel samples from Lucerne #6 and Homer City #1 mines..... 65

29. Concentration of mercury (Hg) in complete- and bench-channel samples from Lucerne #6 and Homer City #1 mines..... 66

30. Mineral and maceral statistical associations..... 71

31. Interpreted depositional settings of rocks associated with the Upper Freeport coal bed, Phase I study area..... 74-75

32. Lithologic maps at 5-ft. increments above the top of C facies of the Upper Freeport coal bed..... 77

33. Isopach of shale above the Upper Freeport coal bed..... 78

Tables

Page

1. Maceral groups and their respective macerals identified in reflected light petrographic analysis in this study..... 14

2. Maceral composition of Upper Freeport coal bed samples by facies 15-17

3. Vitrinite reflectances of 21 complete-channel samples of the Upper Freeport coal bed..... 23

4. Vitrinite reflectances of 22 selected bench-channel samples of the Upper Freeport coal bed..... 24

5. Microscopic iron disulfide classification of coal..... 30

6. Simplified classification of iron disulfide forms and associations..... 31

7. Comparison of megascopic pyrite in selected mine sample locations..... 34

8. Mineralogy of pellet mounts obtained by use of scanning electron microscope..... 48

9. Minerals in the Upper Freeport coal as interpreted from the SEM data..... 40

10. Diffraction spacings of mineral phases in the LTA as determined by XRD, Upper Freeport coal bed, Homer City, Pa..... 42

11. Experimental results for four-phase mineral mixtures..... 46

12. Correlation coefficients and linear equations for a specific phase versus all phases..... 47

13. Statistical correlations of mineral phases..... 49

14. Correlation coefficients, linear equations, and standard error of estimate for regression of known weight percent (Y) on measured intensity (X)..... 49

15. Summary: Mineralogy, relative percent by facies..... 50

16. Summary: Mineralogy, whole coal by facies..... 51

17. Summary: Normalized percent major oxides by facies..... 54

18. Groupings of elements, minerals and macerals based on nonparametric associations..... 72

ABSTRACT

Under an interagency agreement between the U.S. Environmental Protection Agency and U.S. Geological Survey, a four-phase study was initiated to determine the geologic controls on mineral-matter variation in coal and to relate the geologic controls to mining and coal-preparation practices. The first phase of the study has focused on the geology of the Homer City, Pennsylvania, dedicated reserves of the Upper Freeport coal bed.

Field investigations included detailed descriptions and sampling of the coal and associated rocks (21 complete-channel and 75 bench-channel samples). Laboratory analyses included: 1) determination of the concentrations of 70 elements; 2) ultimate, proximate, and sulfur forms; 3) maceral analysis; 4) pyrite morphological analysis; 5) low temperature ash X-ray mineralogy; and 6) scanning electron microscope and electron microprobe analyses on selected samples.

The Upper Freeport coal bed of the study area is divisible in the field into eight facies--two nonbanded coal facies, four banded coal facies, and two shale partings. The thickness of the coal bed averages 83 inches (211 cm) in the northern part of the area where all eight facies are present. Only the four lower facies are present in the southern part where the thickness averages 48 inches (122 cm).

Laboratory analyses show that each of the six coal facies consists of distinct associations between macerals and mineral matter. Areally, the facies show trends which indicate that a specific set of conditions prevailed during the development of each facies in the ancestral peat-forming environment.

Vertically within the bed, vitrinite reflectance is negatively correlated with low temperature ash content, indicating that increasing ash content may retard coalification.

Microscopic analyses of pyrite and marcasite forms and their petrographic associations show definite differences among the coal facies. Specifically, the bottom facies has framboidal pyrite whereas the other facies tend to contain more massive varieties that should be more amenable to removal during coal preparation.

Based on the analyses using scanning electron microscope, X-ray diffraction, and the electron microprobe, accessory minerals observed in the Upper Freeport coal bed contain most of the trace elements that have been determined chemically.

Parametric and nonparametric statistics were applied to the analytical data of the bench-channel samples ($n = 75$) to determine relationships among elements, forms of sulfur, mineral compositions of low temperature ashes, and maceral concentrations. The same statistical analyses were also conducted on 1) samples with an ash content of 10 percent or less and a Btu of 12,000 or greater ($n = 46$) and 2) all samples from the lower three facies ($n = 37$). Statistical analyses of laboratory data indicate the existence of two distinct groupings of variables. Group I consists of elements, minerals, and macerals that correlate with ash, SiO_2, and Al_2O_3 content. Group II consists of elements, minerals, and macerals that correlate with sulfur.

Variation in mineral-matter content of the Homer City, Pa., dedicated reserves of the Upper Freeport coal bed was controlled primarily by processes operable during the peat stage of coal formation.

Those elements associated with Group I of the statistical correlations are believed to be dominantly derived from the inherent (plant) ash whereas the variation of sulfur and related elements of Group II was primarily controlled by biochemical and chemical processes. A secondary control on sulfur variation is related to roof-rock lithology; elevated sulfur contents occur under sandstone roof conditions.

In summary, it appears that mineral matter in coal is directly and indirectly controlled by the inherent plant ash, the pH, and the hydrologic conditions of the ancestral peat-forming environment. Low-ash and low-sulfur coal is the product of peat that formed under highly acid conditions ($pH < 4.5$) whereas coal having higher ash and sulfur contents formed under pH conditions that ranged from 4.5 to 7.5. We conclude that prediction of mineral-matter variation in coal is best approached by use of detailed geologic analysis of a given coal body which includes paleoenvironmental parameters of plant communities, water chemistry, and hydrologic conditions.

ACKNOWLEDGMENTS

The completion of Phase I of the Geology of Contaminants in Coal Project is the result of the efforts of many individuals. The conceptualization and planning of the project resulted from discussions with James D. Kilgroe U.S. Environmental Protection Agency (EPA) and Charles Statler, Francis Martino, and Edward Zawadski (Pennsylvania Electric Company). Sample planning and the logistics of sampling underground were made possible through the efforts of Francis Martino and officials of the Rochester and Pittsburgh Coal Company and the North American Coal Company.

The U.S. Bureau of Mines/Department of Energy performed coal analyses under supervision of Forest Walker. Major, minor, and trace element analyses were conducted by the U.S. Geological Survey (USGS). Electron microprobe analyses were conducted by Jean Minkin (USGS). Oriented block samples and thin sections of coal were supplied by E. C. T. Chao (USGS). Scanning electron microscope investigations were carried out by R. B. Finkelman (USGS). Sample preparations and portions of the microscopic analyses were conducted by Derek Widmayer (USGS).

Numerous helpful discussions regarding the geology of the Homer City dedicated reserves were held with William Bragonier and William Clark of the Rochester and Pittsburgh Coal Company. The expertise of Peter Zubovic (USGS) regarding the origin of mineral matter in coal was used extensively. Alfred Bodenlos (USGS) was instrumental in our recognition of the importance of the relationship between microbial activity and sulfur fixation in coal. Sharon D. Allshouse (Pennsylvania State University) assisted in the initial formulation and actualization of project activities.

Finally, we acknowledge the continued encouragement and support of EPA project officers David Kirchgessner and Robert Lagemann.

INTRODUCTION

The Geology of Contaminants in Coal Project was established to determine the geologic factors that control the variability of mineral matter in coal. The efficiency of coal usage can be maximized and the effects of deleterious elements can be minimized with a better understanding of factors that control quality aspects of coal feedstock. Mineral-matter variability (including sulfur) complicates design problems and may increase the construction and operation costs of coal preparation plants, power plants, or conversion plants. In addition, certain forms of mineral matter and their variability may cause equipment fouling; certain elements and minerals are believed to affect catalysts in coal conversion. Thus, there exists an ever increasing need to better understand the basic raw material that may become the primary source of the nation's energy supply. Coal resource predictive models can 1) minimize exploration and development costs, 2) delineate zones of coal beds that can cause mining and processing problems, 3) maximize the utilization of existing geological, chemical, and engineering data, 4) aid in the determination of the best technical uses (conversion, combustion, cokemaking), and 5) aid in the prediction of possible environmental consequences.

The project consists of four phases, the first of which is the subject of this report. Phase I focused on the geologic controls and mineral-matter variability of the Homer City, Pennsylvania, dedicated reserves of the Upper Freeport coal bed. Phase II is designed to relate the geologic factors of Phase I to sulfur and ash removal by coal preparation. The objective of Phase III is to investigate geologic controls on the regional variation of mineral matter in the Upper Freeport coal bed. Phase IV will test models developed for the Upper Freeport coal bed on at least three other major producing coal beds of the United States.

The primary objectives of Phase I were to determine the geologic factors that controlled the variability of 1) total and pyritic sulfur, 2) the forms and size of pyritic sulfur, 3) the concentration of major, minor, and trace elements, 4) the dominant mineral phases, and 5) maceral composition and mineral-matter associations.

GEOLOGIC SETTING OF THE HOMER CITY STUDY AREA

GENERAL GEOLOGY

The study area is in Indiana County, west-central Pennsylvania (fig. 1). Indiana County is in the Appalachian Plateau and is characterized by mild stream dissection and rolling topography. The region was not glaciated. Other than anticlinal structures, topographical relief is limited; surface elevations range from 1000 to 1350 feet (300 to 400 meters).

Structurally, the dedicated reserves of the Upper Freeport coal bed are situated in the southwestward-plunging Latrobe syncline. The elevation of the coal along the trough is approximately 950 feet (290 meters) in the southern part of the reserve area and 550 feet (170 meters) in the northern part. The Latrobe syncline is flanked on the east by the Chestnut Ridge anticline and on the west by the Indian Springs anticline. The Upper Freeport coal bed crops out along the eastern limb of the Latrobe syncline and also to the west of the Homer City study area. Faults (structural) have not been encountered in the dedicated reserve area although minor faulting has been reported (Puglio and Iannacchione, 1979). The roof is commonly jointed, and joints apparently serve as conduits for ground water. The combination of jointing and groundwater movement commonly causes hazardous roof conditions beneath stream valleys. Cleating of the coal is of variable intensity.

STRATIGRAPHY

The rock units considered in this investigation include those associated with 1) the Upper Freeport limestone interval, 2) the Upper Freeport coal bed, 3) the Mahoning Sandstone interval, and 4) the Brush Creek shale interval (fig. 2). The Upper Freeport limestone interval is overlain by the Upper Freeport coal and contains the uppermost units of the Allegheny Formation. Rock units of the Conemaugh Formation considered in this report consist of the Mahoning sandstone interval, and the Brush Creek shale as shown in figure 2.

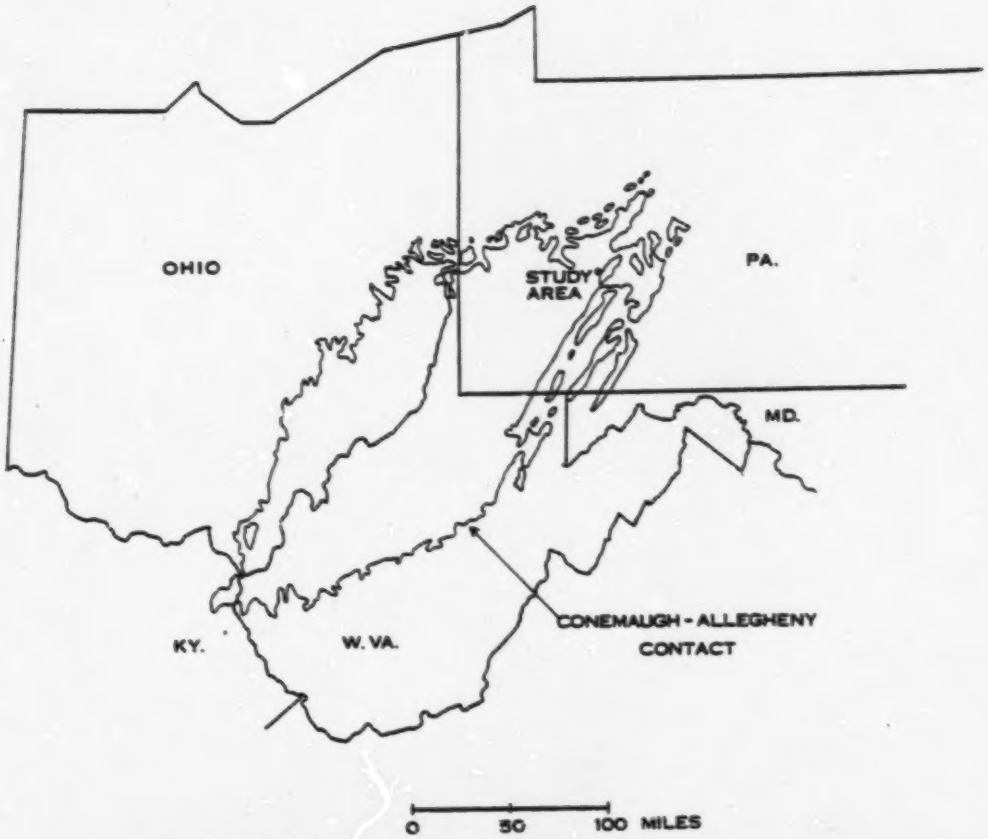

FIGURE 1 - INDEX MAP OF THE HOMER CITY, PA. STUDY AREA AND CONEMAUGH-ALLEGHENY CONTACT.

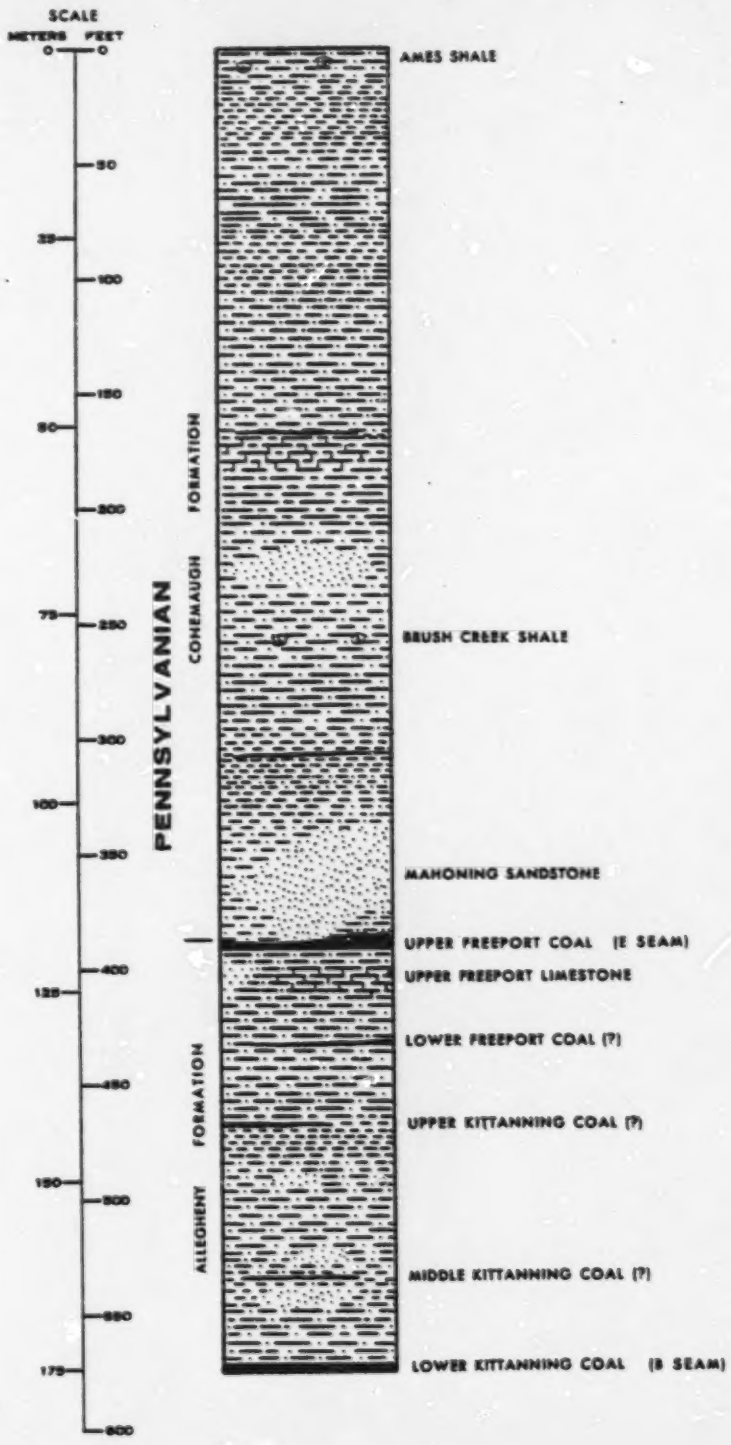

FIGURE 2. GENERALIZED STRATIGRAPHIC COLUMN OF ROCKS IN THE HOMER CITY STUDY AREA.

FIELD STUDIES

SAMPLING

During two trips to the Homer City area (fig. 1), a total of 21 complete-channel samples and 75 bench-channel samples of coal were collected from 21 locations in the Homer City #1 and Lucerne #6 mines (fig. 3).

Sampling of the coal bed was based on field descriptions of facies within the bed. These facies are continuous throughout the mining reserve area and nearby surface exposures. The field descriptions were based on physical appearance and characteristics. The primary variables that control the differentiation of the coal facies are hardness, fracture, blocky character, and degree of banding and brightness.

Samples were obtained by cutting channels for the entire height of the bed or bench of coal. All of the coal removed from each channel was collected. Between 10 and 15 pounds of coal were obtained from each of 96 samples. At each location, two to eight facies were sampled depending on their thickness and physical characteristics. At most sample locations, shale partings were included in the samples to represent the coal as mined. Sample locations and numbers are shown in figure 3; individual sample thicknesses are given in Appendix B.

Sample numbers were chosen to identify each sample logically. For example, decoding of sample number H2-42P-1.2 is as follows:

H2	42P	1.2
Homer City #1 Mine (H) Second trip (2)	No. 4 entry (4) at No. 2 panel (2P) in mine	First sample location (1) in this part of mine; Second bench-channel (.2)

Sample numbers that end in zero designate complete-channel samples; all other integer endings designate bench-channel samples.

COAL STRATIGRAPHY

Differences in coal bed facies were recognized both vertically and laterally. The stratigraphic relations of facies within the Upper Freeport coal bed of the study area are illustrated in figure 4, which is a fence diagram based on field descriptions at sample locations, and on field observations made between the sample locations.

Figure 5 shows a generalized section of the Upper Freeport coal bed. All facies are shown in this section including their minimum and maximum thickness. The lower split of the coal bed (facies C, D, and E) persists throughout the study area. The upper split of the coal bed (facies A, B, and in some places A') is present in the Lucerne #6 mine but pinches out and is not present in the Homer City #1 mine. Facies A and A' are both nonbanded coal types. They differ in that Facies A' is discontinuous whereas A is present at the top of the upper split.

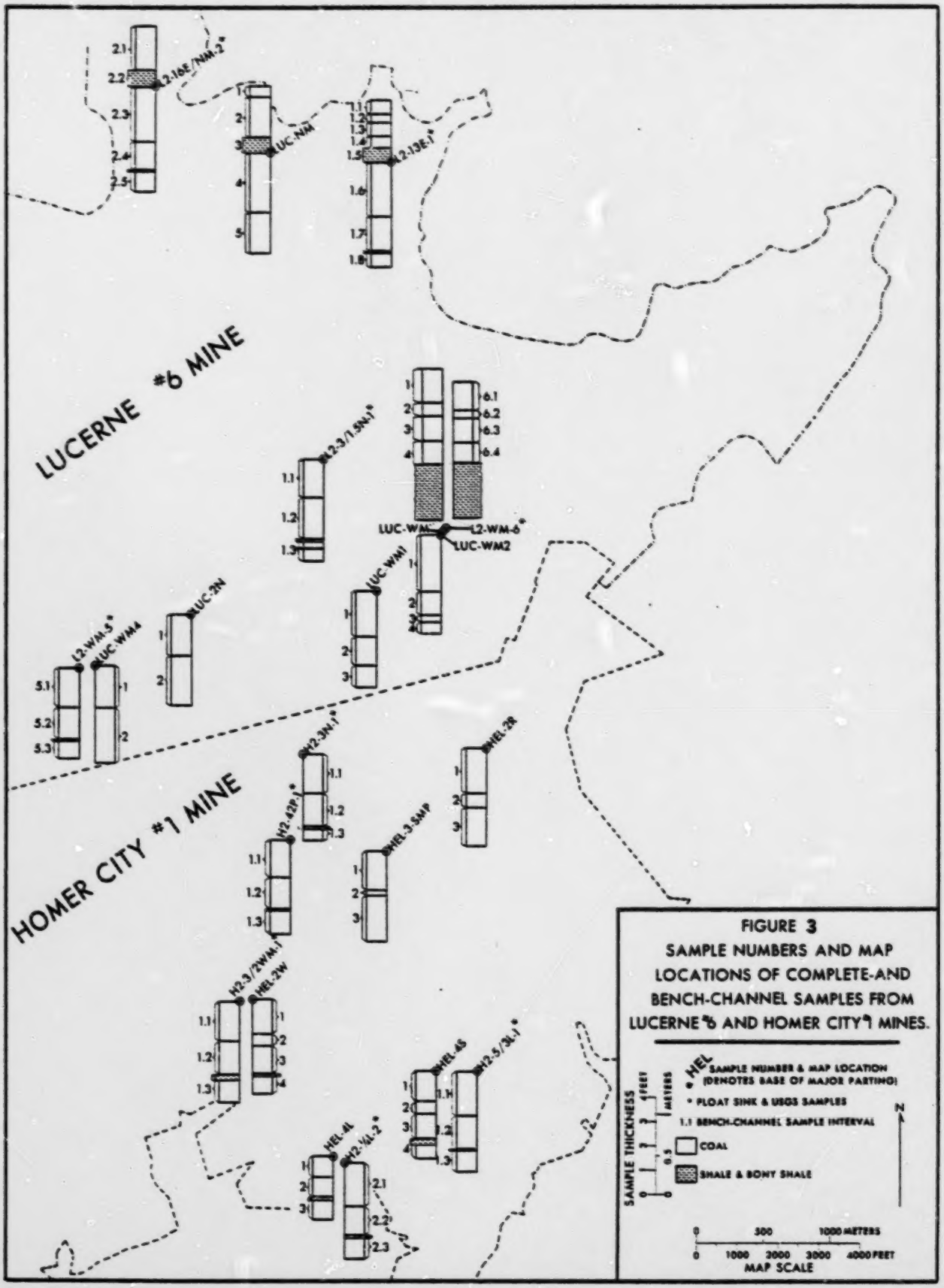
LUCERNE #6 MINE
HOMER CITY #1 MINE
2.1
2.2
2.3
2.4
2.5
2-16E/NM-2*
LUC-NM
1.1
1.2
1.3
1.4
1.5
1.6
1.7
1.8
2-13E-1*
6.1
6.2
6.3
6.4
H2-3/1.5N-1*
LUC-WM1
L2-WM-6*
LUC-WM2
LUC-2N
L2-WM-5*
LUC-WM4
5.1
5.2
5.3
H2-3N-1*
H2-42P-1*
HEL-2R
HEL-3-SMP
H2-3/2WM-1
HEL-2W
HEL-4S
H2-5/3L-1*
HEL-4L
H2-4/L-2*
2.1
2.2
2.3
FIGURE 3
SAMPLE NUMBERS AND MAP LOCATIONS OF COMPLETE-AND BENCH-CHANNEL SAMPLES FROM LUCERNE #6 AND HOMER CITY #1 MINES.
HEL SAMPLE NUMBER & MAP LOCATION (DENOTES BASE OF MAJOR PARTING)
* FLOAT SINK & USGS SAMPLES
1.1 BENCH-CHANNEL SAMPLE INTERVAL
COAL
SHALE & BONY SHALE
SAMPLE THICKNESS
FEET
METERS
N
0 300 1000 METERS
0 1000 2000 3000 4000 FEET
MAP SCALE

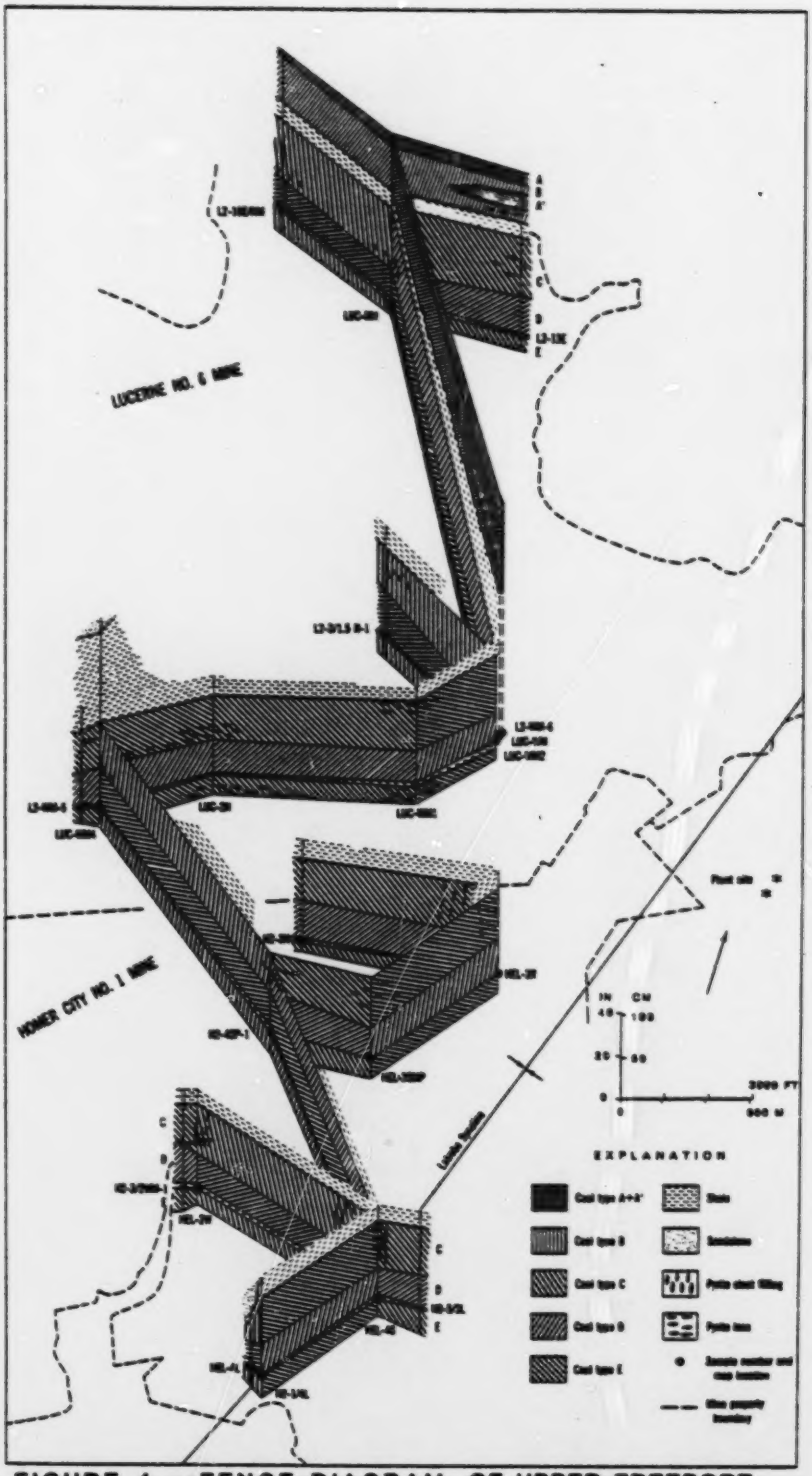

FIGURE 4 - FENCE DIAGRAM OF UPPER FREEPORT COAL FACIES/LUCERNE #6 - HOMER CITY #1 MINES

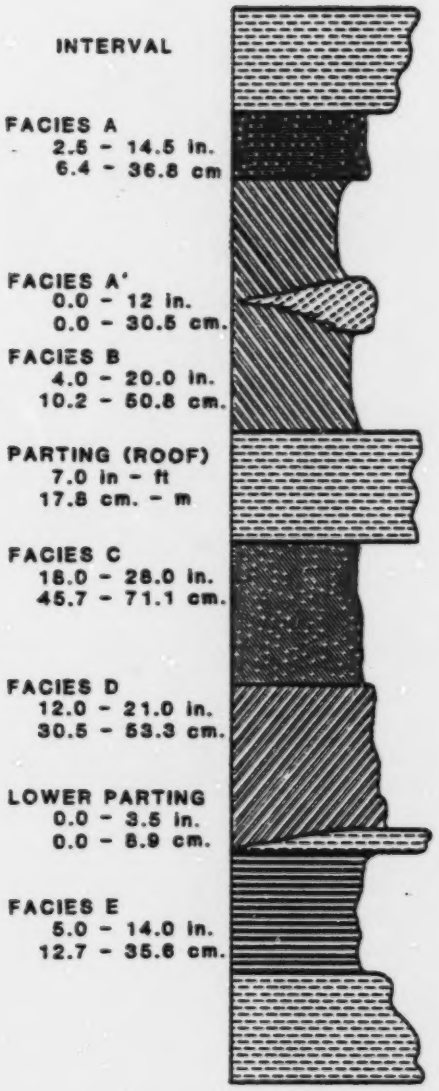

FACIES A - Hard blocky,nonbanded,impure coal: shaley sometimes displaying fissility: calcite along cleats.

FACIES B - Hard,blocky, banded coal with bright bands 2 to 3 mm thick alternating with attrital (dull) bands 3 to 20 mm thick ; fusain abundant at top of facies:scattered pyrite lenses in basal portion

FACIES A' - Hard,blocky,nonbanded,impure coal: concheidal fracture: moderately bright, resinous luster: granular texture. Facies absent in someplaces.

PARTING(ROOF) FACIES - Very dark, gray claystone and shale: basal portions commonly dark gray grading upward into medium gray.

FACIES C - Bright, banded coal, columnar fracture: bright bands 3 to 4 mm thick alternating with attrital bands 6mm thick: distinct fusain layers associated with pyrite: fusain chips at top: calcite and pyrite commonly fill cleats.

FACIES D - Hard, banded coal broken in large blocks; dull luster: bright bands 3 to 15 mm thick; some cleat calcite, very little pyrite; some fusain layers and chips.

LOWER PARTING - Dark gray shale to claystone someplaces absent.

FACIES E - Very hard, blocky, banded coal: very dull luster: numerous shale layers; abundant pyrite in lenses and cleats; some calcite in cleats: bright bands 3 to 4 mm thick; dull bands 2 to 3 cm. thick: slickensides parallel stratification in shale layers near base.

FIGURE 5 - GENERALIZED STRATIGRAPHY OF THE UPPER FREEPOF COAL BED/LUCERNE #6 - HOMER CITY #1 MINES.

DEPOSITIONAL HISTORY

The Upper Freeport coal bed of the Homer City dedicated reserve area is underlain by a complex of underclay, shale, siltstone, brecciated limestone, and flint clay. The lithologies underlying the coal are the result of a variety of processes which began with the deposition of the Upper Freeport limestone in a freshwater environment (Williams and others, 1968). From core data and outcrop data, the Upper Freeport limestone is interpreted to have undergone extensive subaerial exposure after deposition and prior to peat accumulation. This interpretation is consistent with the presence of 1) extensive brecciation, 2) subaerial crusts, and 3) a highly irregular microkarst surface which was partially covered with clays and silt prior to the formation of the ancestral peat-forming environment.

The peat-forming environment developed on the calcium carbonate-rich surface of the Upper Freeport "limestone" interval. Formation of the E facies resulted from peat accumulation that was interrupted by deposition of a parting precursor over much of the area. Peat accumulation resumed with the deposition of the precursors of facies D and C. Peat accumulation (coal facies C) was terminated by drowning and the formation of a freshwater lake or slough in which clay and silt were deposited. The clay and silt became the roof rock where only coal facies D, E, and C are present. In the northeastern part of the area, peat deposition resumed probably on a topographic high in the form of a long linear peat island (Clark, 1979). Coal facies A', B, and A resulted from variations of peat types which accumulated on this peat island. Lateral to the island, clays and silts continued to be deposited contemporaneously with the peat types which became coal facies A', B, and A.

Peat accumulation was terminated by flooding of the island, and clay and silt were deposited over the entire area.

Sands of the Mahoning sandstone interval were then deposited over much of the area as part of a fluvial sequence which prograded into the lake environment. In some places, the streams which transported the sands eroded the previously deposited silts and clays, and sand was deposited directly on the peat. The thin and discontinuous Mahoning coal resulted from peat that accumulated adjacent to stream channels as the sands and associated clays and silts of the Mahoning interval prograded into the freshwater "lake" environment.

Clays and silts were again deposited over the area following deposition of the lithologies of the Mahoning interval. Deposition of the shale above the Mahoning interval apparently occurred in a shallow freshwater environment. Deposition in this environment resulted in conditions which were favorable for scattered peat deposits to form the precursor of the Brush Creek coal. The Brush Creek coal bed is thin, discontinuous, and high in ash and sulfur; thus, it is not of economic value in the study area. The Brush Creek coal bed is overlain by the marine Brush Creek shale. The Brush Creek coal bed may have been deposited originally in a marginal marine environment. This interpretation is based on the thin and discontinuous nature of the bed, the high ash and sulfur content, and the presence of the overlying marine Brush Creek shale which represents a transgressive phase of sedimentation.

The peat-forming environment of the Upper Freeport coal bed in the study area is interpreted to consist entirely of nonmarine swamps and marshes. The Brush Creek shale interval is the first recognizable marine sediment above the Upper Freeport coal bed (fig. 2). The depositional history of the Upper Freeport coal bed and associated units is discussed in detail in Interpretations and Conclusions.

LABORATORY STUDIES

SAMPLE HANDLING

Samples were transported to the laboratory in sealed plastic bags, opened, air dried at room temperature, pulverized, and split for various analyses. Figures 6 and 7 detail the sequence of analyses and the flow of each sample through different stages of pulverizing and splitting.

COAL PETROGRAPHY

Maceral composition

Minerals and macerals are the basic microscopically recognizable constituents of coal (Stopes, 1935). Macerals may have textural characteristics either inherited from the original plant material or resulting from degradation or coalification of plant materials. Macerals do not have definite chemical compositions, are noncrystalline, and have distinct reflectance in polished sections. Minerals, on the other hand, have definite chemical compositions and characteristic crystallographic properties. Because coal is composed predominantly of organic material, maceral composition is valuable quantitative information that can be used to delineate variations among samples. Differences are the result of (1) different original plant types and components; (2) conditions of deposition and preservation, such as flooding, drowning, dry conditions, carbonization/oxidation, and bacterial decomposition; and (3) diagenetic processes during coalification.

Macerals are classified according to petrographic properties such as morphology, color, reflectance, anisotropy, density, polishing relief, and microhardness. Table 1 lists the maceral groups and respective macerals that were recognized by reflected light analysis in this study. Detailed definitions of terms can be found in Stach and others (1975) and ICCP (1963, 1971 Suppl.).

Other published studies concerning the petrographic composition of the Upper Freeport coal (Thiessen and Voorhees, 1922; Davis and others, 1943; Koppe, 1963, 1967) present data obtained from thin sections and polished pellets. Samples analyzed in these studies were not obtained at or near Homer City, Pennsylvania; thus, results of previous petrographic work are not discussed in this report.

Samples for petrographic analysis were prepared by curing an epoxy-coal (-20 mesh) mixture in cylindrical molds (diameter 2.5 cm) and polishing the ends to a flat, scratch-free surface (ASTM, 1977a). Maceral compositions were estimated by point counting components visible in a microscope field. A total of 1000 points were counted per sample at a magnification of 500X.

Because coal is a mixture of both macerals and minerals, the maceral values are presented on a mineral-free basis and a whole-coal basis. Appendix C lists the three representations of the data. These three tables are 1) mineral-matter-free basis (mmf); 2) whole-coal basis [Parr mineral-matter formula (Pmm) corrected]; and 3) whole-coal basis [low temperature ash (LTA) corrected]. Table 2A-C lists the averages by facies for each macearal and maceral group.

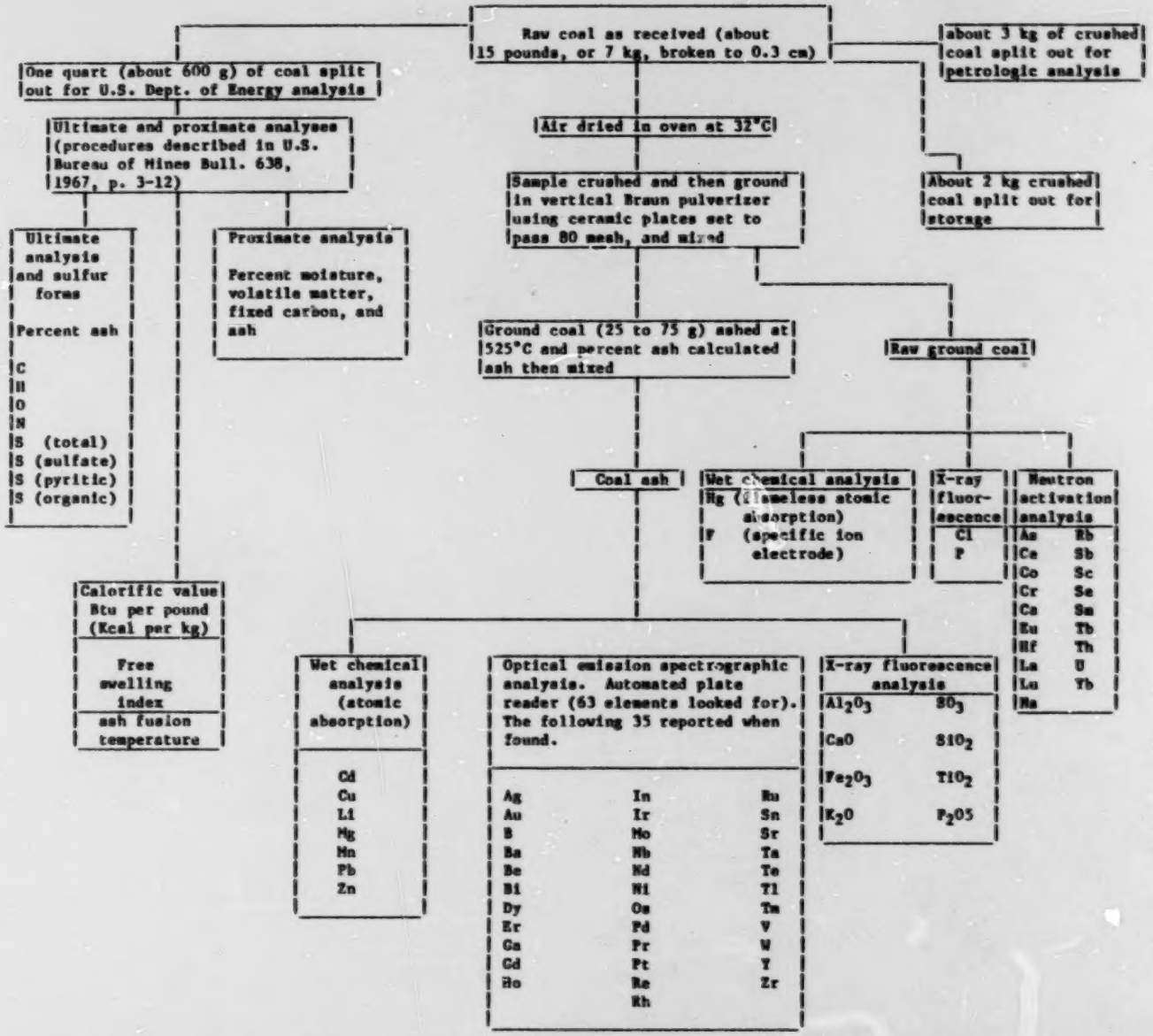

Figure 6 - Analyses performed on coal samples.

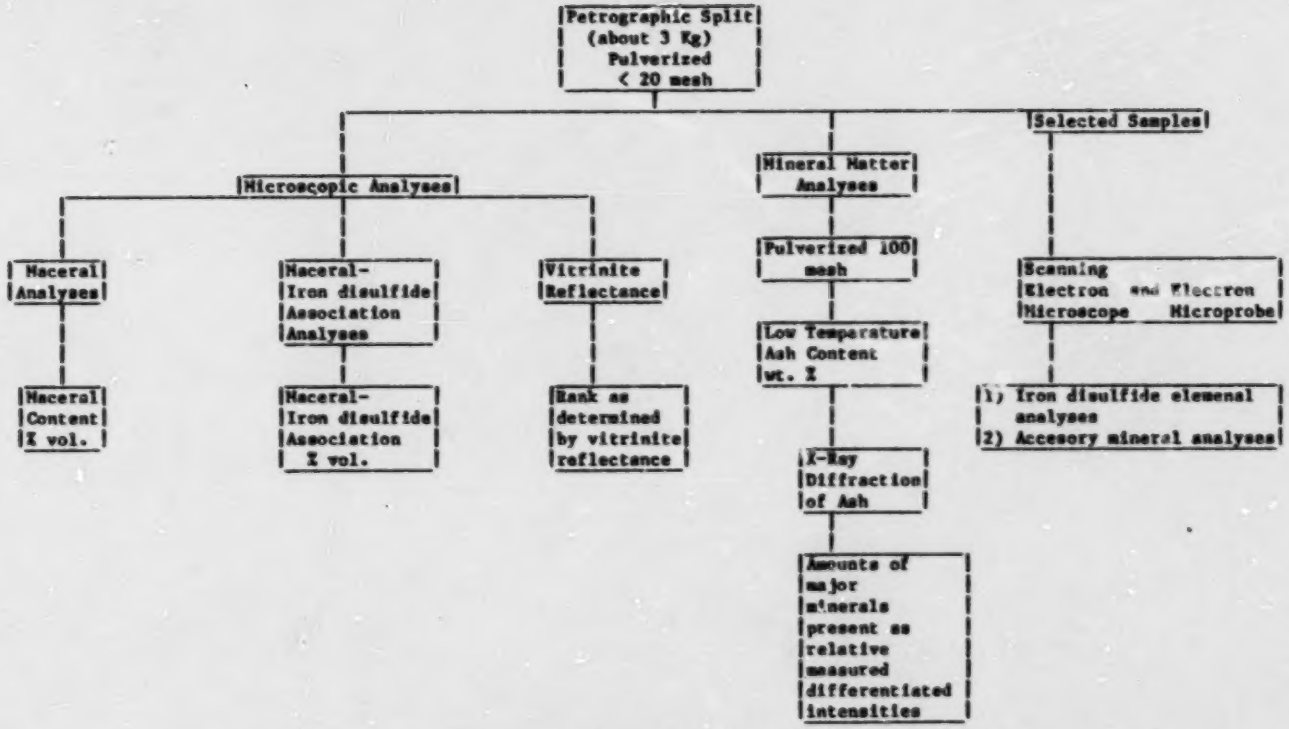
Petrographic Split (about 3 Kg) Pulverized < 20 mesh
Microscopic Analyses
Mineral Matter Analyses
Selected Samples
Maceral Analyses
Maceral Content % vol.
Maceral-Iron disulfide Association Analyses
Maceral-Iron disulfide Association % vol.
Vitrinite Reflectance
Rank as determined by vitrinite reflectance
Pulverized 100 mesh
Low Temperature Ash Content wt. %
X-Ray Diffraction of Ash
Amounts of major minerals present as relative measured differentiated intensities
Scanning Electron and Electron Microscope Microprobe
1) Iron disulfide elemenal analyses
2) Accesory mineral analyses

FIGURE 7

PETROGRAPHIC AND MINERALOGIC ANALYSES PERFORMED ON COAL SAMPLES

Table 1. Maceral groups and their respective macerals identified by reflected light petrographic analysis in this study.

Maceral Group	Maceral
Vitrinite	Collinite and telinite
	Vitrodetrinite
Exinite	Sporinite
(Liptinite)	Cutinite
	Resinite
	Alginite
	Liptodetrinite
Inertinite	Inertodetrinite
	Fusinite
	Semifusinite
	Macrinite
	Micrinite
	Sclerotinite

TABLE 2A: MACERAL COMPOSITION OF UPPER FREEPORT COAL SAMPLES BY FACIES.
(Mineral-free, volume percent basis; C&T=collinite and telinite;
VD= vitrodetrinite; SP=sporinite; CU=cutinite; R=resinite; FU=fusinite;
SF=semifusinite; MI=micrinite; MA=macrinite; SC=sclerotinite;
ID= inertodetrinite; VIT=vitrinite; EX=exinite; INT=inertinite;
LMM=LTA mineral matter[table 2C]; PMM=Parr mineral matter[table 2B]).

	MACERAL VARIETIES											GROUP SUMMARIES		
FIELD NO.	C&T	VD	SP	CU	R	FU	SF	MI	MA	SC	ID	VIT	EX	INT
:::: COMPLETE CHANNELS ::::														
N= 21	84	-	2	T	-	3	4	4	1	-	1	84	3	13
:::: FACIES A ::::														
N= 4	45	6	T	T	-	2	13	3	12	-	17	51	2	47
:::: FACIES B ::::														
N= 7	72	-	2	T	-	4	7	7	6	-	2	72	2	26
:::: FACIES A & B ::::														
N= 1	71	-	6	T	-	3	12	5	-	-	2	72	7	22
:::: FACIES A' ::::														
N= 3	58	2	1	T	-	1	2	28	2	-	4	61	2	38
:::: PARTING FACIES ::::														
N= 3	82	T	T	T	-	3	11	-	1	-	1	82	T	17
:::: FACIES C ::::														
N= 21	86	-	4	T	-	2	3	5	-	-	-	86	4	10
::::FACIES D ::::														
N= 14	89	-	T	T	-	4	4	T	-	-	-	89	2	9
:::: LOWER PARTING FACIES ::::														
N= 1	77	-	T	T	-	5	13	T	2	-	1	78	-	22
:::: FACIES E ::::														
N= 13	89	-	T	T	-	3	5	1	-	-	1	89	1	10
:::: FACIES D & E ::::														
N= 7	90	-	T	T	-	3	4	1	-	-	-	90	1	9
:::: FACIES E (less shale) ::::														
N= 1	94	-	T	T	-	1	3	-	-	-	-	94	T	5

TABLE 2B: PETROGRAPHIC COMPOSITION OF UPPER FREEPORT COAL SAMPLES BY FACIES (Whole-coal, volume percent basis using LTA correction for mineral matter; abbreviations are defined in table 2A).

	MACERAL VARIETIES											GROUP SUMMARIES			
FIELD NO.	C&T	VD	SP	CU	R	FU	SF	MI	MA	SC	ID	PMM	VIT	EX	INT
:::: COMPLETE CHANNELS ::::															
N= 21	76	-	2	T	-	2	4	3	1	-	1	9	77	2	12
:::: FACIES A ::::															
N= 4	34	4	T	T	-	1	10	2	9	-	13	25	38	1	35
:::: FACIES B ::::															
N= 7	66	-	1	T	-	3	7	7	5	-	2	8	67	2	24
:::: FACIES A & B ::::															
N= 1	66	-	5	T	-	3	11	4	-	-	1	8	66	6	20
:::: FACIES A' ::::															
N= 3	43	2	1	T	-	1	2	21	2	-	3	27	44	1	28
:::: PARTING FACIES ::::															
N= 3	46	-	T	T	-	2	6	-	T	-	T	44	46	-	10
:::: FACIES C ::::															
N= 21	82	-	4	T	-	2	3	5	-	-	-	5	82	4	9
::::FACIES D ::::															
N= 14	82	-	T	T	-	4	3	T	-	-	-	7	82	1	9
:::: LOWER PARTING FACIES ::::															
N= 1	57	-	T	T	-	4	9	T	2	-	T	27	57	-	16
:::: FACIES E ::::															
N= 13	75	-	T	T	-	2	4	T	-	-	T	16	75	1	8
:::: FACIES D & E ::::															
N= 7	81	-	T	T	-	3	4	T	-	-	-	10	81	1	8
:::: FACIES E (less shale) ::::															
N= 1	86	-	T	T	-	1	3	-	-	-	-	9	86	T	4

TABLE 2C: PETROGRAPHIC COMPOSITION OF UPPER FREEPORT COAL SAMPLES BY FACIES (Whole-coal, volume percent basis using LTA correction for mineral matter; abbreviations are defined in table 2A).

	MACERAL VARIETIES											GROUP SUMMARIES			
FIELD NO.	C&T	VD	SP	CU	R	FU	SF	MI	MA	SC	ID	LMM	VIT	EX	INT
:::: COMPLETE CHANNELS ::::															
N= 21	77	-	2	T	-	2	4	4	1	-	1	8	77	3	12
:::: FACIES A ::::															
N= 4	35	4	T	T	-	1	10	2	10	-	13	23	39	2	36
:::: FACIES B ::::															
N= 7	67	-	1	T	-	3	7	7	5	-	2	6	68	2	24
:::: FACIES A & B ::::															
N= 1	68	-	6	T	-	3	11	4	-	-	1	5	68	6	21
:::: FACIES A' ::::															
N= 3	42	2	1	T	-	T	2	20	2	-	3	27	44	1	27
:::: PARTING FACIES ::::															
N= 3	45	-	T	T	-	2	6	-	T	-	T	45	45	-	10
:::: FACIES C ::::															
N= 21	83	-	4	T	-	2	3	5	-	-	-	4	83	4	9
::::FACIES D ::::															
N= 14	83	-	T	T	-	4	3	T	-	-	-	7	83	1	9
:::: LOWER PARTING FACIES ::::															
N= 1	56	-	T	T	-	4	3	T	2	-	T	27	57	-	16
:::: FACIES E ::::															
N= 13	75	-	T	T	-	2	4	T	-	-	T	15	75	1	8
:::: FACIES D & E ::::															
N= 7	81	-	T	T	-	3	4	T	-	-	-	9	81	1	8
:::: FACIES E (less shale) ::::															
N= 1	85	-	T	T	-	1	3	-	-	-	-	10	85	T	4

The Parr correction is given by the following formula (ASTM, 1977b):

$$Pmm = \frac{100\,[(1.08A + 0.55S)/2.8]}{[(100-(1.08A + 0.55S))/1.35] + [(1.08A + 0.55S)/2.8]}$$

where A = high temperature ash (750°C)

S = total sulfur

1.35 = density of organic components

2.8 = density of inorganic components

The LTA correction uses the following formula derived during this study:

$$\text{Mineral Matter (Vol\%)} = \frac{100\left(\frac{L-2P}{2.62} + \frac{2P}{5.01}\right)}{\frac{100-L}{1.22} + \frac{L-2P}{2.62} + \frac{2P}{5.01}}$$

where L = LTA (wt. %)

P = Pyritic Sulfur (wt. %)

1.22 = density of organic components

2.62 = density of ash minerals other than pyrite

5.01 = density of pyrite

Compared to the Parr correction, the LTA correction may be a more representative figure for comparing coal samples that differ significantly in pyrite content. Further explanation of the derivation of this relation is given in Appendix D.

One of the objectives of this study was to determine relationships among macerals and among macerals, minerals, and elements. Using the generally accepted groupings of vitrinite, exinite, and inertinite as end members, differences could not be determined for coal facies C, D, and E. The differentiation among the groupings of inertinite, vitrinite, and exinite is based on their relative reflectances, which do not necessarily indicate a similar maceral genesis within a group or different geneses among groups. Micrinite and fusinite are both classified as inertinite although the processes responsible for their origin were completely different. Therefore, characterization of coal samples based solely on the commonly used groupings of vitrinite, exinite, and inertinite (fig. 8) may be of little value in considering facies and/or genetic relationships. For the purpose of this study, more useful differentiation among samples may be made using groupings that are based on maceral concentrations that resulted from the relative enrichment by specific independent processes (deposition, preservation, plant-type abundance, etc.).

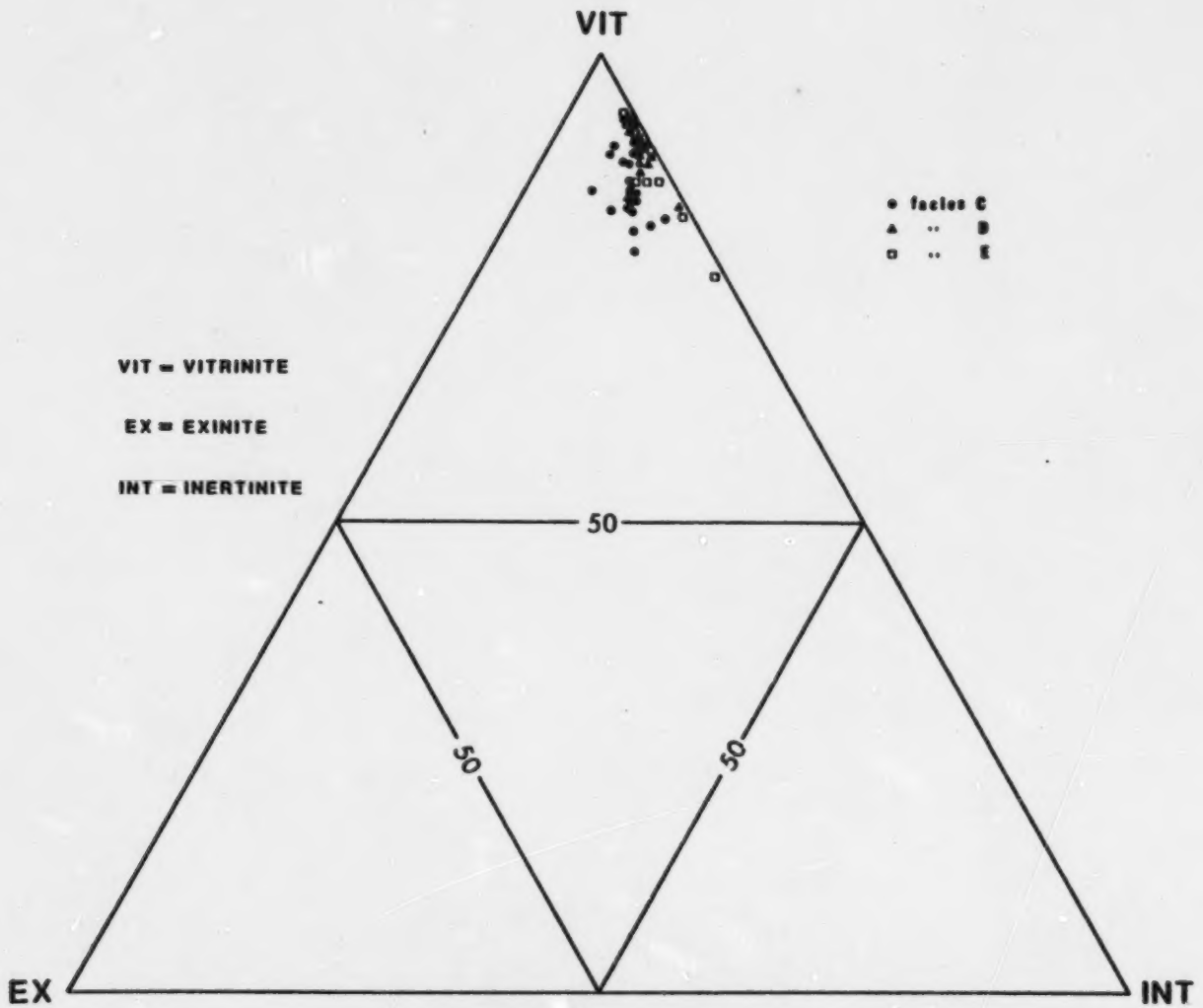

FIGURE 8 - MACERAL COMPOSITIONS OF 46 BENCH - CHANNEL SAMPLES /UPPER FREEPORT COAL,HOMER CITY,PA.

Thus, to differentiate among samples in this study on a mineral-matter-free basis, the following groupings of macerals were chosen:

Group I = inertodetrinite + vitrodetrinite + micrinite + sporinite + resinite

Group II = collinite + telinite + sclerotinite + cutinite

Group III = fusinite + semifusinite + macrinite + mineral matter (LTA corrected)

These groupings were chosen on the basis of possible genetic relationships and statistical correlations among certain macerals. However, even these groupings may not fully explain the differences among samples, and all the maceral varieties themselves in each grouping may not be genetically similar. Notwithstanding, these groupings permit differentiation among samples that was not possible using the groupings of vitrinite, exinite, and inertinite. Although these differences may not be indicative of particular environments of deposition within a peat-accumulating area, they are results of differing degrees of preservation and, therefore, if anything, are indicative of environments of degradation.

A triangular diagram (fig. 9) of the data in terms of the above groupings permits graphical distinction between samples of facies C, D, and E. Compositionally, samples of facies C contain more micrinite and sporinite than those of facies D and E, which are similar to each other in composition; Facies E contains more minerals than facies C or D.

The major factor in separating facies D from E in field sampling was the occurrence of a shale parting that separated the two facies. This shale may have resulted from a temporal change in the environment such as an abrupt change in water depth thereby increasing degradation. After deposition of the organic-matter-rich mud that later formed the parting, peat accumulation continued under somewhat similar conditions that prevailed during the deposition of facies E.

Vitrinite Reflectance

The reflectance of the maceral vitrinite can be used as an accurate measure of the degree of metamorphism or coalification (Hoffman and Jenkins, 1932). In bituminous coal, rank (fixed carbon) is a function of both the degree of metamorphism and maceral composition. Vitrinite reflectance, however, is considered a property directly related to metamorphism.

In this study, the maximum reflectance was recorded and the average of all the readings was reported (mean maximum reflectance, ASTM, 1977c). The vitrinite reflectances for the complete-channel samples are listed in table 3. Their areal relation is shown in figure 10.

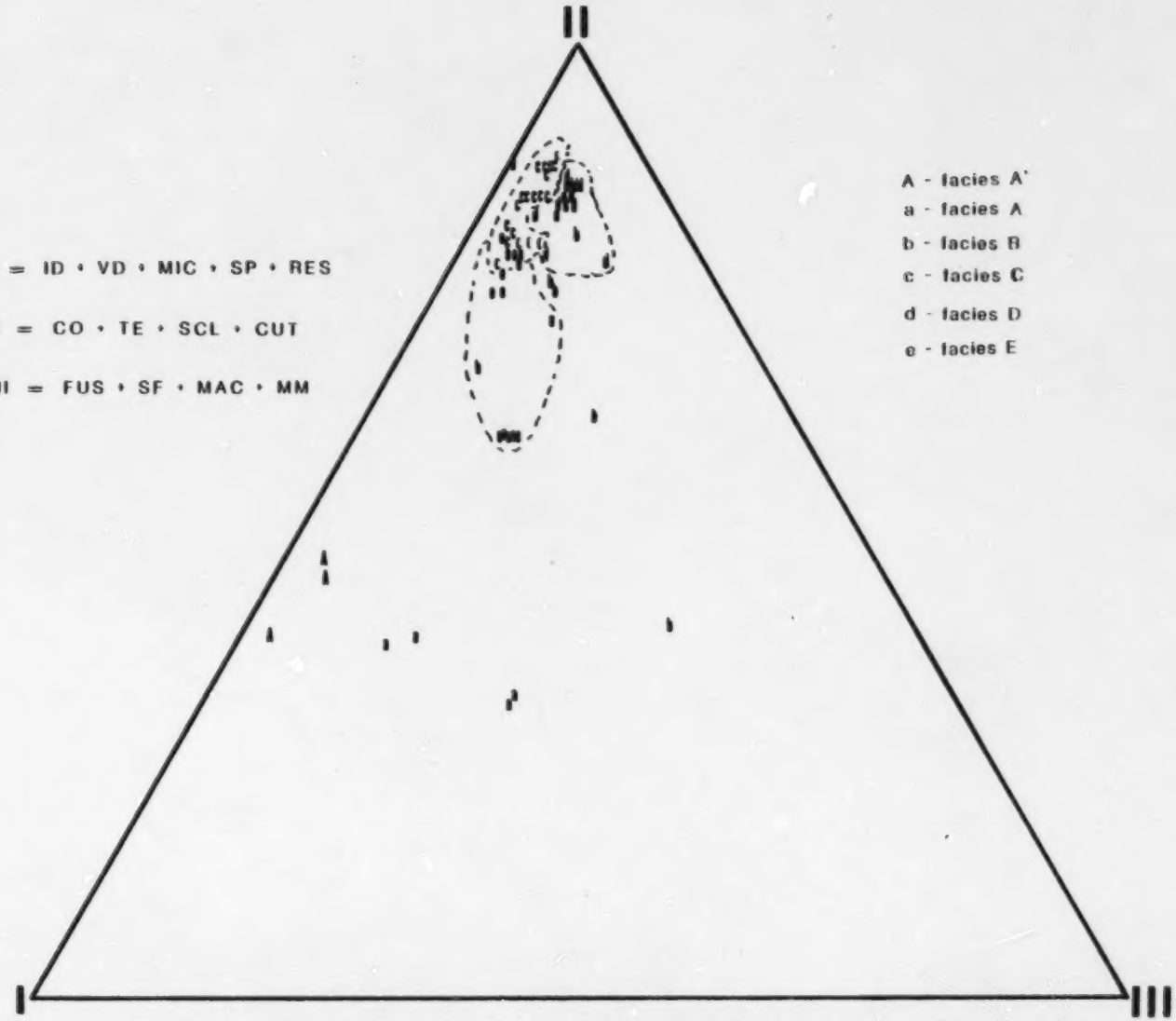
II
I
III
GROUP I = ID + VD + MIC + SP + RES
GROUP II = CO + TE + SCL + CUT
GROUP III = FUS + SF + MAC + MM
A - facies A'
a - facies A
b - facies B
c - facies C
d - facies D
e - facies E

FIGURE 9 – MACERAL VARIETY COMPOSITIONS OF BENCH-CHANNEL SAMPLES/UPPER FREEPORT COAL, HOMER CITY, PENNSYLVANIA.

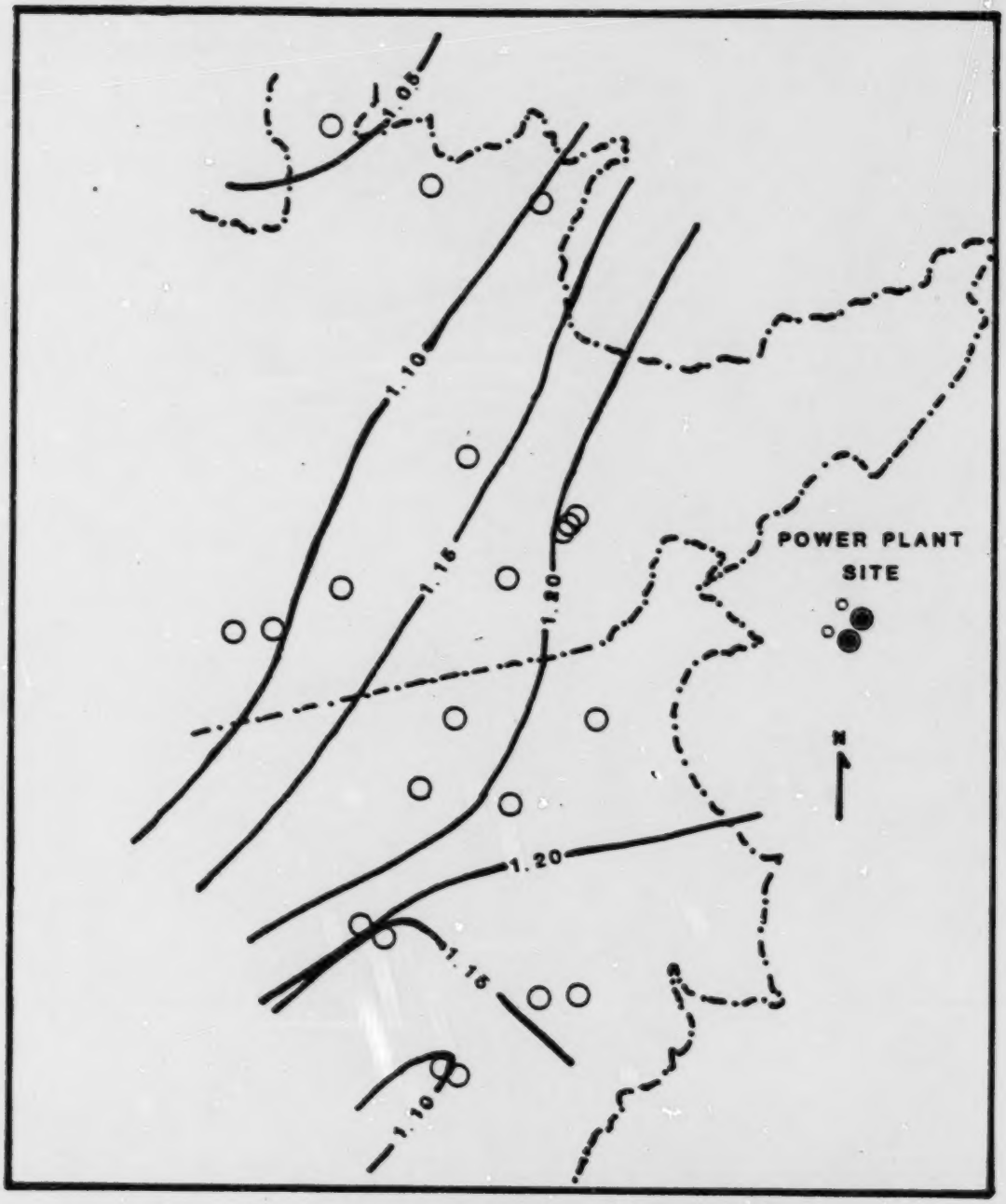

FIGURE 10 - ISOPLETH MAP OF VITRINITE REFLECTANCES /UPPER FREEPORT COAL BED - HOMER CITY, PA.

Table 3. Vitrinite reflectances of 21 complete-channel samples of the Upper Freeport coal bed

Sample No.	R_{omax}	S.D.
HEL-4L-0	1.06	.05
HEL-2W-0	1.15	.05
HEL-2R-0	1.21	.06
HEL-3SMP-0	1.20	.06
HEL-4S-0	1.16	.05
LUC-NM-0	1.09	.05
LUC-WM4-0	1.10	.04
LUC-WM1-0	1.17	.05
LUC-WM-0	1.20	.04
LUC-2N-0	1.12	.04
H2-42P-1.0	1.19	.06
H2-3/2WM-1.0	1.20	.06
H2-1/4L-2.0	1.14	.04
H2-5/3L-1.0	1.17	.05
H2-3N-1.0	1.19	.06
L2-WM-5.0	1.09	.05
L2-WM-6.0	1.20	.03
L2-3/1.5N-1.0	1.13	.05
L2-16E/NM-2.0	1.04	.05
L2-13E-1.0	1.10	.05
LUC-WM2-0	1.21	.05
Arithmetic mean ($\bar{x}$) =	1.15	$\bar{x}$ = .05
Standard deviation (s) =	.05	

The reflectances of bench-channel samples from five locations are listed in table 4. In figure 11, a correlation can be observed between the fixed carbon content and vitrinite reflectance. The fixed carbon content does not appear to show the variation that the vitrinite reflectance shows. Specifically, the vitrinite reflectance is not constant throughout a vertical section of coal as might be expected. Furthermore, an inverse relation exists between vitrinite reflectance and the amount of low temperature ash (mineral matter) (fig. 12) particularly below an LTA of 20 wt. percent. A possible explanation of this correlation is that some element or mineral composing the LTA may have either 1) a retarding effect on the organic maturation and/or degree of degradation or 2) an effect on the vitrinite-reflectance measurement. Thus, the vitrinite reflectance may be affected by ash as well as by pressure and temperature.

A good correlation exists between fixed carbon content (dmmf)--on a dry mineral-matter-free basis and vitrinite reflectance (fig. 13). Scatter along the X-direction (similar vitrinite reflectances but different fixed carbon contents) can be attributed to composition differences, particularly maceral composition. Scatter along the Y-direction (similar fixed carbon contents but different vitrinite reflectances) is not easily explained. These differences may be due, in part, to compositional effect of some ash constituent.

Table 4. Vitrinite reflectances of 22 selected bench-channel samples of the Upper Freeport coal bed

Sample Number	R_{omax}	S.D.
H2-42P-1.1	1.19	.05
H2-42P-1.2	1.19	.04
H2-42P-1.3	1.15	.03
HEL-4L-1	1.06	.05
HEL-4L-2	1.09	.04
HEL-4L-3	1.03	.06
LUC-WM2-1	1.29	.04
LUC-WM2-2	1.25	.04
LUC-WM2-3	1.17	.04
LUC-WM2-4	1.12	.04
L2-WM-6.1	.99	.05
L2-WM-6.2	1.07	.04
L2-WM-6.3	1.06	.04
L2-WM-6.4	1.24	.04
L2-13E-1.1	.94	.05
L2-13E-1.2	.99	.04
L2-13E-1.3	.94	.05
L2-13E-1.4	1.01	.04
L2-13E-1.5	1.05	.05
L2-13E-1.6	1.19	.04
L2-13E-1.7	1.11	.04
L2-13E-1.8	1.06	.04

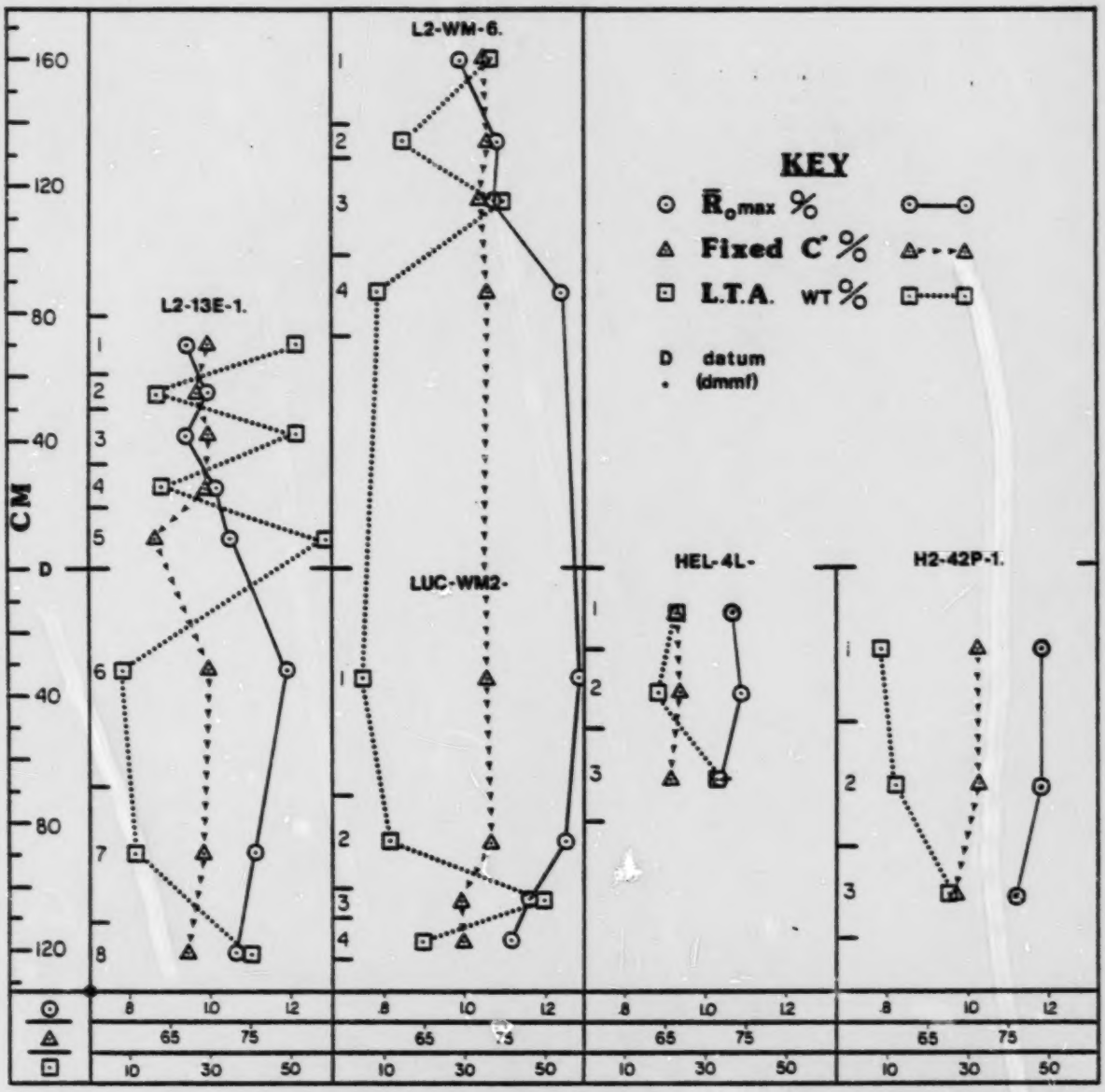

FIGURE 11 - VITRINITE REFLECTANCES, FIXED CARBON CONTENTS, AND LOW TEMPERATURE ASH CONTENTS OF 22 SELECTED BENCH-CHANNEL SAMPLES/UPPER FREEPORT COAL, HOMER CITY, PA.

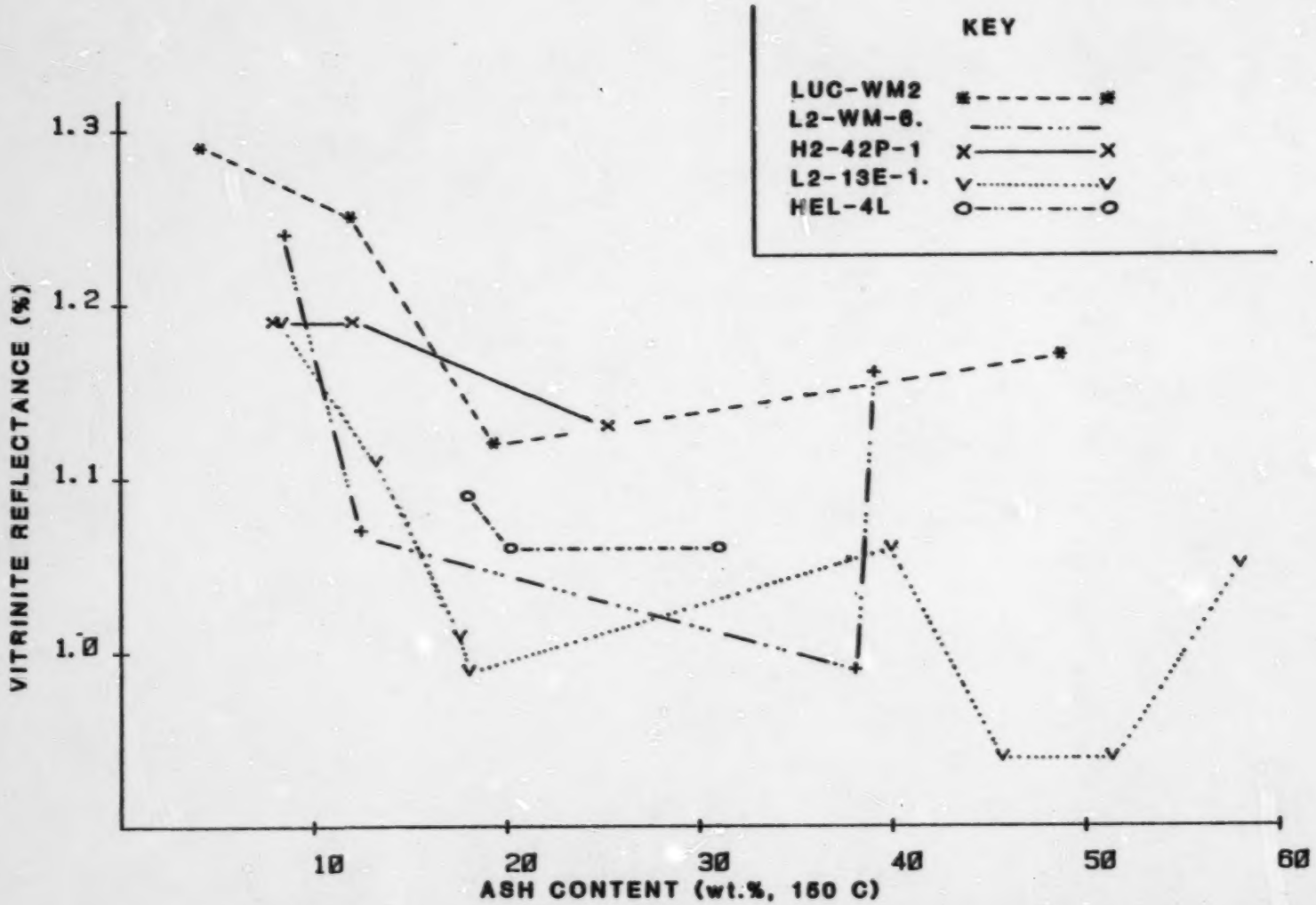

FIGURE 12 -VITRINITE REFLECTANCES VS. ASH CONTENTS OF 22 BENCH CHANNEL SAMPLES FROM THE UPPER FREEPORT COAL BED, HOMER CITY, PA.

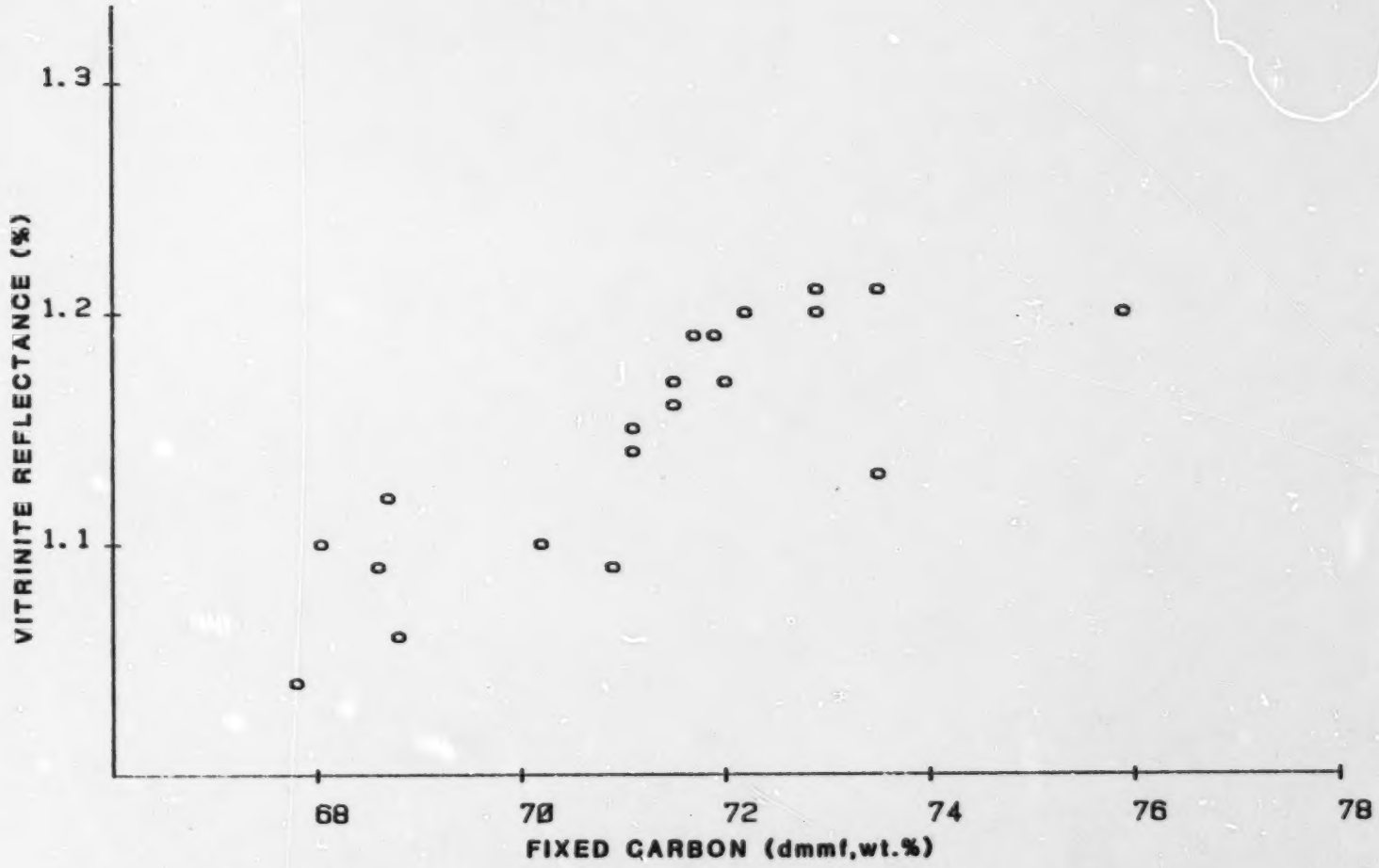

FIGURE 13 - VITRINITE REFLECTANCES VS. FIXED CARBON CONTENTS OF 21 COMPLETE CHANNEL SAMPLES FROM THE UPPER FREEPORT COAL BED, HOMER CITY, PA.

Differences in random reflectances among vitrinite of coal, shale, and limestones of the same sedimentary section have been studied by Bostick and Foster (1973). On the basis of their comparisons of lithology to random reflectances, they suggested the possible need for some correction factor for more precise comparisons of vitrinite reflectances.

In the present study, a stronger correlation of values was obtained because:

1) the samples were stratigraphically closer (within a single bed)

2) the low temperature ash (LTA) value is a more quantitative measure of the amount of minerals present than is general lithologic differentiation (such as coal, shale, etc.)

3) the Upper Freeport samples represent only part (the organic-matter-rich part) of the spectrum of samples compared by Bostick and Foster (1973)

4) mean maximum reflectance as a technique may have less scatter in measured values than random reflectance.

The negative correlation between vitrinite reflectance and LTA may aid in the understanding of: 1) maceral-mineral relationships; 2) the concentrating effect of mineral matter by degradation of plant material, and 3) the contribution of inorganic elements derived from plants to the total mineral-matter content of coal.

Analyses of Sulfur in Coal

Sulfur is bound both organically (in macerals) and inorganically (in minerals) in coal. Much of the organic sulfur is bound during peat accumulation and is affected by chemical changes during diagenesis. The organic sulfur may be bound in compounds such as thiols and thiophenes (Neavel, 1966). Sulfur in the organic form is difficult to analyze by standard chemical means and impossible to detect by optical microscopic techniques.

With the use of a scanning electron microscope (SEM) equipped with an energy dispersive X-ray detector, maps can be constructed showing the sulfur distribution in polished sections of coal. By comparing the elemental distribution maps for sulfur, iron, and zinc, areas can be delineated in which sulfur is not associated with iron or other metallic ions. In such areas, sulfur is assumed to be organically bound. This technique is not quantitative but does give an indication where organic sulfur is concentrated in coal macerals. The electron microprobe has also been used for organic sulfur determinations (Harris and others, 1977; Soloman and Manzione, 1977; Raymond, 1978; Minkin and others, 1979a).

Chemical analysis determines organic sulfur (ASTM, 1977d) by difference. After analyzing for total sulfur (ASTM, 1977e), pyritic, and sulfate sulfur, organic sulfur is determined on the whole-coal basis by subtracting the sum of the pyritic and sulfate sulfurs from the total sulfur. This method does not yield information on sulfur concentrations in macerals.

The accuracy of chemical analysis may be also adversely affected by finely disseminated pyrite encapsulated in macerals or minerals (Edwards and others, 1964). However, the chemical method is currently the best available for determination of sulfur forms.

Sulfur-bearing minerals in coal are sulfides and sulfates. Sulfide minerals are dominantly pyrite and marcasite, and less dominantly sphalerite, galena, and chalcopyrite. With the exception of barite, the sulfate minerals are believed to be weathering products of the sulfide minerals and generally are not present in significant concentrations (Neavel, 1966). Because the organic sulfur contents of the Upper Freeport coal samples differ little, the variation of sulfur in the Upper Freeport coal can be considered primarily a function of the variation of the amounts of pyrite and marcasite.

The methods discussed above cannot distinguish pyrite from marcasite and by themselves cannot determine maceral-mineral associations. However, reflected light microscopy of polished coal specimens can be used to 1) distinguish iron disulfides from other mineral and maceral entities with which they are associated; (2) differentiate pyrite, marcasite, and sphalerite; and (3) observe the forms (size and shape) of the iron disulfides. The iron disulfides are highly reflective in polished sections allowing easy identification. Marcasite generally can be distinguished from pyrite by using crossed polarized reflected light. Marcasite is anisotropic and therefore shows prismatic colors as the specimen is rotated through 360 degrees, whereas pyrite is isotropic and shows no colors or change in brightness during rotation.

A classification based on modes of occurrence can be used to characterize the variation of iron disulfides within a coal bed. Numerous classifications of iron disulfide forms in coal have been devised and used (Whelan, 1954; Gray and others, 1963; Neavel, 1966; Reyes-Navarro and Davis, 1976; Khawaja, 1975; Grady, 1977; King, 1978). Some of these classifications differentiate pyrite forms according to their association with macerals and minerals.

Table 5 depicts the detailed classification devised for this study. Each iron disulfide occurrence is classified by both form and association. The terminology is compiled from the literature and from microscopic observations of many coal samples to be as inclusive as possible. Table 6 is a simplified version of the classification which was found to be the most significant in sample to sample comparisons for this study.

Polished pellets of Upper Freeport coal (as used for maceral analysis) are analyzed in accordance with the above classification. For this analysis, a pellet is examined in reflected light at 500x magnification. Depending on the abundance of iron disulfide in the samples, 500 or more grains may be counted. In pellets containing few iron disulfide grains, the entire polished surface of the pellet is scanned to maximize the number of points. The point-count data are then calculated to 100 volume percent of the total amount of iron disulfide present in the sample.

The total amount of iron disulfides in any individual sample can be expressed on a whole-coal basis: (1) as a weight percent of pyritic sulfur (derived from chemical extraction) or (2) as a volume percent from microscopic estimation (point counting). The first method has a precision of 0.05 wt. percent for a sample containing 1.00 percent pyritic sulfur (ASTM, 1977d). The second method has a precision of 1.5 volume percent (Stach and others, 1975). To compare the precision of chemical

Table 5

MICROSCOPIC IRON DISULFIDE CLASSIFICATION OF COAL

ASSOCIATION / FORM			MACERAL										MINERAL ENCAPSULATION						FRACTURE AND CLEAT FILLING	
			CELL FILLING			ENCAPSULATION							PYRITE							
			TELINITE	INERTINITE	REPLACEMENT	UNKNOWN	TELINITE	COLLINITE TELO-	COLLINITE DESMO/ CORPO-	EXINITE	INERTINITE	FRAM.	DEND.	MARCASITE	CLAY	SIDERITE	OTHER	MICROCLEAT (BRECCIA)	ISOLATED
PYRITE	CRYSTALS	BLEBS																		
		EUHEDRAL																		
	FRAMBOIDS AND PATCHES	DISCRETE																		
		COALESCENT																		
	SPHERULITES																			
	DENDRITIC	PLUMOSE																		
		COLLOFORM																		
		MASSIVE																		
MARCASITE	PERIPHERAL																			
	MASSIVE																			
ACCICULAR																				

Table 6. Simplified classification of iron disulfide forms and associations.

		Association				
		Cell filling	Maceral Replacement	Maceral Encapsulation	Mineral Encapsulation	Fracture or cleat filling
F O R M	Pyrite crystals					
	Pyrite patch or framboid					
	Dendrite or irregular pyrite					
	Marcasite					

and microscopical determinations, the density of pyrite, 5.01 g/cm^3 must be considered. The precision of the first method can be made comparable to that of the second method by the following:

$$\frac{.05}{5.01\ g/cm^3} = .01$$

where .05 = precision of ASTM method (by weight)

where .01 = precision of ASTM method (by volume)

The precision of microscopic point counting 1000 points is, at best, 1.5 wt. percent. To obtain a precision of 0.01 by microscopical techniques alone, more points (about 500,000) would be required. Manually counting so many points would be nearly impossible. Therefore, for the purposes of this study, to obtain weight percentages of pyritic sulfur in terms of irondisulfide forms on a whole-coal basis, the volume percent of any particular form (determined microscopically) is divided by 100 and multiplied by the weight percent pyritic sulfur (ASTM sulfur-forms determination). The results can be used quantiatively for sample to sample comparison.

Pyrite grain-size distribution also can be obtained. In conjunction with the iron disulfide forms/association analysis, each point counted is also categorized according to the size of the particle. The resulting distribution is in volume percent of the total amount of iron disulfide present in the coal. For this study, where minus twenty-mesh coal is used in polished pellets, arbitrary categories corresponding to reticle cell dimensions are used. The significance of these data is not the actual size of the particles but relative variation of the grain-size distributions vertically and laterally within the coal.

Selected bench-channel samples were chosen for initial analysis of iron disulfide forms and associations. The analysis will be applied primarily to the estimation of float-sink characteristics, which will be the focus of the Phase II study.

Figures 14 and 15 are graphic depictions of iron disulfide data from bench-channel samples. Values of iron disulfides as weight percent pyritic sulfur are given as well as grain-sizes of occurrences based on microscopical measurement. These data show not only that the sizes of the iron disulfides are different vertically within the bed but also that the forms and the associations of these occurrences also differ. It is an objective of the second phase of this study to empirically develop criteria for the prediction of washing characteristics as indicated from the examination of whole-coal samples such as cores. These data (figs. 14 and 15) suggest that facies C, D, and E differ in the forms of pyrite on both a volume-percent basis and weight-percent whole-coal basis.

Facies C is dominated by irregular masses of pyrite. These forms are primarily associated with macerals and cleats or fractures. The maceral pyritization probably occurred early in the peat stage because many of the particles show uncompressed plant impressions and casts. The cleat and fracture filling could have resulted from secondary mobilization of replacement pyrite following development of cleat.

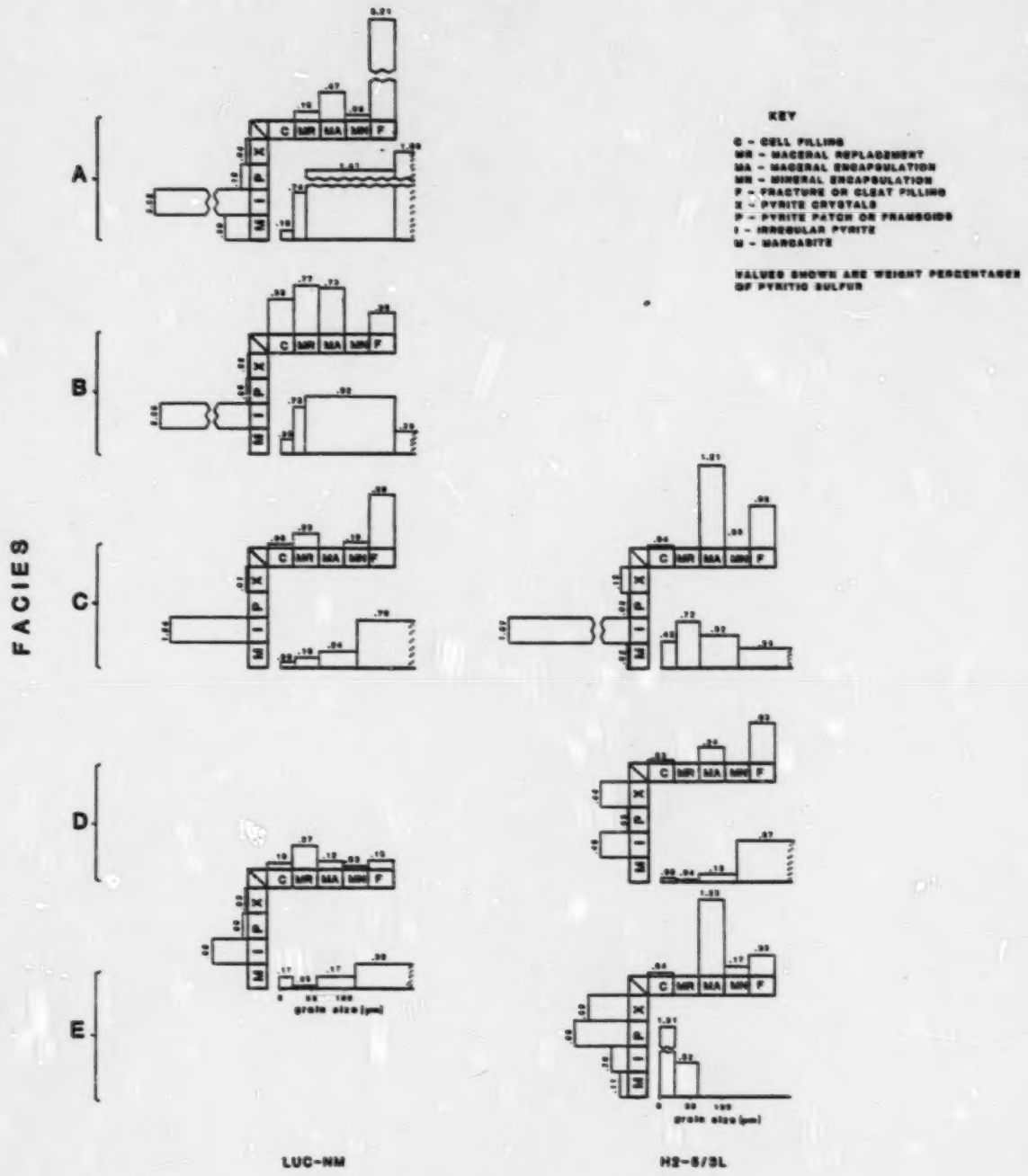

FIGURE 14 - IRON DISULFIDE FORMS, ASSOCIATIONS, AND GRAIN SIZES IN SAMPLES FROM LUC-NM AND H2-5/3L, UPPER FREEPORT COAL / HOMER CITY, PA.

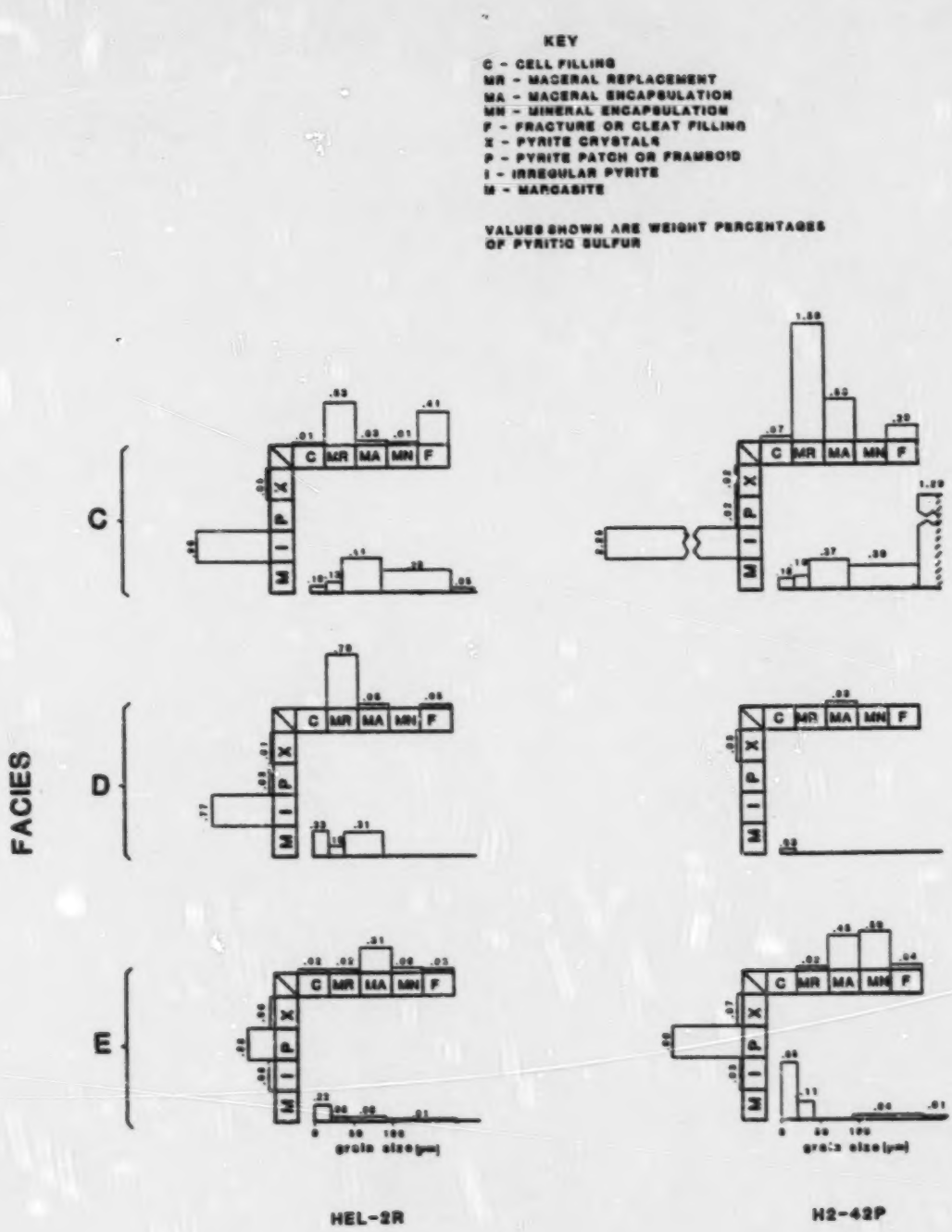

FIGURE 15 - IRON DISULFIDE FORMS, ASSOCIATIONS, AND GRAIN SIZES IN SAMPLES FROM HEL-2R AND H2-42P, UPPER FREEPORT COAL/HOMER CITY, PA.

Facies D generally contains less pyritic sulfur than any other facies. The relative abundance of forms present in facies D differs in each sample. However, a consistent amount of framboids and patches is present.

Facies E contains primarily framboid and crystals encapsulated in macerals (vitrinite) and minerals (clay).

Megascopic Iron Disulfide Occurrences

Megascopic FeS_2 samples (lenses, nodules, cleat deposits) were collected at four sample locations. Two types of sample mounts were prepared--(1) hand block for megascopic and low magnification observation and (2) polished block sections mounted in pellet molds for high magnification microscopic examination. Polished block sections were initially examined at high magnification in reflected light (500x) and later by use of the SEM.

Table 7 is a comparison of microscopic descriptions of each megascopic FeS_2 zone sampled. In three of the sample locations, the forms and associations of the FeS_2 (i.e., fusinite cell fill) are similar.

In samples from location H2-3/2WM, siderite was identified by X-ray diffraction (XRD). The boundaries between siderite and pyrite appear sutured. The outlines of grains having inner cores of siderite surrounded by zones of pyrite suggest replacement of siderite ($FeCO_3$) by pyrite (FeS_2). In the same samples, a clay mineral, probably "kaolinite," was also observed. The formation of siderite over pyrite requires a low concentration of dissolved sulfide, high dissolved carbonate, near neutral pH, low Eh, and high Fe^{+2}/Ca^{+2} ratio (Berner, 1964; Garrrels and Christ, 1965). The near neutral pH of the peat would also be a favorable chemical environment for bacterial sulfate reduction (Postma, 1977). As a result of the increase in dissolved sulfide over dissolved carbonate, pyrite would form over siderite.

In samples from H2-1/4L at the 35-40-inch interval, different forms (table 7) of iron disulfide occur as layers. The layers consist of (a) submicron-sized pyrite in corpocollinite, (b) massive void filling pyrite along spore layers, (c) massive cell replacement pyrite, (d) pyrite framboids along spore and clay layers, (e) pyrite framboids and patches and spherulite pyrite, and (f) pyrite framboids in vitrinite.

In samples from location L2-3/1.5N, zones of pyrite filling telinite cells grade into pyrite filling broken cells which, in turn, grade into pyrite filling cracks in collinite; the gradation strongly indicates secondary mobilization of the pyrite.

Scanning Electron Microscopy of Minerals

To more fully understand the apportionment of trace elements of environmental interest during combustion, liquefaction, gasification, cleaning, weathering, or leaching of coal, one must know the mode of occurrence of these elements, that is, the way in which the element is chemically bound and how it is physically distributed throughout the coal. To obtain information on trace element-mineral associations, selected samples of the Upper Freeport coal were studied by use of scanning electron microscope (SEM). The SEM, used in conjunction with an energy-dispersive X-ray analysis system is effective in the identification of in-situ minerals in coal (Finkelman, 1978; Finkelman and Stanton, 1978; Lee and others, 1978; Stanton and Finkelman, 1979).

Table 7. Comparison of megascopic pyrite in selected mine sample locations.

Interval (inches)	Sample: H2-3/2WM-1	L2-3/1.5N-1	H2-1/4L-2	L2-WM-5
0			Plumose dendrites of pyrite that grade into massive pyrite; no organic structures apparent	
5				
				Pyrite in fusinite cells and vitrain voids and cracks; cell replacement with some vitrinite cell filling that is compressed indicating pyritization after compaction.
10				
	Pyrite crystals (20 microns) in mosaic of siderite and "kaolinite"; siderite appears replaced by pyrite.			
15				
		Pyrite filling open and broken cells of telinite and filling cracks in vitrinite.		
20				
35			Pyrite rich zones as: massive cell replacement; framboids and patches; Coal layers are wrapped around pyrite framboids; blebs less than 1/2 micron in corpocollinite; spherulites or discs showing ringed structure.	
40				

The SEM has a wide range of useful magnifications (10-10,000x), good depth of field, and excellent resolution (<200 angstrom). The solid-state energy-dispersive X-ray detector can determine the presence of all elements heavier than neon (atomic numbers greater than 10) that are present in concentrations above 1 wt. percent. The SEM-energy dispersive system allows the observation and analysis of individual mineral grains as small as one-half micron (um) in diameter.

Four basic sample types were studied in SEM work on Upper Freeport coal:

1) polished pellets also used in routine coal petrographic examinations

2) oriented polished blocks cut from column samples (supplied by E. C. T. Chao)

3) polished thin section (supplied by E. C. T. Chao) prepared from oriented column samples

4) polished and unpolished grain mounts of minerals separated by their densities from the residue of low temperature ashing

A preliminary investigation was conducted on pellets of samples H2-42P-1.1, H2-42P-1.2, and H2-42P-1.3. Table 8 contains a summary of this work. The three samples can be differentiated by the abundance and morphology of pyrite or carbonates as well as the major and trace inorganic element distributions. The samples can also be differentiated by the relative variation of accessory minerals.

Although pellet mounts offer a representative sample that can be used for both SEM and petrographic studies, they have certain disadvantages. The grain size (<20 mesh) is small enough to disrupt the continuity of the coal structure thus making difficult the study of the mineral-maceral relationships. Also, the particles are from a broad stratigraphic range (an entire facies), thus precluding detailed correlation of features. For these reasons, limited use was made of the pellets beyond this preliminary study.

The minerals identified from the SEM study of the Upper Freeport coal samples appear in table 9. Examples of SEM photographs of pyrite forms and clay-minerals are shown in figures 16 and 17.

Mineral identifications based solely on major element data obtained by use of the SEM are not conclusive (throughout the report, they are designated by quotation marks); confirmation of mineral identification requires optical characterization or X-ray diffraction data. Nevertheless, the tentative nature of some mineral identifications does not diminish the usefulness of the data.

The relative abundances of SEM characterized minerals differ considerably. Some were observed in only one or two samples, whereas other minerals were found in almost every sample studied.

Lumina (cell cavities) in fusinite and semifusinite in the Upper Freeport coal are commonly filled by "kaolinite". In some lumina, the "kaolinite" appears to have been replaced by "siderite" (having a varying Ca content). Other mineral occurrences in the lumina include sphalerite (ZnS), "clausthalite" (PbSe), and, more rarely, "chalcopyrite" ($CuFeS_2$) and "apatite" ($Ca_5(PO_4)_3(F,OH,Cl)$). Some resin bodies and/or megaspores contain sphalerite and in one case "barite" ($BaSO_4$).

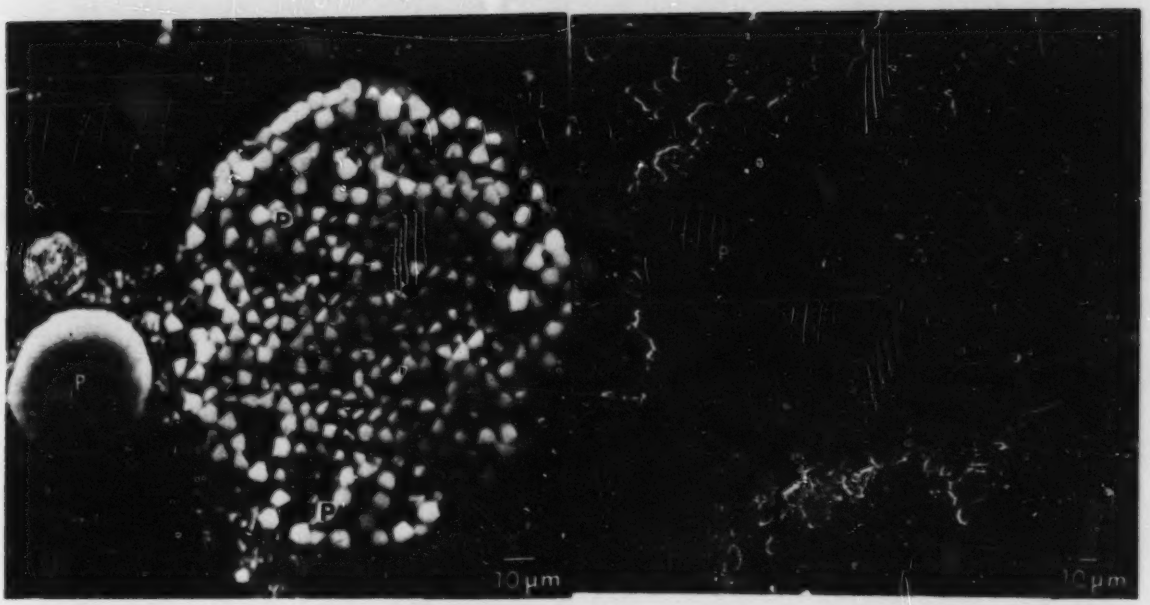

FIGURE 16 - SEM PHOTOGRAPHS OF TWO COMMON FORMS OF PYRITE (P) IN UPPER FREEPORT COAL. PYRITE FRAMBOIDS ARE ON LEFT AND DENDRITIC MASSIVE REPLACEMENT PYRITE IS ON RIGHT.

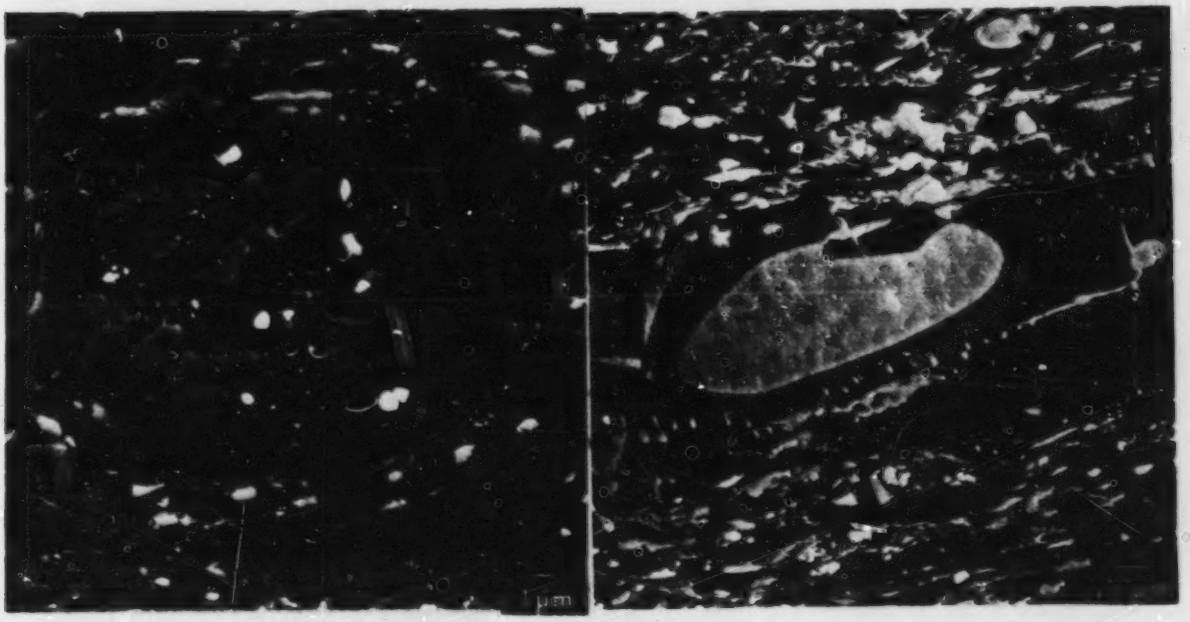

FIGURE 17 - SEM PHOTOGRAPHS OF CLAY MINERALS (C) IN FUSINITE(I).

Table 8. Mineralogy of pellet mounts obtained by use of a scanning electron microscope. [Quotation marks indicate mineral identifications based primarily on major-element data.]

Sample	H2-42P-1.1	H2-42P-1.2	H2-42P-1.3
Total mineral matter	low 5% of surface area	high 15% of surface area	very high >20% of surface area
Iron disulfides	rare but generally massive	none	abundant (50% of mineral matter) framboids, euhedral crystals, some replacements etc.
"Carbonates"	none	abundant vein fillings, fragments, calcite, ankerite and siderite	scarce calcite laths, some pore fillings, some ankerite and siderite
"Kaolinite"	in bogen structure bands with pyrite	in fusinite and vein fillings, filmy	associated with pyrite
"Illite"	in attrital lenses and films	in attrital lenses	filmy and in attrital lenses
"Quartz"	localized in attrital lenses	same	same

Table 9. Minerals in the Upper Freeport coal as interpreted from the SEM data

Major minerals

calcite
$CaCO_3$

kaolinite
$Al_2Si_2O_5(OH_4)$

illite (and mixed layer clays)
$(K, H_3O)\ (Al, Mg, Fe)_2\ (Al, Si)_4\ O_{10}\ [(OH)_2, H_2O]$

pyrite-marcasite
FeS_2

quartz (and opal)
SiO_2

siderite
$FeCO_3$

Accessory minerals*

"ankerite"
$Ca\ (Fe, Mg, Mn)\ (CO_3)_2$

apatite
$Ca_5\ (PO_4)_3\ (F, OH, Cl)$

"argentite"
Ag_2S

"barite"
$BaSO_4$

calcium sulphate
$CaSO_4$

chalcopyrite
$CuFeS_2$

chlorite
$(Mg, Fe)_5\ (Al, Si)_4\ O_{10}\ (OH)_8$

"clausthalite"
PbSe

crandallite
$CaAl_3\ (PO_4)_2\ (OH)_5\ H_2O$

"diaspore"
AlO (OH)

feldspar (potash)
$KAl\ (Al, Si)\ Si_2O_8$

"galena"
PbS

magnetite
$(Fe, Fe_2)\ O_4$

halite
NaCl

Iron-titanium-oxide
$FeTiO_3$

manganese silicate
$MnSiO_3$

"monazite"
$(Ce, La)\ PO_4$

"olivine"
$(Mg, Fe)_2\ SiO_4$

"pyrrhotite"
FeS

"rutile"/"anatase"
TiO_2

sphalerite
ZnS

"xenotime"
YPO_4

zircon
$ZrSiO_4$

*Quotation marks indicate mineral identifications based primarily on major-element data. All other identifications have been substantiated by X-ray diffraction.

The abundance of the PbSe phase in the Upper Freeport samples suggests that substantial amounts of lead and selenium are tied up in this mineral. Nevertheless, the associations of selenium in the Upper Freeport coal appear to be quite complex. Minkin and others (1979b) detected low levels (as much as 0.2 weight percent) of selenium in some pyrite grains.

LOW TEMPERATURE ASH (LTA) MINERALOGY

Approximately 150 minerals have been found in and associated with coals (Mackowsky, 1968; Rao and Gluskoter, 1973; Renton and Hidalgo, 1975; Ward, 1977). The 13 minerals listed in table 10 are the phases identified by X-ray diffraction (XRD) in the suite of samples of Upper Freeport coal collected for Phase I of this study. Illite, kaolinite, quartz, calcite, and pyrite are the phases found most consistently in detectable quantities. These minerals are the only ones considered on a semiquantitative basis. All the X-ray data are listed in Appendix E, table 1.

Methodology and Experimental Studies with Mineral Standards

The method used for the characterization of the mineral phases in the Upper Freeport samples is as follows.

1) 1-2 grams of <150 um (100 mesh) whole coal is low temperature ashed in a four-chamber plasma asher to constant weight using 35-45 watts per chamber.

2) The ash is pulverized and sieved to <73 um (200 mesh).

3) The ash is evenly dispersed in a 28.5-mm-diameter vacuum pellet mold on a smoothed backing of 1.7 grams of a 1:1 mixture of methyl cellulose and boric acid and compressed to 15 tons (2.35 tons cm^2) in a motorized hydraulic press.

4) Pellets are stored in a desiccator until they are analyzed by XRD.

The analysis was conducted on an automated polycrystalline diffractometer (APD). The samples were X-rayed from 3° to at least 59° 2θ with copper, fine focus, X-radiation utilizing a theta compensating slit, a graphite monochromator, and a pulse-height analyzer. The potential on the anode was set at 40 KV and the current through the tube was 20 ma. Data in the form of maximum peak intensity minus background were collected using the Peak Search mode of the APD system (Jenkins and others, 1971) with a counting time of 0.75 sec per 0.02° 2θ and the peak to background ratio (threshold for significance of a peak) of 1.25. Data in the form of integrated intensities minus background were collected for the two principal clay-mineral peaks using the Line Profile mode of the APD system. The goniometer was stepped from 7.0° to 9.5°2θ and 11.5° to 13.0°2θ at an increment of 0.02°2θ per sec. for the illite and kaolinite determinations, respectively.

Table 10

Diffraction spacings of mineral phases in LTA as determined by XRD, Upper Freeport coal bed, Homer City, Pa.

Phase	Diffraction Spacing, Å								
Illite	10.0	4.97	4.47	2.56	2.38				
Kaolinite	7.14	4.46	3.58	2.56	2.50	2.38	2.33	1.98	1.79
Gypsum	7.56	4.27	3.06						
Quartz	4.26	3.34	2.46	2.28	2.24	2.13	1.98	1.82	1.67
Anatase	3.52	2.38	1.89	1.70	1.67				
Marcasite	3.44	2.32	1.76						
Rutile	3.25	2.49	1.69						
Pyrite	3.13	2.71	2.42	2.21	1.92	1.63			
Calcite	3.04	2.85	2.29	2.10	1.91	1.88			
Dolomite	2.89	2.19							
Siderite	2.79								
Coquimbite	8.26	2.76	5.45						
Ankerite	2.90								

The semiquantitative characterization method involved summing the measured maximum intensity minus background values for each of the five principal phases. The five major phases, their respective diffraction spacing (dÅ), and crystallographic indices (hkl) used in the measurement are listed below:

Phase	dÅ	hkl
illite (ill)	10	001 (1M) 002 (2M)
kaolinite (kaol)	7.14	001
quartz (qtz)	4.26	100
calcite (cal)	3.04	100
pyrite (py)	2.71	200

Each intensity value was divided by the sum of all intensity values, and a relative percent intensity factor was calculated. This factor was further multiplied by the fractional value for the percent low temperature ash of the particular sample resulting in relative percent intensity on a whole-coal basis. Figure 18 illustrates the calculation procedure on a hypothetical set of intensity data.

Two clay ratios were calculated from: 1) the integrated intensity of kaolinite divided by the integrated intensity of illite; 2) the integrated intensity of kaolinite divided by the sum of the integrated intensities of illite and kaolinite.

$$1)\ \frac{\text{kaol}}{\text{illite}} \quad \text{and} \quad 2)\ \frac{\text{kaol}}{\text{kaol + illite}}$$

Because the method chosen is specific for instrumentation used in this study, it cannot be directly compared with other semiquantitative methods. The method is designed to maximize the precision, and by being internally consistent, the method enables a large amount of diffraction data to be analyzed and compared. The calculated relative percent of measured intensity values for each mineral does not represent the actual weight percent. The following experiments with blends of mineral standards demonstrate a relationship between the actual weight percent of a mineral phase and the relative percent intensity factor.

The mineral standards used were as follows:

Quartz - Ottawa Sand, Fisher Scientific S-23
pulverized to < 73 um

Calcite - crystal from Germany Valley, W. Va.
pulverized to < 73 um

Kaolinite - EPK Georgia Kaolinite
pulverized to < 73 um

Pyrite - massive pyrite lens from the Pittsburgh coal bed pulverized to <73 um, treated with 10 percent HCl to remove calcite.

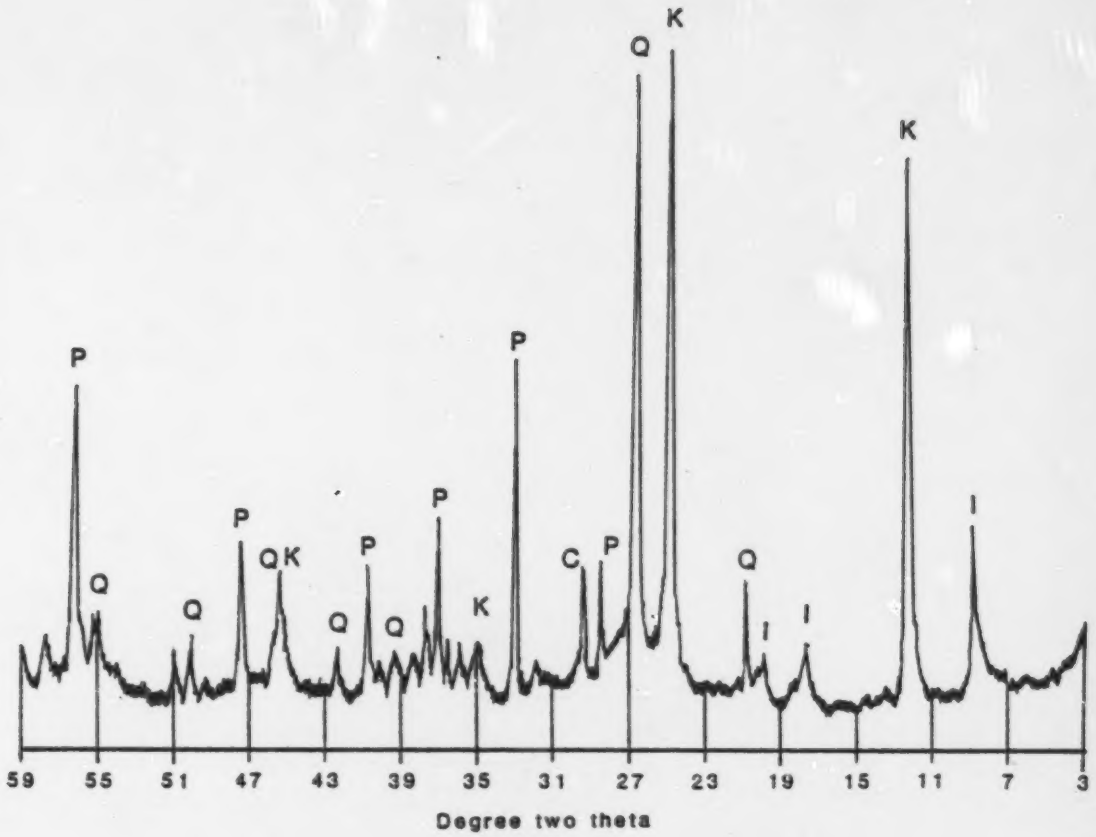

	ill(I)	kaol(K)	qtz(Q)	cal(C)	py(P)	Row Sum	% Ash
Intensity	513	1899	343	340	1036	4130	15
Relative Percent	13	46	8	8	25	100	
Percent Whole Coal	2	7	1	1	4	15	

FIGURE 18 - XRD Intensity - percent Calculation

All standards were X-rayed separately and determined to be monomineralic. Ten, four-component mineral mixes were weighed out to the nearest 0.01 mg in a random fashion and their respective weight percents were calculated (table 11). The samples were pressed into pellets and scanned from 11° to 39°2θ at a rate of 0.02° per 0.75 sec. using the APD Peak Search Mode. The peak intensities minus background determined for selected peaks, and their calculated relative intensities are shown in table 11.

Quartz ranges from 4-35 weight percent with corresponding intensity values of 155 and 1469. The weight percents and intensity measurement intervals for calcite are 9-46 and 2402-12184, those for pyrite are 7-37 and 734-2782, and those for kaolinite are 21-57 and 1032-3004, respectively.

The correlation coefficients and the linear regression equations were derived to determine the percent of one mineral phase with respect to all phases in the multicomponent system (table 12). For all equations, variable X is the sum of the measured intensity for each of the respective phases in the system divided by the intensity of the phase in question. Variable Y is a transformation of the known weight percent of the phase in question which is divided into 100 and has 1 subtracted from it. The equation used is a synthesis and simplification of equations used by Moore (1965 and 1968) and Chung (1974) for quantitative multicomponent analysis.

The equations represent a deterministic linear model for relating the measured intensity at the specific d-spacing for the particular four-phase system and demonstrate the intrinsic relation between the actual weight percent and the measured X-ray diffracted intensity.

The standard error of estimate (SEE), which is the scatter in the vertical (Y) direction of the observed points about the regression line, can be used as a measure of the accuracy of the linear model in estimating a weight percent of a mineral from the measured intensity values. $(SEE)^2$ is an estimate of that part of the variance of Y (s^2_y) left unexplained by the regression of Y on X. The s^2_y and SEE and their corresponding weight percent error window for each regression equation from table 12 are listed below.

Mineral	s^2_y	SEE	SEE^2	WT%
Quartz	75.52	1.64	2.69	+ 4.94, - 9.78
Calcite	11.09	0.59	0.35	+ 2.11, - 2.68
Pyrite	12.31	2.09	4.37	+ 5.89, - 14.33
Kaolinite	0.94	0.60	0.26	+ 2.11, - 2.68

The specific relationship between the known weight percent and the calculated relative percent of diffracted intensity is verified by 1) regressing the latter (X) on the former (Y), and 2) calculating a nonparametric Spearman Rank correlation coefficient. The results of this analysis are presented in table 13.

Table 13 demonstrates both parametrically and nonparametrically that a relationship exists between the actual weight percent of a mineral phase and the measured relative percent intensity factor. The parametric correlation coefficient (r) is a measure of the association among the random variables, known and calculated percent, for each mineral. The coefficients

Table 11. Experimental results for four-phase mineral mixtures.

Spl#	Phase	Actual weight %	dÅ	Measured intensity	Relative % intensity
1	Qtz	35	4.26	1469	19
	Cal	9	3.03	2652	34
	Py	15	2.71	1553	20
	Kaol	41	7.14	2035	26
2	Qtz	8	4.26	296	3
	Cal	20	3.03	5317	53
	Py	32	2.71	2398	24
	Kaol	41	7.14	2016	20
3	Qtz	30	4.26	811	12
	Cal	10	3.03	2402	35
	Py	35	2.71	2612	38
	Kaol	25	7.14	1111	16
4	Qtz	20	4.26	561	6
	Cal	27	3.03	6061	61
	Py	29	2.71	2170	22
	Kaol	25	7.14	1073	11
5	Qtz	21	4.26	1249	12
	Cal	15	3.03	5362	52
	Py	7	2.71	734	7
	Kaol	57	7.14	3004	29
6	Qtz	4	4.26	155	2
	Cal	22	3.03	5433	53
	Py	37	2.71	2782	27
	Kaol	37	7.14	1817	18
7	Qtz	17	4.26	686	7
	Cal	19	3.03	5468	55
	Py	21	2.71	1693	17
	Kaol	42	7.14	2160	22
8	Qtz	31	4.26	1356	18
	Cal	9	3.03	2563	34
	Py	14	2.71	1351	18
	Kaol	46	7.14	2282	30
9	Qtz	17	4.26	673	4
	Cal	46	3.03	12184	80
	Py	16	2.71	1265	8
	Kaol	21	7.14	1032	7
10	Qtz	4	4.26	158	1
	Cal	32	3.03	8658	69
	Py	28	2.71	2159	17
	Kaol	36	7.14	1655	13

Table 12. Correlation coefficients and linear equations for a specific phase versus all phases.

Mineral	r	Equation
Quartz	.984	-1.80 + .320 X = Y
Calcite	.986	-5.51 + 5.23 X = Y
Pyrite	.828	-4.93 + .784 X = Y
Kaolinite	.828	.828 + .117 X = Y

where n = 10, significant r (99%) = .708

For the determination of quartz, the X and Y variables are as follows:

$$Xqtz = \frac{Iqtz + Ical + Ipy + Ikaol}{Iqtz}$$

$$Yqtz = \left[\frac{100}{\text{known weight \%}}\right] - 1$$

are significant in all cases at the 0.99 level for 10 samples. The non-parametric Spearman's rank correlation (s) test uses the relative magnitudes of the variables within each of the two sets of data to determine if the two sets are independent (Gibbons, 1976). The standardized normal value is calculated, $z = s\ (n-1)$, where n is the number of paired variables and is used to test the hypothesis of independence. The probability of independence is less than 0.01 for 10 samples.

An even more simplistic quantitative relationship can be shown between the measured intensity for a phase and the known weight percent of that phase in the multicomponent mixture, where X is the measured intensity and Y the actual weight percent. Table 14 presents the derived linear equations and correlation coefficients.

The mineral mixture experiments were run to establish a relationship between measurements of diffracted X-ray intensity and the known weight percent of a particular suite of minerals. We concluded that if the complete mineralogy is known and suitable standards of each mineral are available, the weight percent of each mineral can be estimated from equations similar to those presented in tables 12 and 14. The relationship between known weight percent and relative intensity measurements as presented in table 13 was taken as the basis of comparison between samples for this study. The relative percent intensity measurements for each of the four phases of the mineral blends are related to the actual weight percent of each phase. Intensity factors are adequate for comparison of samples, thus precluding the need for conversion to weight percent. The X-ray data, as collected and presented in Appendix E, are first order measurements. The error is attributable only to the method of sample preparation and the inherent random fluctuation of the diffraction setup. The usefulness of these first order data would be obscured by their transformation through deterministic linear models of varying degrees of accuracy.

Table 13. Statistical correlations of mineral phases

	Qtz	Cal	Py	Kaol
Parametric corr. coef. r =	.934	.967	.805	.889
Nonparametric Spearman Rank s =	.973	.961	.803	.945
z =	2.92	2.88	2.41	2.84

(Data are from table 11)

Table 14. Correlation coefficients(r), linear equations, and standard errors of estimate (SEE) for regression of known weight percent (Y) on measured intensity (X).

Mineral	r	equation	SEE
Quartz	.901	3.36 + .021 (X) = Y	±5.09
Calcite	.979	-4.96 + .004 (X) = Y	±2.53
Pyrite	.983	-4.19 + .015 (X) = Y	±1.61
Kaolinite	.994	5.40 + .017 (X) = Y	±1.24

All correlation coefficients are significant at 99%.
(Data are from Table 11)

All slope coefficients were tested and found to be nonzero at the 99 percent level of confidence. They are necessarily small due to the effect of the large intensity values.

Error in the diffraction method can be broadly attributed to two sources: 1) inherent voltage fluctuations in the electronics and 2) the method of sample preparation. The first error was approximated by repeated measurement of a quartz reference standard, normally performed between samples to calibrate the goniometer. In 200 calibrations, the average intensity was 12944 counts/sec. with a standard deviation of 162 counts/sec. or 1.3 percent.

The second error is affected by three factors: 1) nonhomogeneous distribution of minerals within the sample which is commonly a problem in sedimentation mounts on glass slides and to a lesser extent vacuum tile mounts; 2) orientation effects common to loose powder pack mounts which use nonreproducible packing pressures; and 3) particle size differences which are common in sedimentation mounts because of differential settling.

The pressed pellet method used in this study maximizes the orientation effects and minimizes the variability in intensity measurements. The percent deviation determined for this method of preparation was determined to range from 5 to 10 percent.

Mineral Composition

The mineralogy on a percent relative intensity basis for the seven megascopic facies of the Upper Freeport coal bed samples is summarized in table 15. For each facies and its respective number of samples (n), the average percent value (x), and standard deviation (s) is given. The coefficient of variation (cv) is the standard deviation divided by the mean and is a relative measure of variability among facies and phases. Calcite is extremely variable in the facies A, A', B and parting. In the lower three facies, calcite is present in its highest concentration and is less variable. In these three facies epigenetic cleat calcite is commonly found. The parting facies is dominated by the clay minerals illite and kaolinite with addition of a large contribution from quartz and some pyrite. The proportions of minerals in the parting are similar to those in the A' facies, a nonbanded coal facies.

Table 16 presents the data of table 15 on a whole-coal basis; these data were obtained by multiplying the calculated relative percent of the total measured diffracted intensity for each mineral by the fractional percent LTA for the specific sample. This transformation illustrates which facies contains the most mineral matter. The ash values range from a low of 4.3 for a sample from C facies to a high of 68.2 for a sample from the parting facies.

Table 15. Summary: Mineralogy, Relative Percent, by Facies

Facies	n	Ill	Kaol	Qtz	Cal	Py
A	4 $\bar{x}$ =	12.5	35	37	1.0	14.5
	s =	3.0	8.4	7.5	2.0	10.7
	cv =	.24	.24	.20	2.0	.74
	range =	9-15	24-44	26-42	0-4	4-26
A'	3 $\bar{x}$ =	21	42	23	3.3	10
	s =	3.5	5.3	3.8	5.8	6.3
	cv =	.17	.13	.17	1.8	.62
	range =	17-24	38-48	19-26	0-10	3-15
B	7 $\bar{x}$ =	7.3	47	13	15	18
	s =	3.3	19	9.3	15	13.6
	cv =	.45	.40	.72	1	.76
	range =	4-23	27-73	5-33	0-37	0-32
Part	3 $\bar{x}$ =	20	44	25	2.7	8.7
	s =	4.4	3.6	5.0	4.6	4.9
	cv =	.22	.08	.20	1.7	.56
	range =	17-25	41-48	20-30	0-8	3-12
C	15 $\bar{x}$ =	5.8	36	3.5	23	32
	s =	2.7	14	1.9	20	15
	cv =	.47	.40	.54	.90	.49
	range =	2-11	10-57	1-7	0-58	3-66
D	14 $\bar{x}$ =	17	37	12	21	14
	s =	4.9	11	4.6	15	11
	cv =	.29	.30	.38	.71	.79
	range =	10-24	22-60	5-21	0-39	0-31
E w/shale	13 $\bar{x}$ =	11	35	10	17	26
	s =	3	9	6	11	6
	cv =	.27	.26	.60	.65	.23
	range =	6-16	23-51	4-23	0-34	19-39

Table 16. Summary: Mineralogy, Whole Coal, by Facies

Facies	n	Ill	Kaol	Qtz	Cal	Py	% Ash (LTA)
A	4 $\bar{x}$ =	4.9	13.6	14.8	.7	6.3	40.1
	s =	1.4	2.0	3.0	1.2	5.2	6.8
	cv =	.29	.15	.20	1.7	.83	.17
	range =	3.4-6.6	10.8-15.4	12.0-18.0	0-2.1	1.2-11.8	31.3-45.8
A'	3 $\bar{x}$ =	9.1	18.8	10.4	1.8	4.8	45.0
	s =	.29	.90	1.1	3.1	3.4	6.1
	cv =	.03	.05	.11	1.7	.71	.14
	range =	8.8-9.3	17.9-19.7	9.7-11.7	0-5.3	1.2-7.9	39.2-51.4
B	7 $\bar{x}$ =	.88	5.9	1.8	2.3	2.8	13.8
	s =	.26	1.3	1.5	2.7	2.2	4.1
	cv =	.30	.22	.83	1.2	.79	.30
	range =	.46-1.2	4.0-8.0	.88-5.2	0-6.5	0-5.2	8.2-18.1
Part	3 $\bar{x}$ =	12.9	28.0	15.7	1.5	5.6	63.7
	s =	3.5	4.1	3.9	2.5	2.8	5.2
	cv =	.27	.15	.25	1.7	.5	.08
	range =	10.1-16.9	24.9-32.6	11.5-19.2	0-4.4	2.4-7.4	58.0-68.2
C	15 $\bar{x}$ =	.45	2.7	.28	1.9	2.6	8.0
	s =	.21	.93	.19	2.0	1.2	2.0
	cv =	.47	.34	.68	1.1	.46	.25
	range =	.21-1.7	1.2-4.7	.05-.73	0-6.4	.11-4.7	4.3-11.2
D	14 $\bar{x}$ =	2.3	5.1	1.6	2.8	2.1	14.0
	s =	.79	1.3	.79	2.1	1.8	2.5
	cv =	.34	.25	.49	.7	.86	.18
	range =	.43-3.3	2.8-7.4	.20-3.3	0-6.4	0-4.8	9.6-18.0
E w/shale	13 $\bar{x}$ =	3.3	9.8	3.0	5.0	7.1	28.5
	s =	1.0	2.9	2.3	3.6	1.6	4.7
	cv =	.30	.30	.77	.7	.23	.16
	range =	1.6-5.1	7.2-17.7	1.0-9.2	0-11.2	5.2-10.5	21.7-40.0

Table 17 presents the average values for the major oxides by facies. The "R" is the percentage sum of Mg, Na, Mn, Ti, and P. There is a strong association between major-oxide chemistry and major-component mineralogy. Low calcium, iron, and sulfur values correspond with low amounts of calcite and pyrite.

Figure 19 graphically displays the major-oxide data over the corresponding mineralogy data by facies. With an increase in K, there is a corresponding increase in illite. Large amounts of Al and Si are associated with proportional amounts of kaolinite, illite, and quartz. An important item demonstrated by figure 19 is that the X-ray mineralogy data are meaningful and relevant although not absolutely quantitative.

CHEMICAL ANALYSES

Elemental Analyses

The USGS analytical laboratories analyzed all bench-channel and complete-channel samples for 70 elements. Analytical techniques included atomic-absorption, neutron-activation, X-ray fluorescence, and emission-spectrographic analysis (fig. 6). Analytical results for all samples are included in Appendix F. Although elements are determined on sample ash, analytical values are reported on a whole-coal basis.

Standard coal analyses conducted on all bench and complete channel samples by the U.S. Department of Energy (DOE) include: 1) proximate analysis (moisture, volatile matter, fixed carbon, and ash); 2) ultimate analysis (hydrogen, carbon, nitrogen, sulfur, and oxygen); 3) calorific value (Btu/lb); 4) ash-initial deformation, softening, and fluid temperatures: 5) sulfur forms (sulfate, pyritic and organic); 6) free-swelling index; and 7) air dried weight loss. Results for all samples are shown in Appendix G. Summary statistics of USGS and DOE analytical data for all samples are presented in Appendix H. Appendix I lists fixed-carbon and calorific values calculated for ASTM rank determinations. The rank of the Upper Freeport coal bed throughout the study area is medium volatile bituminous.

Vertical and lateral variations of selected major, minor, and trace elements are illustrated graphically (figs. 20-29). The selection of elements was based on their potential deleterious effects on the environment. In this report, major elements are those present in concentrations greater than 1 wt. percent; minor elements range between 1 and 0.1 wt percent; and trace elements are those present in concentrations < 0.1 wt. percent. All elements for which data are displayed in figures 20-29 are trace elements except iron and sulfur which generally are major elements in the Upper Freeport coal of the Homer City reserve.

Table 17. Summary: Normalized Percent Major Oxides, by Facies

Facies	n	K	Al	Si	Ca	Fe	S	"R" (Mg, Na, Mn, Ti, P)
A	4	$\bar{x}$ = 2.3	23	61	0.77	9.4	0.88	2.7
A'	3	$\bar{x}$ = 3.4	27	57	1.0	6.8	1.3	3.0
B	7	$\bar{x}$ = 1.7	23	46	4.3	17.0	4.5	3.2
Part	3	$\bar{x}$ = 3.8	29	57	0.70	5.5	1.1	3.2
C	15	$\bar{x}$ = 1.3	21	32	5.4	32.0	5.3	2.4
D	14	$\bar{x}$ = 3.0	26	50	3.5	12.0	3.0	2.6
E	13	$\bar{x}$ = 3.5	29	49	1.9	11.0	2.0	2.9

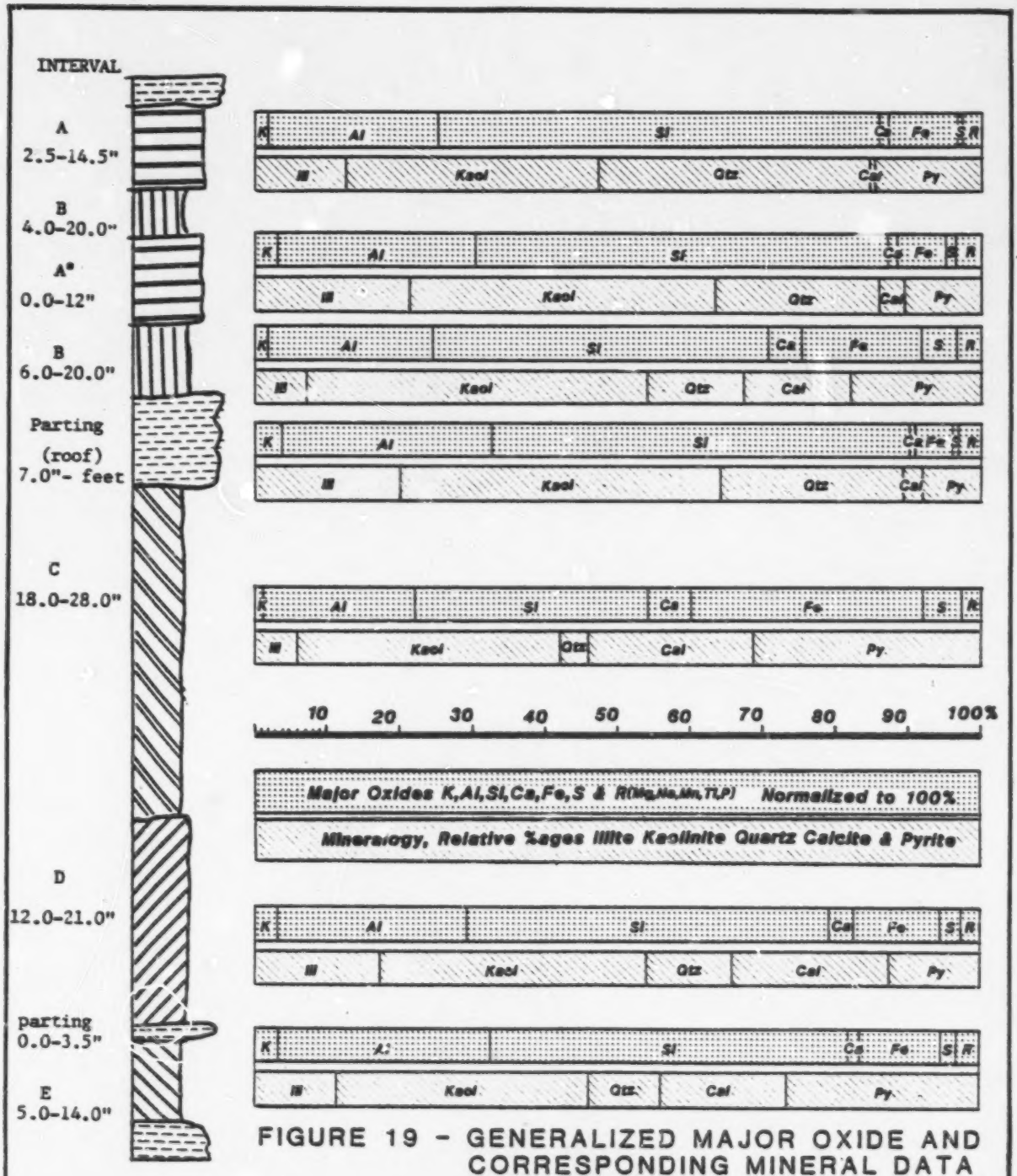

FIGURE 19 - GENERALIZED MAJOR OXIDE AND CORRESPONDING MINERAL DATA BY COAL FACIES

Quality of the coal generally decreases toward the top and bottom of the Upper Freeport coal bed ("contaminant" concentrations tend to increase toward the top and bottom of the bed, see figures 20-29 and Appendices F and G). For the selected elements considered in this report, the following generalizations can be drawn:

1. Arsenic--the concentration of this element appears to be greater in the upper facies (C) than in the middle (D) and lower (E) facies of the Homer City #1 mine (fig. 20). Systematic variations of arsenic are not distinct in the Lucerne #6 mine; however, the lower facies (D and E) tend to have the highest concentrations of arsenic in the southern part of the mine. In the northern part of Lucerne #6, this element tends to be enriched in both the top and bottom facies and is probably associated with pyrite. Anomalous values in HEL-3SMP, H2-3N, H2-3/2WM, and LUC-2N may be due to analytical error and/or real differences in the types of samples (bench-channel vs. complete channel).

2. Cadmium and zinc--the highest concentrations of these elements occur mainly in either the top or bottom benches in both mines (figs. 21 and 22). Cadmium correlates with zinc. This correlation is consistent with results reported by Ruch and others (1974) for other coal beds. Thus, cadmium is probably associated with sphalerite in the Upper Freeport study area and any preparation process which tends to concentrate zinc will also concentrate cadmium. This correlation has been verified using statistical analysis as well as the SEM and other analytical techniques.

3. Iron, pyritic sulfur and total sulfur--a strong correlation exists among iron, pyritic sulfur, and total sulfur values for all samples. The highest concentrations tend to be in the upper facies (figs. 23, 24, and 25). Maximum concentrations are associated with sandstone roof conditions or where the Mahoning Sandstone is within a few inches of the coal as determined from core data and field descriptions. The relationship between higher sulfur content and sandstone roof conditions is well known; however, the actual geologic and geochemical processes by which iron disulfides are enriched because of proximity to sandstone bodies may be related to differing geochemical gradients (see Interpretations and Conclusions).

4. Lead and selenium--much of the selenium may be associated with lead (see SEM discussion) as a lead selenide. These elements tend to be enriched in either the top or bottom facies (figs. 26 and 27). Selenium also occurs in pyrite.

5. Manganese--the greatest concentrations of this element are in the upper or lower facies (fig. 28). An analytical value which appears to be anomalous (H2-3/2WM-1.1) was cross checked with emission spectrographic data and found to be correct. The mineral associations of manganese are primarily in siderite and perhaps other carbonate minerals.

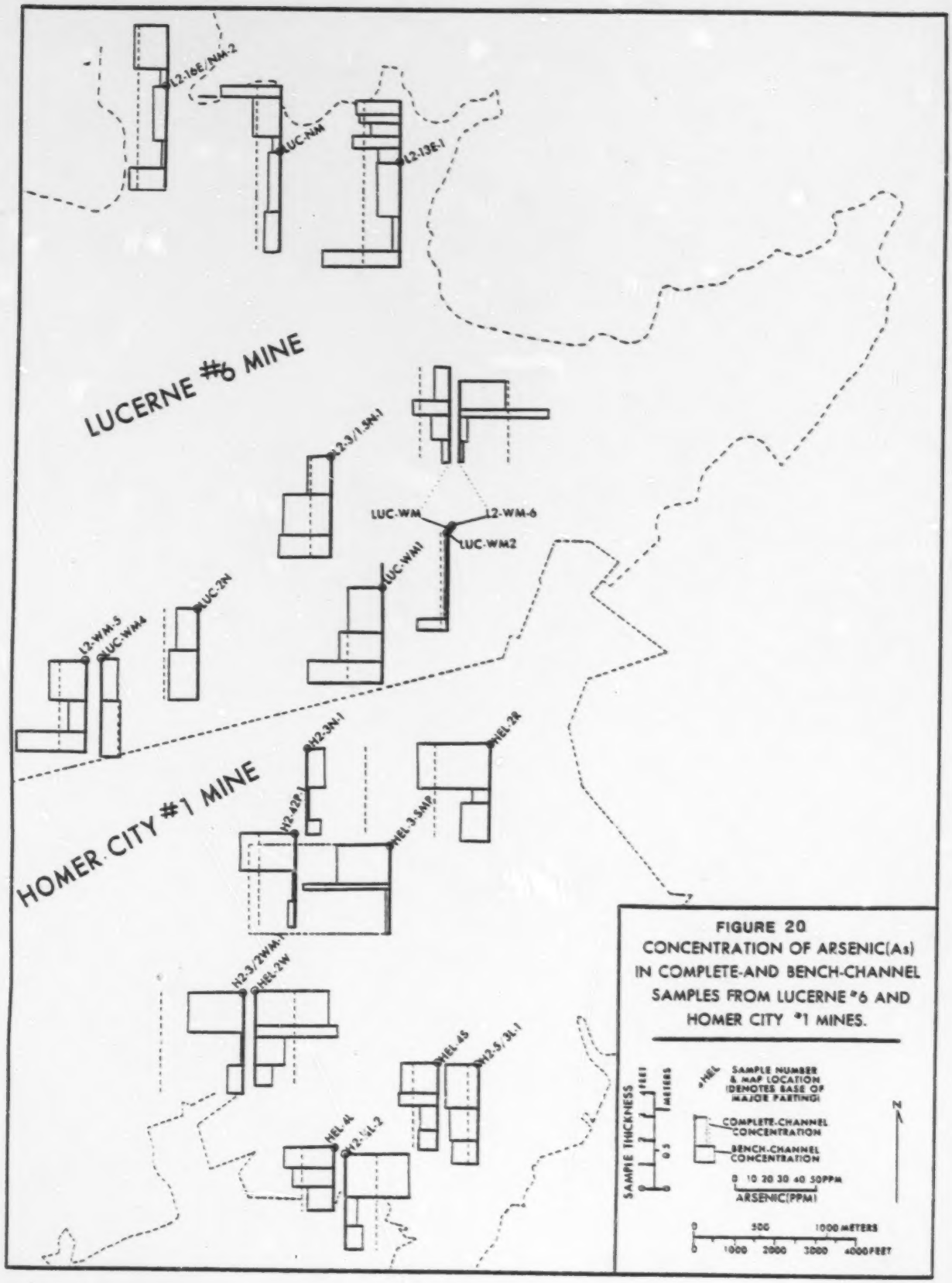

FIGURE 20
CONCENTRATION OF ARSENIC(As) IN COMPLETE-AND BENCH-CHANNEL SAMPLES FROM LUCERNE #6 AND HOMER CITY #1 MINES.

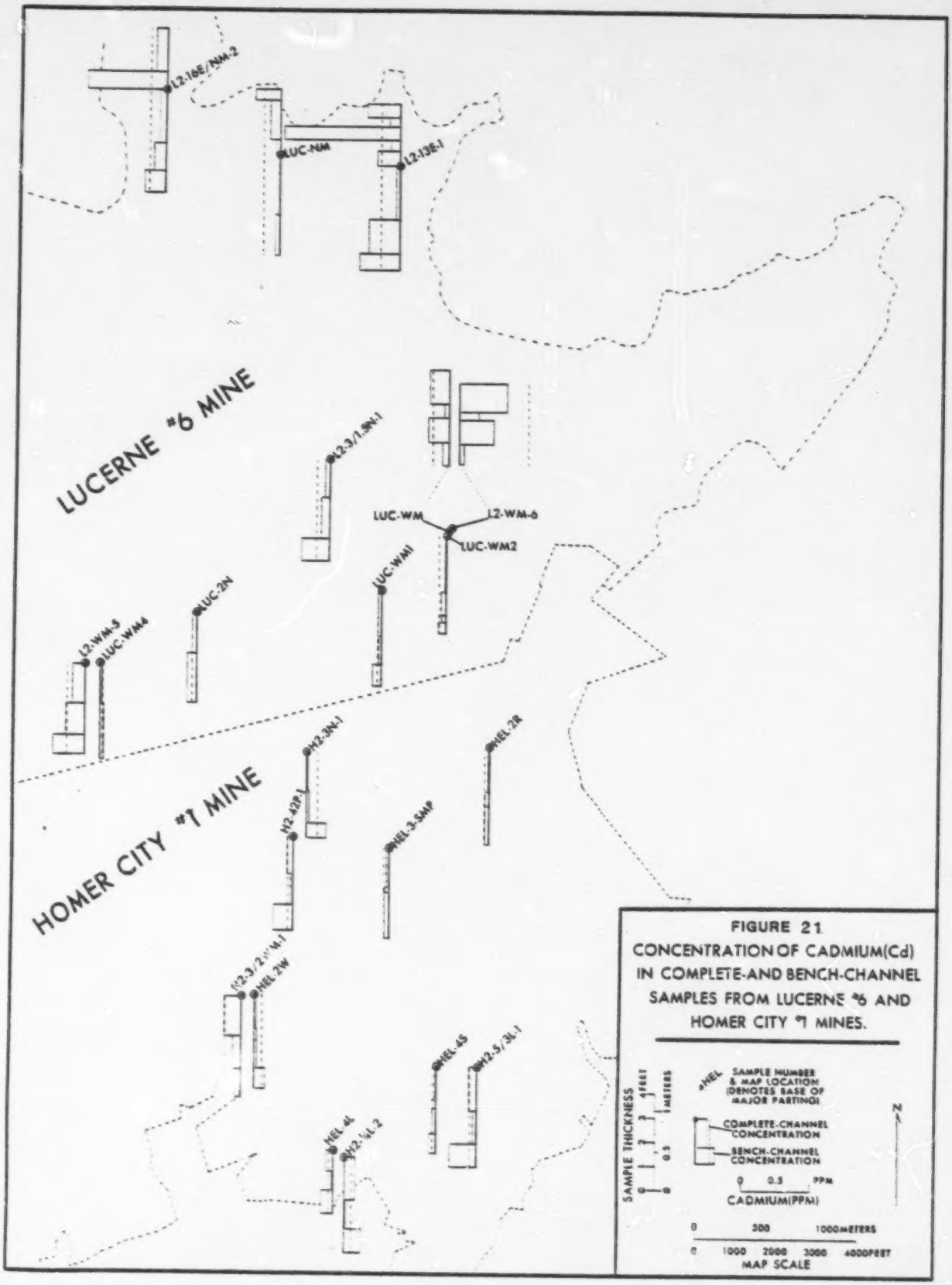

FIGURE 21
CONCENTRATION OF CADMIUM(Cd) IN COMPLETE-AND BENCH-CHANNEL SAMPLES FROM LUCERNE #6 AND HOMER CITY #1 MINES.

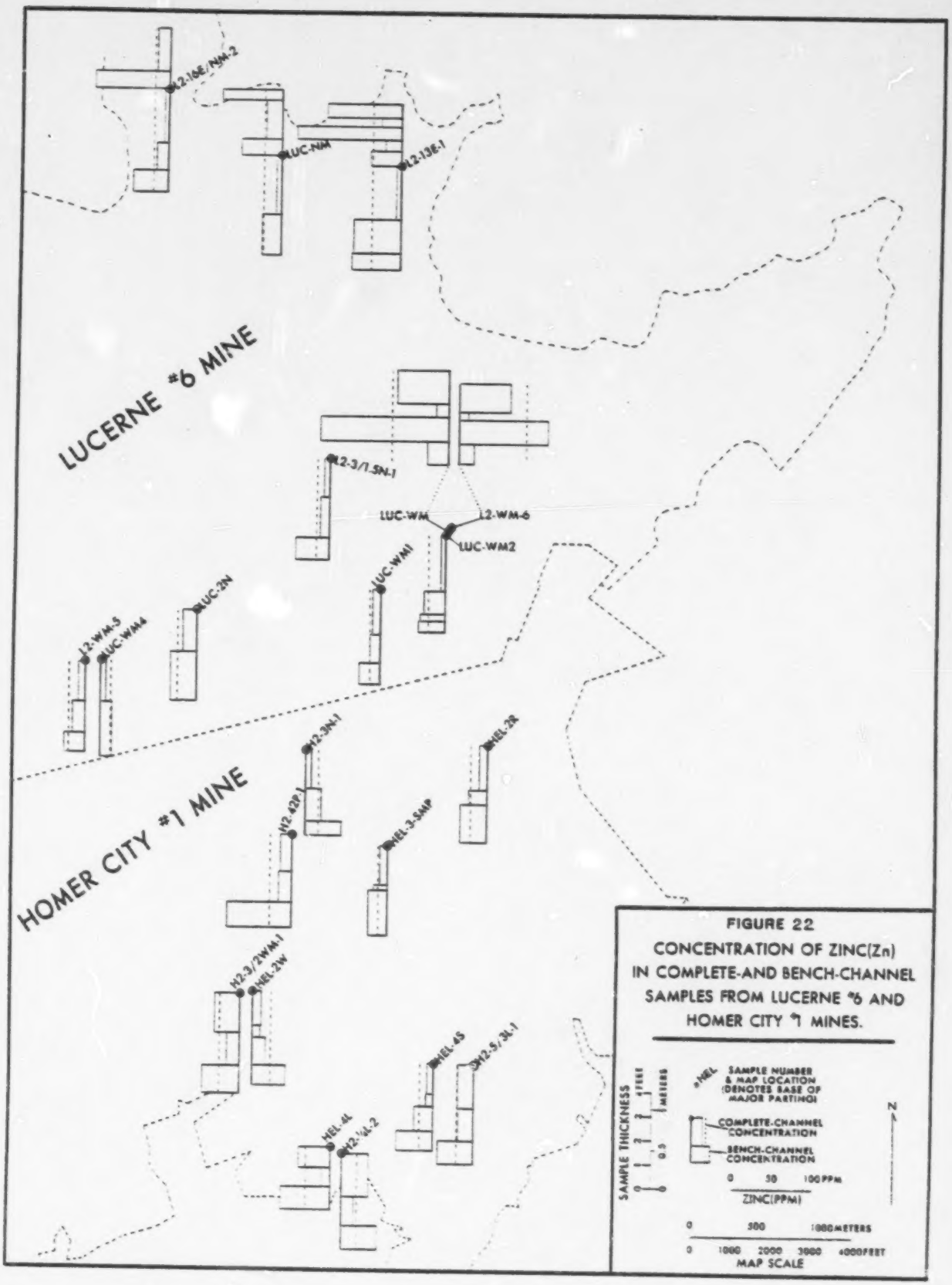

FIGURE 22

CONCENTRATION OF ZINC(Zn) IN COMPLETE-AND BENCH-CHANNEL SAMPLES FROM LUCERNE #6 AND HOMER CITY #1 MINES.

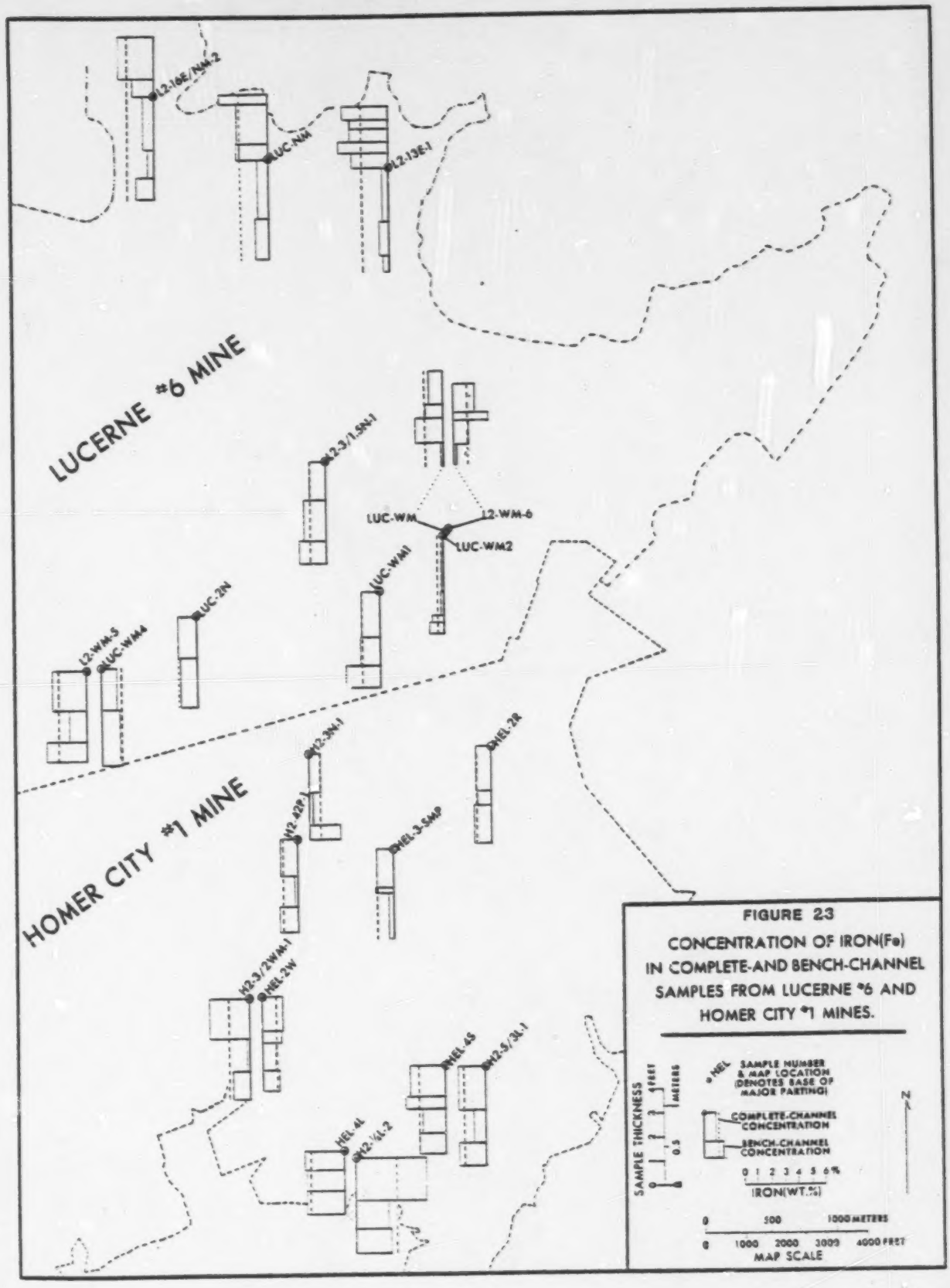
L2-16E/NM-2
LUC-NM
L2-13E-1
LUCERNE #6 MINE
L2-3/1.5N-1
LUC-WM
L2-WM-6
LUC-WM2
LUC-WM1
LUC-2N
L2-WM-5
LUC-WM4
HOMER CITY #1 MINE
H2-3N-1
H2-2P-1
HEL-2R
HEL-3-SMP
H2-3/2WM-1
HEL-2W
HEL-4S
H2-5/3L-1
HEL-4L
H2-4L-2
FIGURE 23
CONCENTRATION OF IRON(Fe) IN COMPLETE-AND BENCH-CHANNEL SAMPLES FROM LUCERNE #6 AND HOMER CITY #1 MINES.
SAMPLE THICKNESS
FEET
METERS
0.5
HEL
SAMPLE NUMBER & MAP LOCATION (DENOTES BASE OF MAJOR PARTING)
COMPLETE-CHANNEL CONCENTRATION
BENCH-CHANNEL CONCENTRATION
0 1 2 3 4 5 6%
IRON(WT.%)
N
0 500 1000 METERS
0 1000 2000 3000 4000 FEET
MAP SCALE

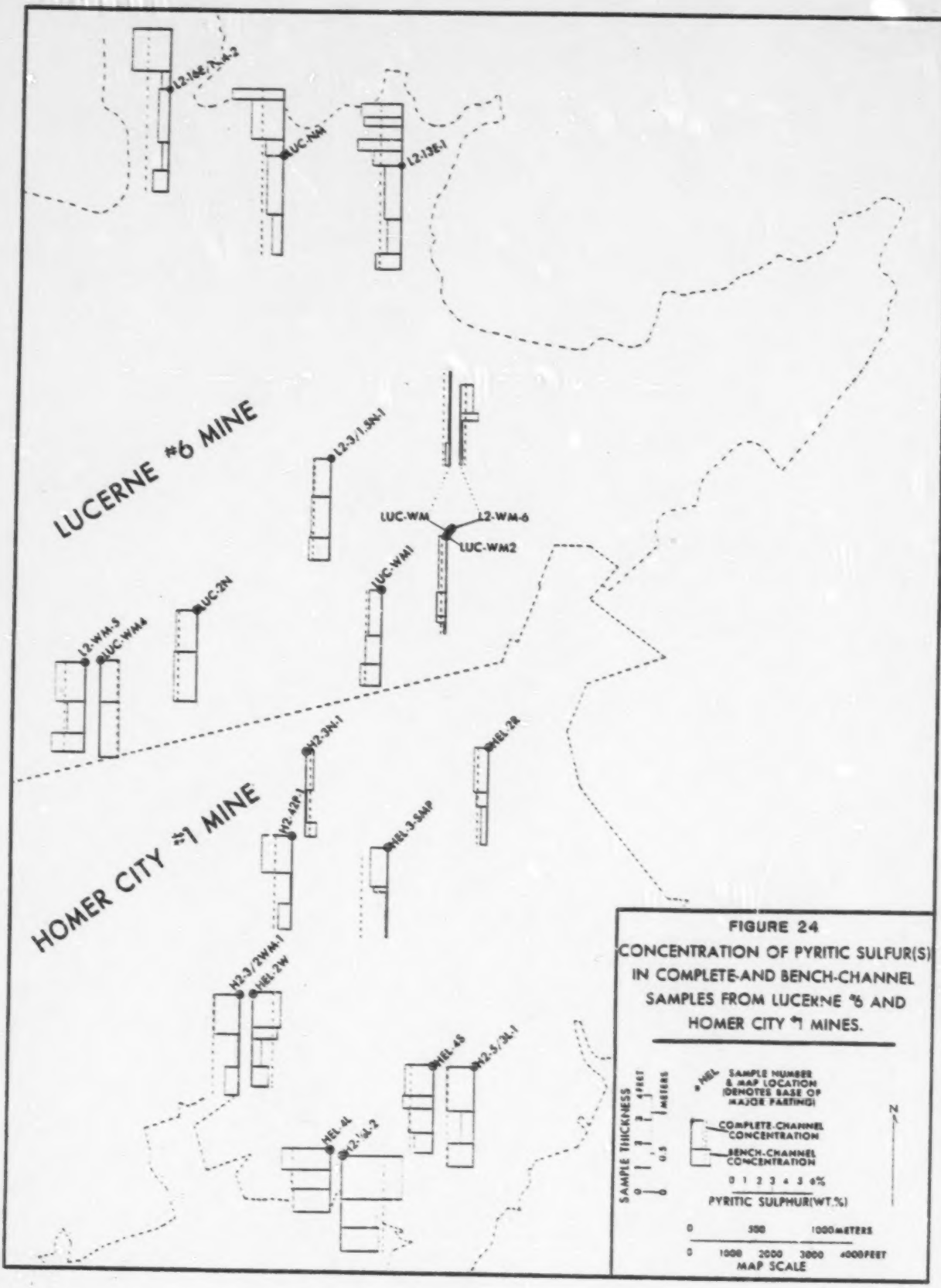
LUCERNE #6 MINE
HOMER CITY #1 MINE
L2-10E/2W-2
LUC-NW
L2-13E-1
L2-3/1.5N-1
LUC-WM
L2-WM-6
LUC-WM2
LUC-WM1
LUC-2N
L2-WM-5
LUC-WM4
H2-3N-1
H2-4SP-1
HEL-2R
HEL-3-SMP
H2-3/2WM-1
HEL-2W
HEL-4S
H2-5/3L-1
HEL-4L
H2-4L-2
FIGURE 24
CONCENTRATION OF PYRITIC SULFUR(S) IN COMPLETE-AND BENCH-CHANNEL SAMPLES FROM LUCERNE #6 AND HOMER CITY #1 MINES.
SAMPLE THICKNESS
FEET
METERS
SAMPLE NUMBER & MAP LOCATION (DENOTES BASE OF MAJOR PARTING)
COMPLETE-CHANNEL CONCENTRATION
BENCH-CHANNEL CONCENTRATION
PYRITIC SULPHUR(WT.%)
MAP SCALE
N

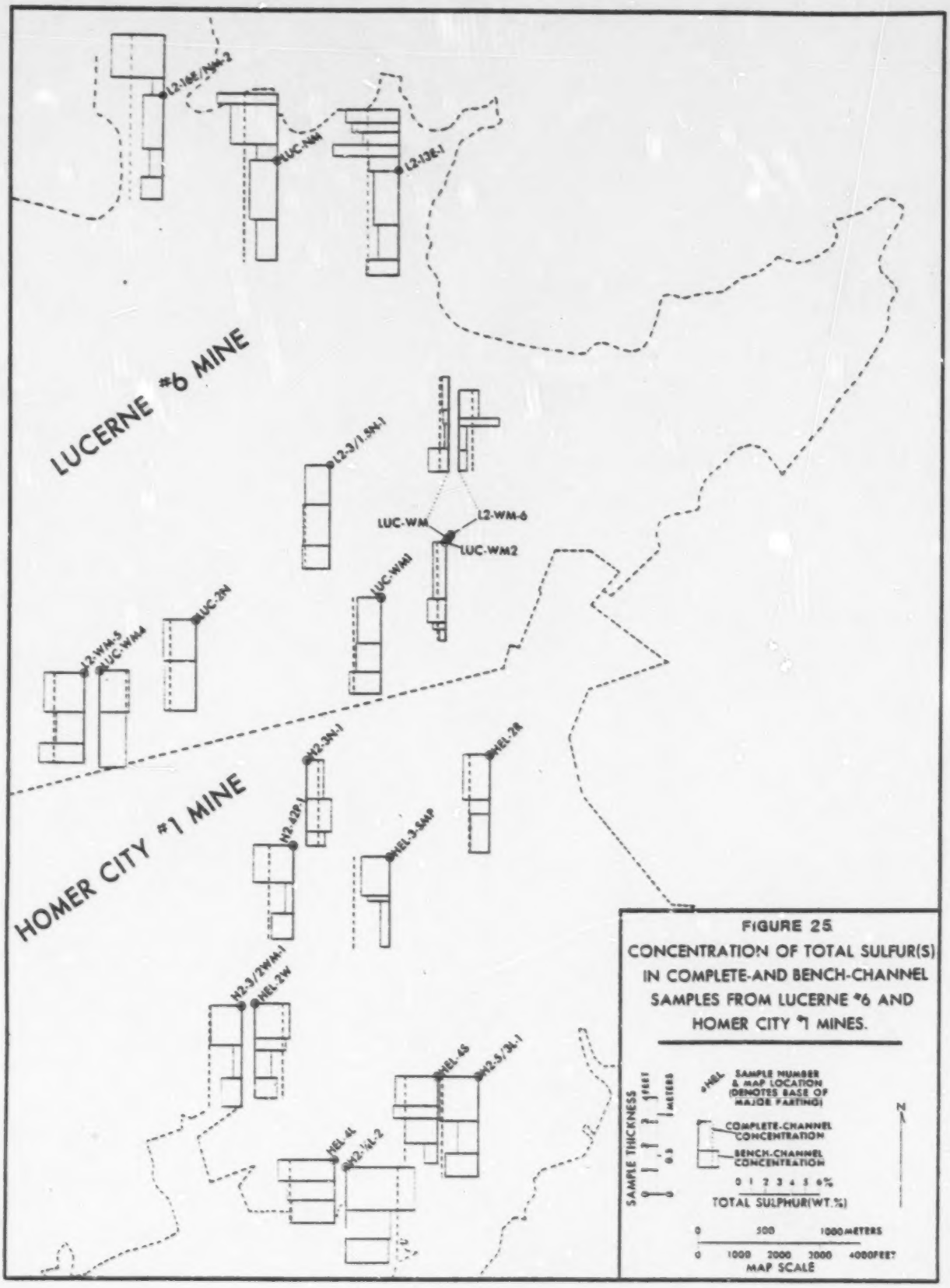

FIGURE 25
CONCENTRATION OF TOTAL SULFUR(S) IN COMPLETE-AND BENCH-CHANNEL SAMPLES FROM LUCERNE #6 AND HOMER CITY #1 MINES.

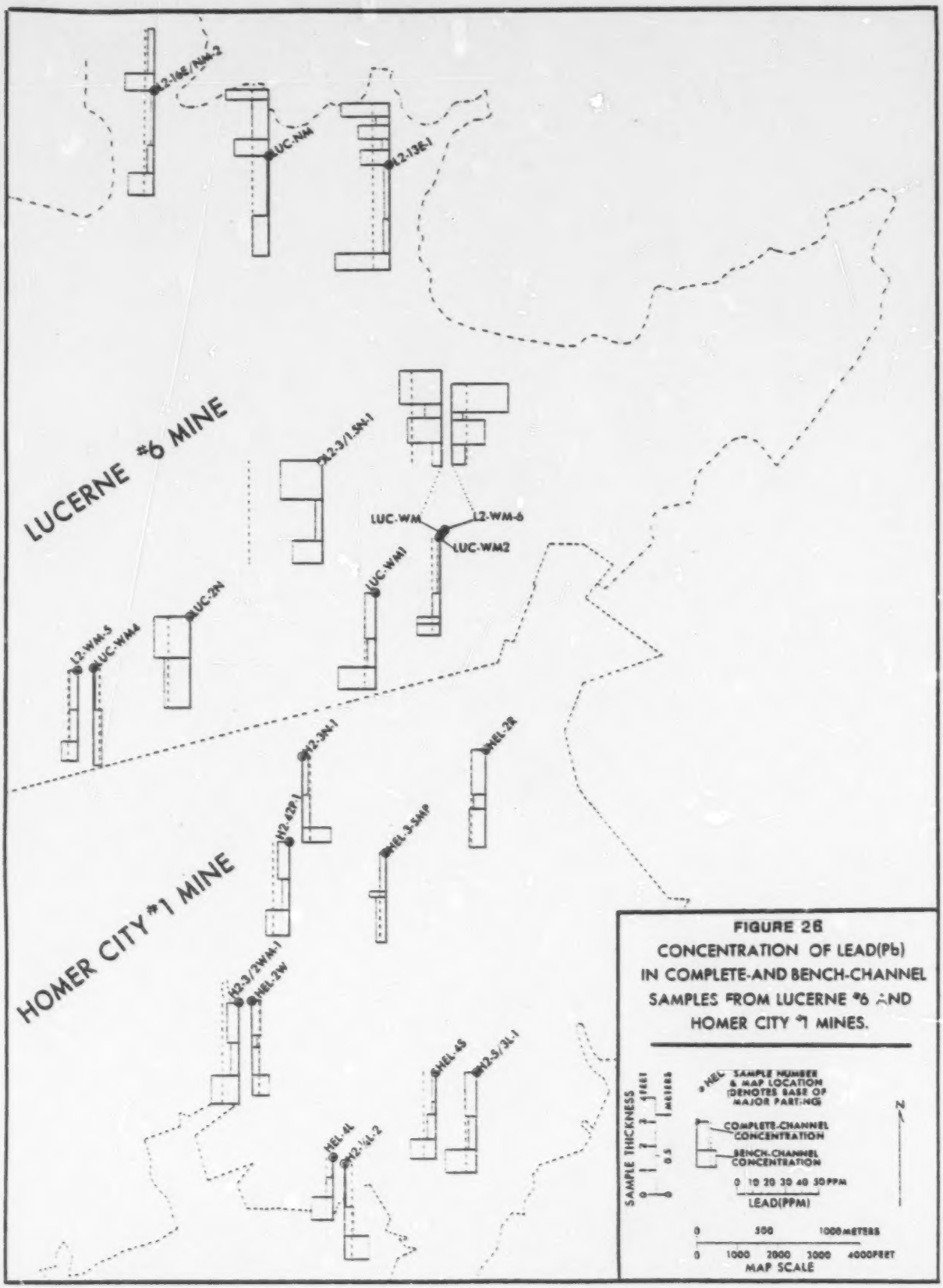

FIGURE 26
CONCENTRATION OF LEAD(Pb) IN COMPLETE-AND BENCH-CHANNEL SAMPLES FROM LUCERNE #6 AND HOMER CITY #1 MINES.

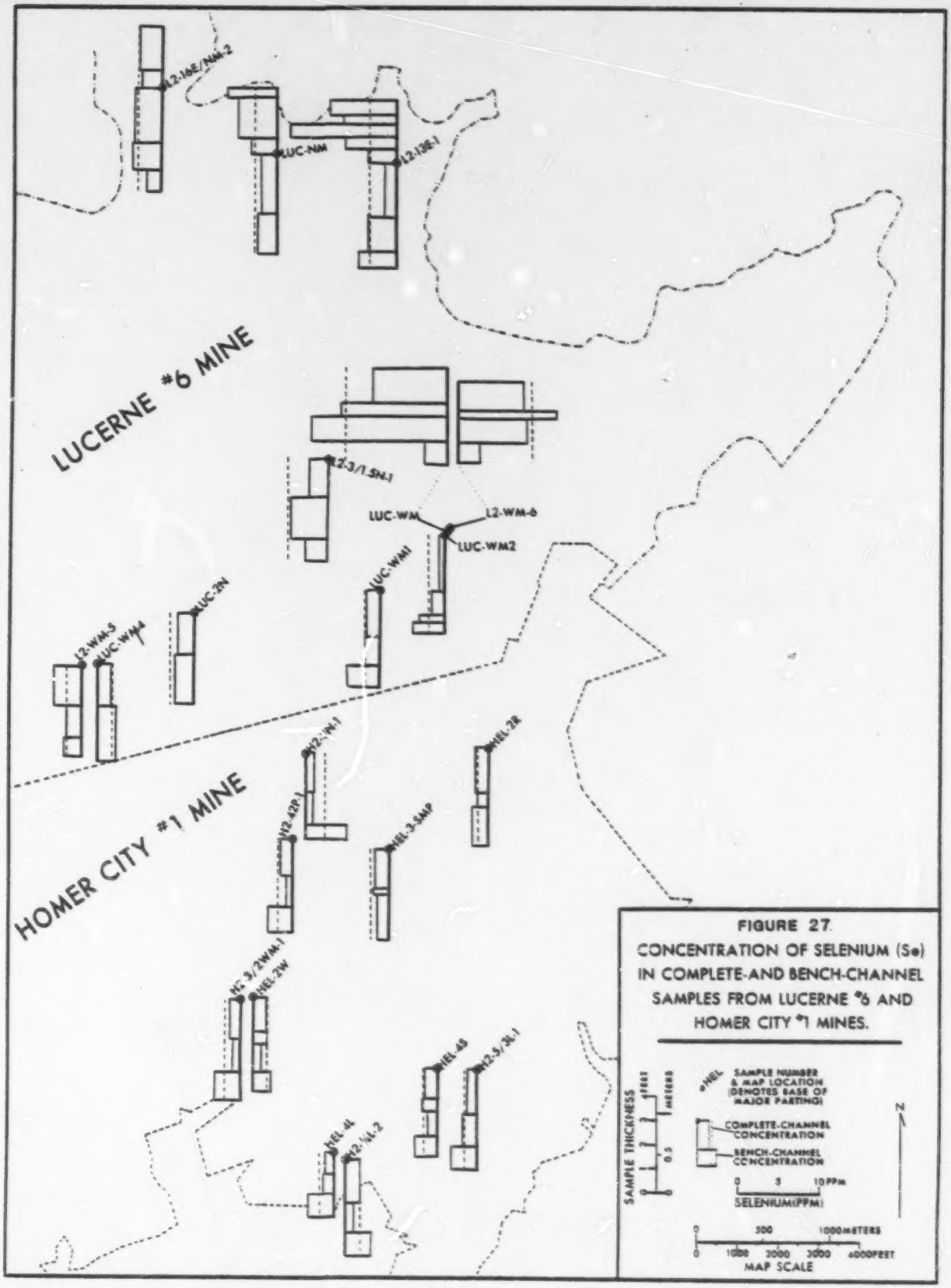

FIGURE 27.
CONCENTRATION OF SELENIUM (Se) IN COMPLETE-AND BENCH-CHANNEL SAMPLES FROM LUCERNE #6 AND HOMER CITY #1 MINES.

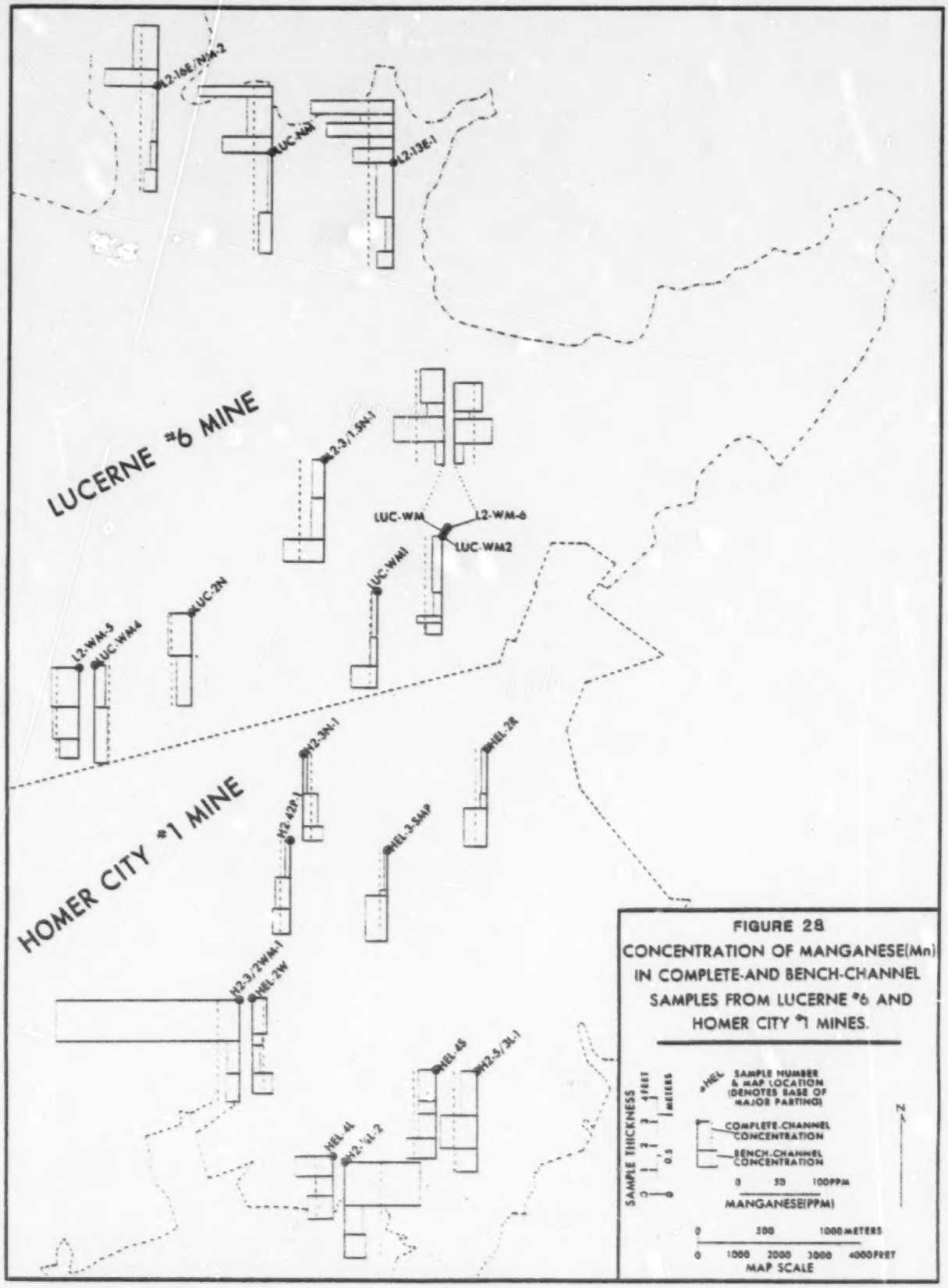

FIGURE 28
CONCENTRATION OF MANGANESE(Mn) IN COMPLETE-AND BENCH-CHANNEL SAMPLES FROM LUCERNE #6 AND HOMER CITY #1 MINES.

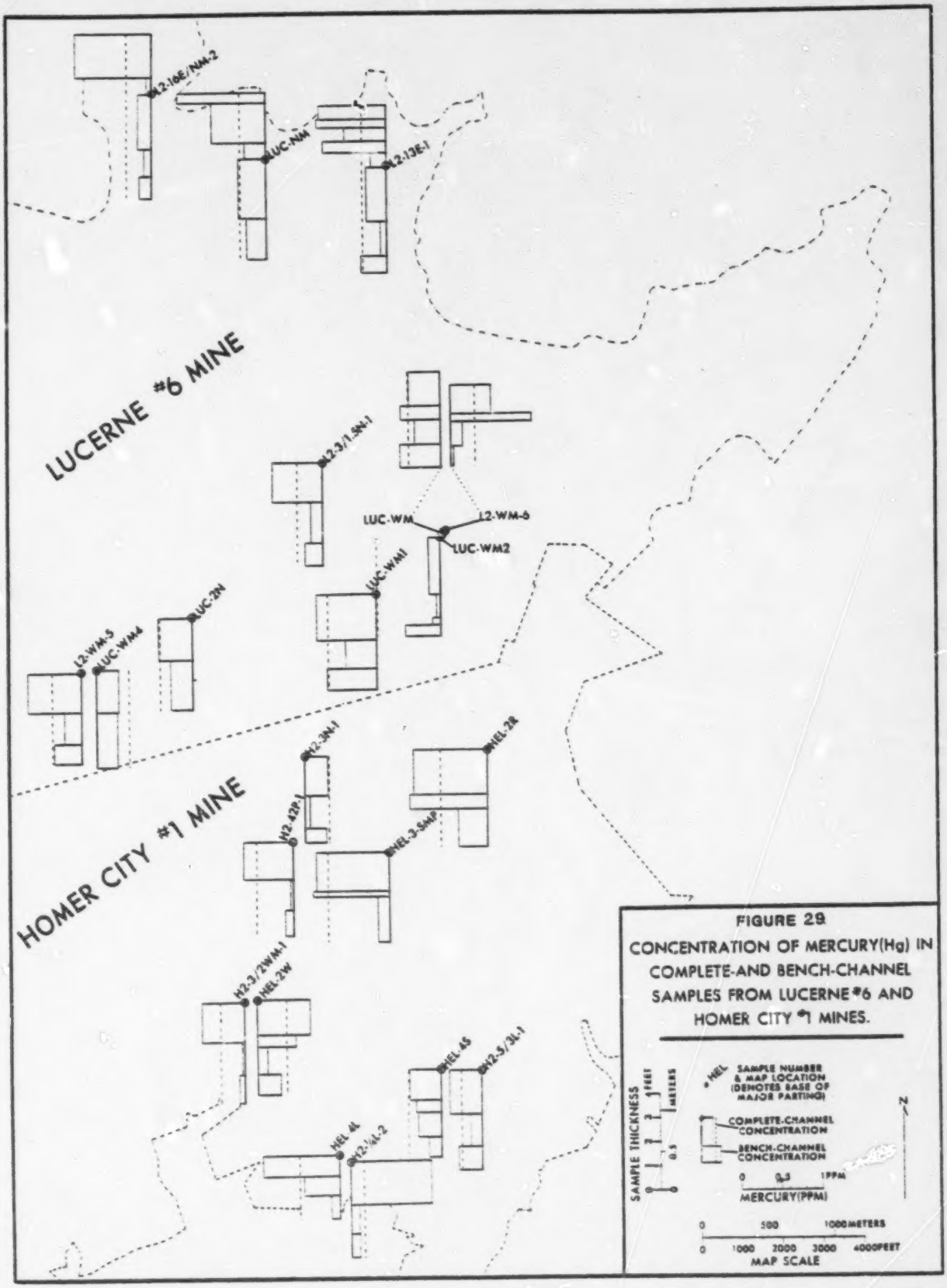

FIGURE 29

CONCENTRATION OF MERCURY(Hg) IN COMPLETE-AND BENCH-CHANNEL SAMPLES FROM LUCERNE #6 AND HOMER CITY #1 MINES.

6. Mercury--Mercury appears to be relatively enriched in the upper facies in both mines (fig. 29). Statistical analysis indicates that mercury is associated with pyrite. In the Phase I study, the mineral association of mercury is based on statistical analysis because this element's mineral associations probably cannot be detected in the whole coal using presently available analytical techniques.

Electron Microprobe Analysis

Relationships among selected elements, minerals, and macerals were investigated on three of the column samples (H2-42P, L2WM5, and L2-13E) by the electron microprobe technique. Complete column samples were collected from five of the sampling stations by E. C. T. Chao. Chao and his coworkers are conducting a companion study on oriented polished blocks using various techniques including electron microprobe analysis.

Results of the electron microprobe analyses completed thus far are summarized as follows:

1) On the basis of statistical analysis of chemical data, arsenic is correlated with pyritic sulfur. Chemical analyses of the coal facies also indicate that both arsenic and pyritic sulfur tend to be concentrated in the top and bottom facies of the bed (figs. 20 and 24). Electron microprobe and SEM analyses of samples having relatively high arsenic content (>50 PPM, whole-coal basis) indicate that arsenic is primarily associated with pyrite. Arsenic tends to be concentrated in outer rims of pyrite grains or along fractures in pyrite (Minkin and others, 1979b). The arsenic is mainly associated with pyrite types that are susceptible to removal from the coal by physical coal preparation.

2) Statistical analysis of the chemical and maceral data indicates a relationship of chlorine to the organic phases of the coal. Electron microprobe analysis of polished blocks confirms that chlorine is bonded organically because this element was not detected in association with any cations (Minkin and others, 1979a). From the chemical and electron microprobe data, we know that chlorine concentrations are lower in the macerals of the partings, bone, and cannel coal than in the macerals of the banded coal. There is no apparent systematic variation in chlorine concentrations of coal facies B, C, D, and E.

3) Electron microprobe determinations of organic sulfur agree with organic sulfur determinations made by conventional methods (Minkin and others, 1979a). Microprobe determinations indicate that organic sulfur concentrations are greater in vitrinite and exinite than in inertinite. There tends to be a slight increase in organic sulfur in vitrinite from the top to the bottom of the bed from approximately 0.5 to 0.6 wt. percent.

STATISTICAL ANALYSIS OF ANALYTICAL DATA

The range of types and units of measurement for the 96 samples collected for this study necessitated the use of a statistical technique that would elucidate relationships among the measurements. For each sample, 148 parameters were measured: 74 chemical variables, 18 ultimate and proximate analysis parameters, 35 petrographic variables and 21 LTA and XRD measurements. The units of measurements include parts per million relative percent, and absolute values of calorific value, temperature, and intensity. Both parametric and nonparametric correlation techniques were investigated.

Only nonparametric statistical tests are applicable to data measured on either a nominal or an ordinal scale. Both parametric and nonparametric methods may be applied to data on an interval or ratio scale of measurement (ratio data is not the same as data on a ratio scale of measurement). Discussions of measurement scales may be found in Griffiths (1967), Siegel (1956), and Gibbons (1976). Interval and ratio data may be analyzed with parametric methods if the assumptions of the parametric statistical model are met. The conditions of classical parametric statistics require that 1) independent data must be measured on at least an interval scale, 2) the observations must be drawn from normally distributed populations, and 3) the populations must be homoscedastic or have a known ratio of variances. Commonly, these conditions are assumed; however, their truth or falsity determines the meaningfulness of the significance of the probability statement (accept or reject H_o) arrived at by the parametric statistical test. We believe that even if slight deviations from these conditions exist within the data, the application of parametric statistics still will be valid. However, there is no general agreement as to what constitutes a "slight" deviation.

A nonparametric statistical model does not require conditions about the parameters of the populations from which the observations are drawn. The assumptions that are associated with nonparametric statistical tests are 1) that the samples are independent and 2) that each variable is continuous. The accuracy of the probability statement arrived at by nonparametric methods does not depend on the distribution of the population, hence the term "distribution free statistics" is often applied to nonparametric methods. Initial histogram plots, utilizing 15 intervals within the range, showed that much of the elemental data appeared to be non-normally distributed and appeared to be lognormally distributed with a larger percentage of values skewed toward the lower end. This distribution is not unexpected because most geochemical data approach, to some degree, a lognormal model (Tennant and White, 1959; Hawks and Webb, 1962; and Sinclair, 1974).

Both the parametric Pearsons Product Moment and the nonparametric Spearman Rank correlation coefficients were determined on all the data. However, the assumptions required for the parametric test are unlikely to be satisfied, as they would have to be based on the minimum possible number of verifiable assumptions; thus, the most logical method of determining associations among data of this study utilizes the nonparametric Spearman Rank correlation coefficient. In the broadest sense, the interpretations of the results are essentially the same regardless of the statistical model. By way of an example, both parametric and nonparametric correlation statistics for ash values are summarized below (data is from Appendix J, table 1, $n = 96$):

	Nonparametric Spearman Rank	Parametric Parsons Product Moment
LTA vs. 550° ash	r_s = .968	r = .961
	z = 9.44	Y = -.045 + .883 (LTA)
LTA vs. 750° ash	r_s = .975	r = .974
	z = 9.50	Y = -.024 + .848 (LTA)
550° ash vs. 750° ash	r_s = .985	r = .994
	z = 9.60	Y = .015 + .968 (550°)

In all cases, the z-values and correlation coefficients are significant at the 99-percent level, and are in good agreement with one another. The strongest association is between the two high temperature ash values.

Detailed comparisons and explanation on the differences and similarities as well as the advantages and disadvantages of parametric and nonparametric statistics are found in both Gibbons (1976) and Siegel (1956).

Using the data from bench-channel samples (n = 75), a matrix consisting of 1) X-ray mineralogy data, 2) maceral concentrations (whole-coal and mineral-matter-matter-free basis), 3) percent major oxides (determined on USGS 550°C ash), 4) percent sulfur, 5) percent carbon, and 6) calorific value was assembled to determine the associations by the Spearman Rank correlation statistical model. The X-ray mineralogy data for each sample consisted of 1) the measured maximum intensity minus background for each of the five major components (illite 10 Å, kaolinite 7Å, quartz 4.26Å, calcite 3.03Å, and pyrite 2.71Å), 2) the calculated relative percent for each component, 3) the calculated relative percent for each component on a whole coal basis, 4) the sum of the measured intensity for the five components, 5) the percent low temperature ash (LTA), and 6) the clay ratios calculated from maximum intensity as well as integrated intensity (area). The significant (95%) positive correlation z-value matrix is reproduced in Appendix J, table 2. The results of the statistical correlation reveal the following associations (fig. 30): 1) The clays (illite and kaolinite) are related to Si, Al, Mg, and K as well as vitrinite, vitrodetrinite, inertrodetrinite, fusinite, semifusinite and macrinite; the clays are not associated with the exinites. 2) Quartz is correlated with Si, Al, Mg, and K and is strongly associated with the inertinites and the clays. 3) Pyrite is associated with C, S, Ca, Fe, and Na as well as all the exinites. 4) Calcite is associated with the calorific value and S, Ca, and Fe and is not associated with any macerals. 5) Ca as CaO is associated with sporinite and micrinite.

Correlations among 127 variables include the standard U.S. DOE coal analyses, 73 elements, and coal macerals (Appendix J, tables 3-7). Presentation of the statistical analysis of the data utilizes the nonparametric model. Spearman Rank correlation coefficients were determined for different groupings of the samples and are given in Appendix J. The groupings included 1) all 75 bench-channel samples (bcs); 2) bcs with Btu greater than 12,000 and ash 10 percent or less (n = 46); 3) all bcs from coal facies C, D, and E (n = 37); 4) samples without partings (n = 53); and 5) samples with partings (n = 22). Correlation coefficients were determined with the elemental data on an ash basis as well as on a whole coal basis for each of the different groupings and are presented on the latter basis.

The parameters that were positively correlated at the 95% confidence level are divisible into two groups (table 18). Group I consists of elements, minerals, and macerals that correlate with ash, SiO_2, and Al_2O_3 contents. Group II consists of elements, minerals, and macerals that correlate positively with sulfur. The two distinct groups of elements, minerals, and macerals are probably related to processes by which the elements were incorporated during the peat stage of coal formation.

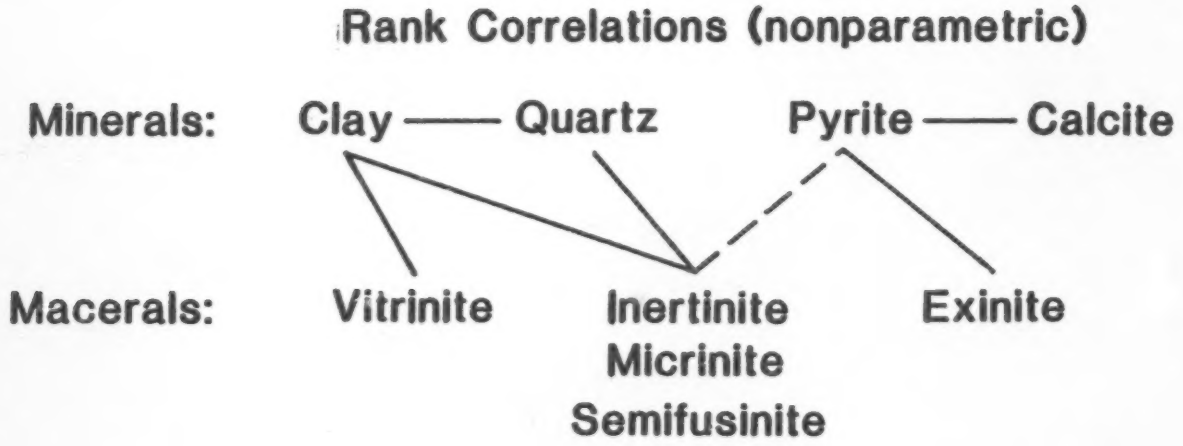

Figure 30. Mineral and maceral statistical associations

Table 18. Grouping of elements, minerals, and macerals based on nonparametric associations.

	Group I			Group II
Macerals	Vitrinite Fusinite Semifusinite			Sporinite Micrinite
Elements, Oxides, and Sulfur forms	SiO_2	Eu	Sb	CaO
	Al_2O_3	F	Sc	Pyritic Sulfur
	MgO	Ga	Se	Total Sulfur
	Na_2O	Gd	Sm	Organic Sulfur
	K_2O	Hf	Sn	Fe_2O_3
	TiO_2	La	Tb	As
	B	Li	U	Ge
	Ba	Lu	V	Hg
	Be	Nb	Y	
	Cd	Nd	Yb	
	Ce	Ni	Zn	
	Cr	Pb	Zr	
	Cs	Rb		
	Cu			
Minerals	Quartz Illite Kaolinite			Pyrite Calcite

INTERPRETATIONS AND CONCLUSIONS

SEDIMENTATION AND PEAT ACCUMULATION

Figure 31 illustrates interpreted depositional settings of rocks associated with the Upper Freeport coal bed. The ancestral peat of the Upper Freeport coal began to form (E facies) on a broad flat surface of the Upper Freeport "limestone." The Upper Freeport limestone had been lithified and subaerially exposed prior to peat formation as indicated by extensive brecciation, subaerial crusts, and the formation of a microkarst surface. In some areas, clastic sediments were deposited on the microkarst surface probably in topographic lows by small streams and/or in sloughs. Following deposition of the clastic material, peat began to accumulate over the entire Homer City study area and beyond. "Normal" peat accumulation was disrupted and the material that now constitutes a thin parting and bone coal layer (0 to 7 cm) accumulated at the top of the E facies, as a mixture of organic attritus and mineral matter. Variation in thickness of the parting and bone coal layer may be related to topographic highs and lows in the peatforming environment. The organic attritus and mineral matter accumulated in drowned topographic lows. Variations in thickness of the E coal facies underlying the parting support this interpretation although the available data are inconclusive. "Normal" peat accumulation continued in areas that were topographically high, perhaps as peat islands.

The Upper Freeport limestone and associated sediments may have indirectly influenced mineral-matter concentrations in the Upper Freeport coal bed, particularly during the early stages of peat accumulation. Acid water generated during peat formation may have been neutralized or partially neutralized by dissolved calcium carbonate species derived from the underlying limestone horizon. This neutralization may have 1) fixed calcium in the peat, 2) allowed sulfate-reducing bacteria to function, and 3) limited the amount of leaching of those elements whose solubility is increased under acid conditions.

Facies C and D resulted from peat that accumulated under conditions of occasional subaerial exposure as indicated by relatively abundant fusinite and semifusinite. These two coal macerals are generally believed to be the product of carbonization probably resulting from fires during the peat stage of coal formation. Carbonization and/or oxidation have the effects of 1) concentrating mineral matter giving rise to "mineral charcoal" bands and 2) creating neutral to alkaline micro-chemical environments through hydrolysis of the alkaline earth ions. Such conditions associated with fusain bands may be favorable for pyrite formation. The pyrite-rich fusain bands of facies C probably formed as a result of these favorable geochemical conditions. Because of the relatively large particle size, most pyrite formed under these conditions can be removed by coal preparation techniques. Deposition of the ancestral peat of facies C was terminated by drowning and the formation of a large lake or slough which had an influx of clay and silt. The clay and silt became the roof "shale" of the Helen mine and part of the Lucerne #6 mine where only C, D, and E facies are present. The shale is present as a parting which thins and contains progressively more organic matter away from the edge of the A, A', and B facies (fig. 31).

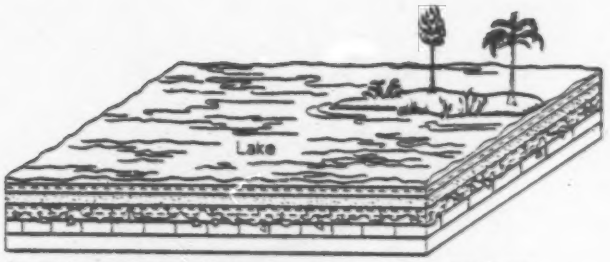

Stage 4. Secession of peat accumulation (coal facies E) and deposition of shale parting and bone coal

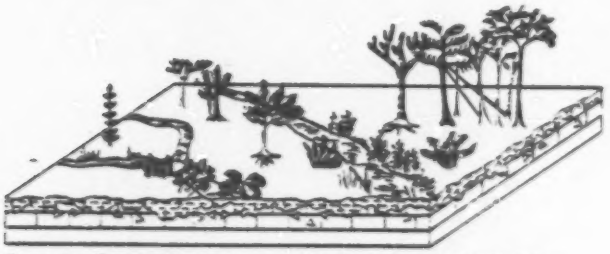

Stage 3. Deposition of clay and silt—formation of microkarst surface; incipient peat accumulation

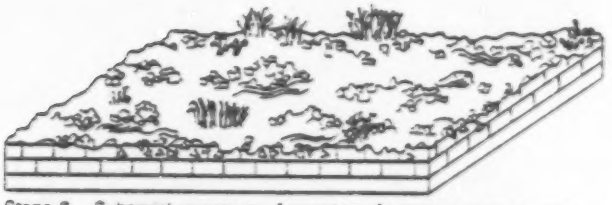

Stage 2. Subaerial exposure—formation of microkarst topography, limestone brecciation, and flint clay development

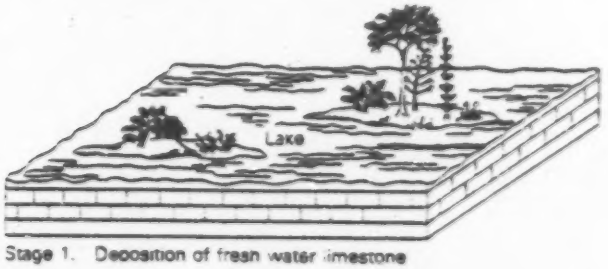

Stage 1. Deposition of fresh water limestone

FIGURE 31 - 'NTERPRETED DEPOSITIONAL SETTINGS OF ROCKS ASSOCIATED WITH THE UPPER FREEPORT COAL BED, PHASE I STUDY AREA.

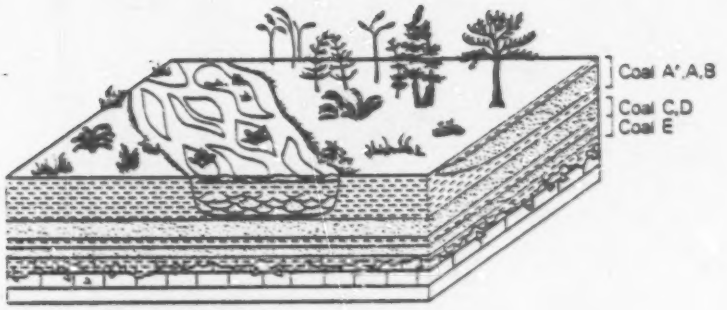

Stage 8. Fluvial progradation

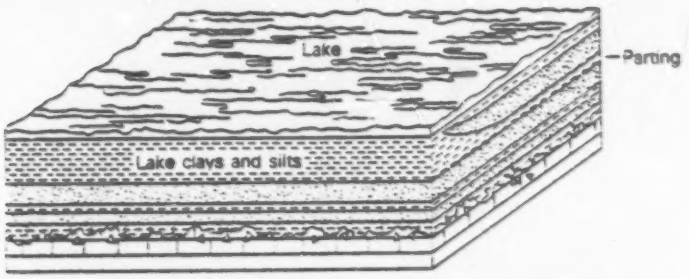

Stage 7. Flooding, clay-silt deposition

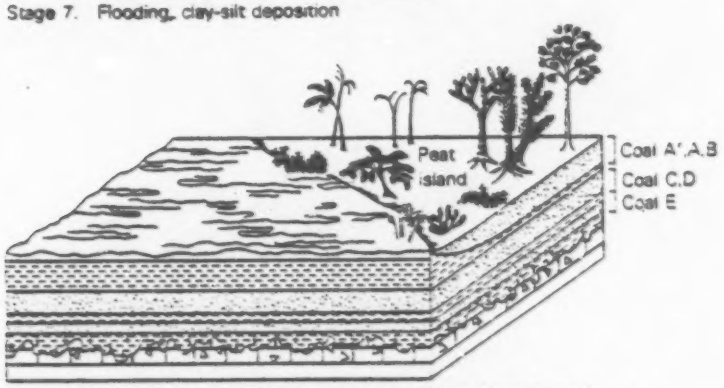

Stage 6. Formation of peat island, deposition of peat (coal facies A, A', and B)

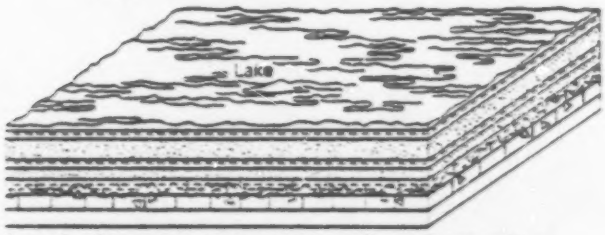

Stage 5. Deposition of peat (coal facies D and C) followed by flooding and deposition of clay and silt

FIGURE 31 (continued)

Facies B represents a resumption of peat deposition in the form of a peat island probably on a topographic high. Marginal to the island, silt and clay continued to accumulate as lake sediments. Coal type A' is probably a result of partial drowning of the island which was followed by resumption of deposition of B facies.

Coal facies A probably resulted from drowning of the peat island and a high degree of peat degradation with subsequent mixing of attrital organic debris and mineral matter. This was the final phase of peat deposition during Upper Freeport time.

As a result of drowning, peat deposition was terminated and clay and silt were deposited over the entire area in a lacustrine environment. Sand and associated sediments of the Mahoning sandstone interval were then deposited as part of an alluvial sequence that prograded over the lacustrine clays and silts. In some areas, scour of the previously deposited silt and clay occurred, and sand was deposited directly on the peat. At these locations, the upper part of the peat was enriched in sulfur.

Stratigraphic cross sections (based on core data), illustrating vertical and lateral lithologic changes within the Lucerne No. 6 and Homer City No. 1 mine area have been constructed (Stanton and Cecil, unpub. data, 1981). In addition, lithologic maps were drawn at 5-foot increments starting at 5 feet above the top of the C facies (fig. 32). Figure 33 is an isopach map of the shale above the coal bed. From the diagrams, cross sections, and descriptions from surface exposures, we interpret the Mahoning sandstone interval above the Upper Freeport coal bed as a braided stream depositional environment. This interpretation is favored over other types of sands depositional systems because: 1) there is no evidence to suggest deposition in a coastal marine environment such as barrier bars of tidal channels; 2) there are few if any point bars, cut and fill channel features, crevasse splays, or levee deposits typical of a meandering stream system; 3) there is little or no evidence to suggest distributary channel systems of a lower delta plain; and 4) internal structures such as large-scale cross stratification, small-scale cross stratification, horizontal stratification, and parallel stratification typical of a braided stream environment as described by Coleman (1969) are common. Furthermore, we believe the overall geometry of the sandstones of the Mahoning interval is highly consistent with the geometry to be expected from a migrating braided stream system or systems. The braided stream interpretation is preliminary in nature, and data on a regional model are currently being compiled for consideration in Phase III of the study.

ORIGIN OF MINERAL MATTER IN THE COAL

The primary objective of Phase I of the Upper Freeport coal bed study was to determine the geologic factors that control the origin, concentrations, and variability of mineral matter in coal. During the peat stage of coal formation, mineral matter may be derived from 1) inherent plant ash, 2) detrital minerals that were washed or blown into the peat-forming environment, 3) sorption of ions in solution on surfaces of peat particles, and 4) precipitation from solution by chemical and/or

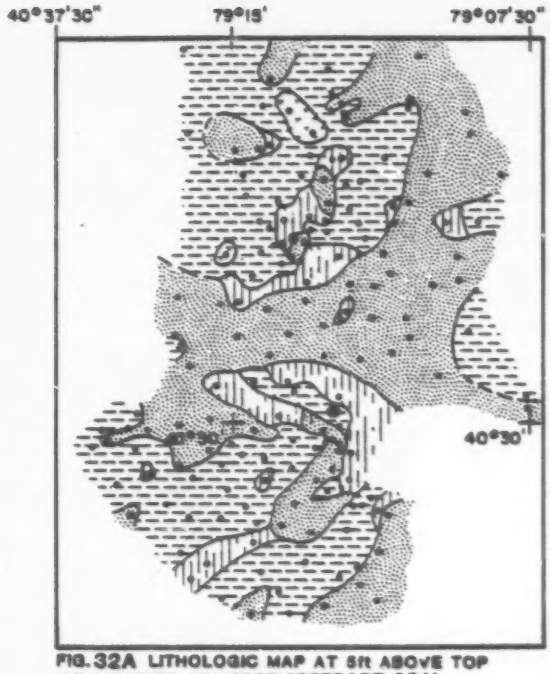

FIG. 32A LITHOLOGIC MAP AT 5ft ABOVE TOP OF C FACIES OF UPPER FREEPORT COAL

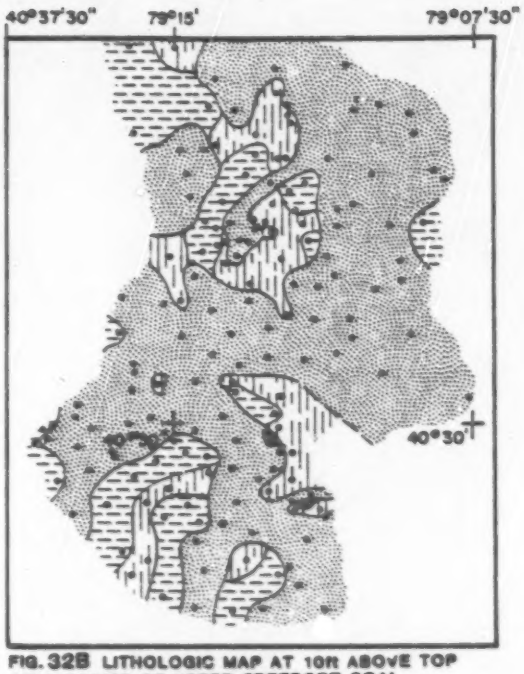

FIG. 32B LITHOLOGIC MAP AT 10ft ABOVE TOP OF C FACIES OF UPPER FREEPORT COAL

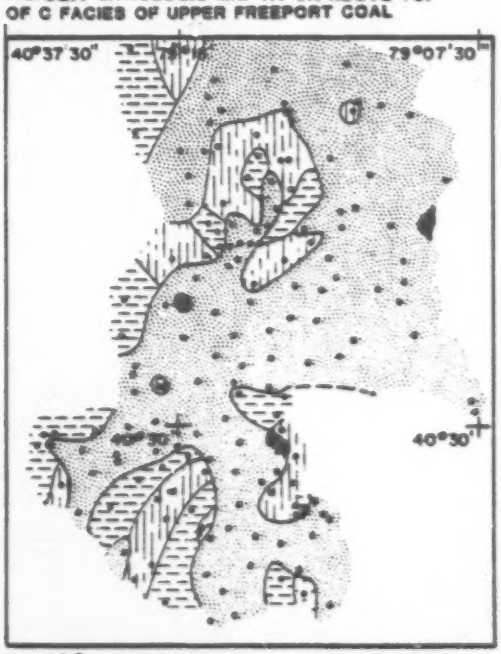

FIG. 32C LITHOLOGIC MAP AT 15ft ABOVE TOP OF C FACIES OF UPPER FREEPORT COAL

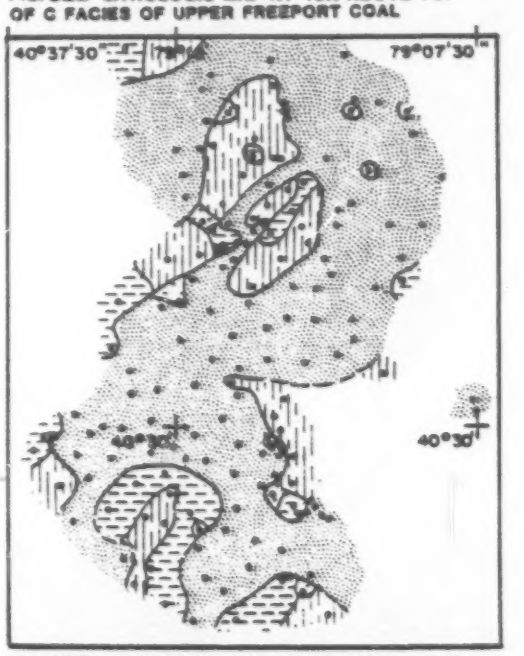

FIG. 32D LITHOLOGIC MAP AT 20ft ABOVE TOP OF C FACIES OF UPPER FREEPORT COAL

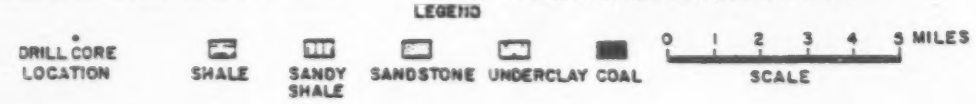

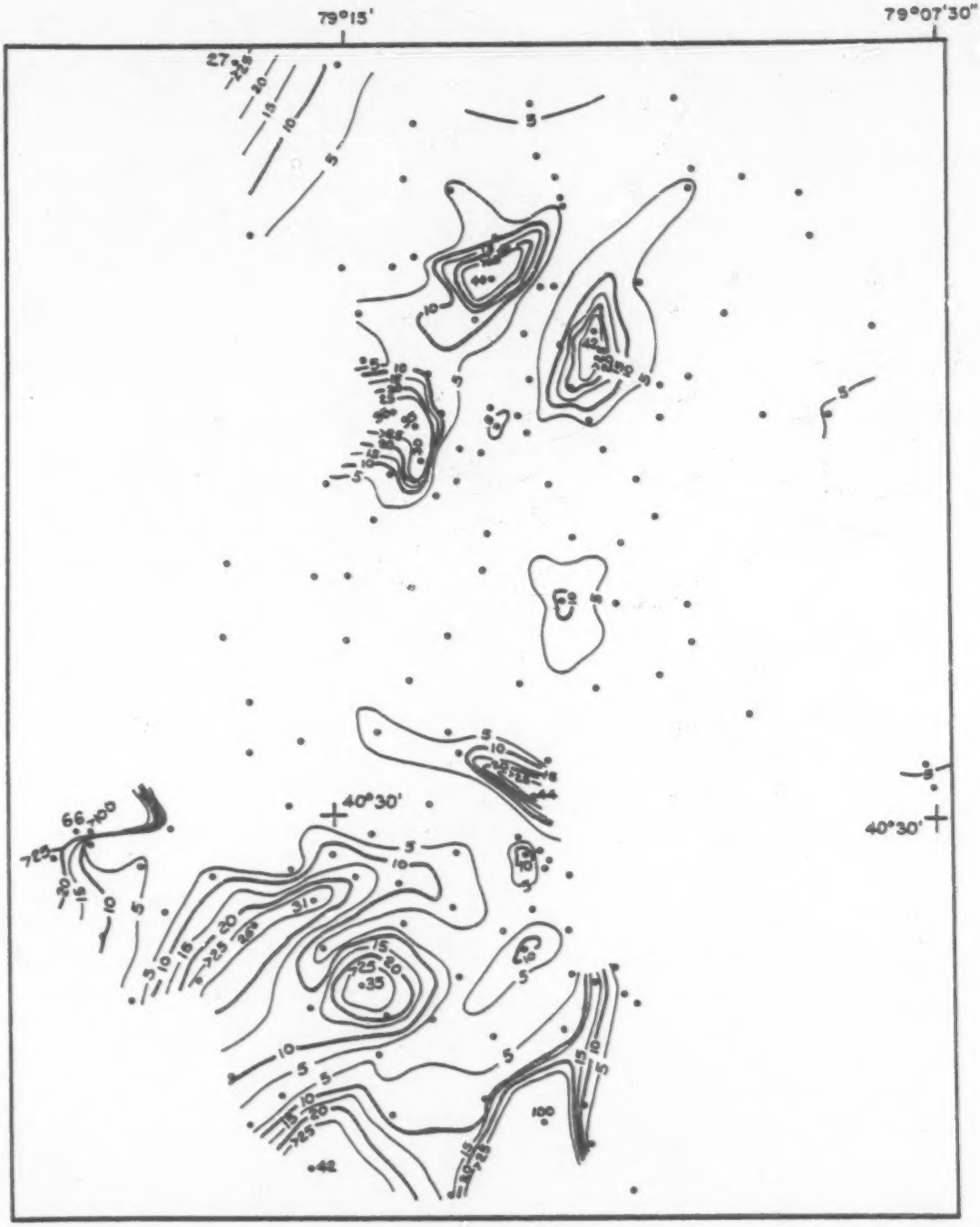

FIGURE 33 ISOPACH OF SHALE ABOVE UPPER FREEPORT COAL. THICKNESS MEASURED FROM TOP OF COAL TO THE FIRST CHANGE TO LITHOLOGY OTHER THAN SHALE. VALUES FOR THICKNESS GREATER THAN 25 FEET ARE SHOWN.

CONTOUR INTERVAL 5 FEET

biochemical processes. After burial, mineral matter may be precipitated from formation waters in pores and fractures. This later stage of mineral-matter fixation may be the result of diagenetic processes operating on mineral matter already present in the coal, or it may be the result of enrichment of elements from ground water moving through the coal. Historically, it has not been possible to determine which source was the major contributor to mineral-matter concentrations; thus, it has not been possible to explain and/or predict variations in mineral-matter content ahead of mining and coal preparation.

In the transformation of plant material to peat and then to coal, all the processes that operate result in a loss of organic matter. Therefore, at any stage of coal formation, loss of organic matter will have the effect of concentrating the mineral matter. Furthermore, from experimental work and theoretical considerations, we postulate that the transformation of well-preserved peat (from the Okefenokee Swamp to Georgia) into a medium-volatile bituminous coal equivalent in rank to the Upper Freeport coal involves a minimum compaction ratio of 10:1 and a 50 percent weight loss of the original peat organic matter. This compaction ratio means that 10 cm of peat having 10 percent ash (dry basis) will become 1 cm of bituminous coal having an ash content of 18 percent, assuming that mineral matter is not added or lost during coalification. A peat having 25 percent ash would be transformed into a bituminous coal having 40 percent ash. Changes of these magnitudes have profound implications on the interpretations of the sedimentary history and depositional environments of coal beds. For example, a 6-inch (15 cm) parting or bone coal layer containing 50 wt. percent ash (20 percent by volume) represents the coalification product of 60 inches (150 cm) of peat whose ash content (dry basis) would have been approximately 33 wt. percent (13 percent by volume). This hypothetical parting or bone coal layer would not be visibly recognizable as such in the peat stage of coal formation. This difficulty of visualizing the effects of compaction probably explains why laterally extensive parting precursors are rarely if ever recognized in modern peat-forming environments. Such parting precursors have the physical appearance of "normal" peat in that they are nonbanded and mineral matter is dispersed. However, during compaction, coalification, and diagenesis, fissility and/or banding (often confused with sedimentary layering) forms, and the mineral matter appears in discrete bands. Banding is generally not pronounced even at the lignite stage of coalification. Thus, the commonly held opinion that all mineral-rich bands are detrital in origin does not have a sound physical or theoretical basis.

Low ash coal (<10 percent) must result from very low ash peats (<5 percent dry-weight basis) or from peats that had significant quantities of mineral matter removed during coalification. Although we cannot determine the ash content and/or composition of the plant precursors of the Upper Freeport coal, it does seem reasonable to assume that Pennsylvanian plants did contain ash. From this and additional studies we conclude that both the content and variability of ash and sulfur in modern peat-forming environments are affected by the pH of the peat-forming environment. High-ash and high-sulfur peats are associated with nearby neutral pH conditions, and low-ash and low-sulfur peats are associated with acid peat conditions (pH 3-4). The most probable origin of the mineral-matter is plant ash.

The possible significance of the plant ash contribution to mineral matter in the Upper Freeport coal bed initially was recognized from the statistical analysis of the data. Those elements that correlate positively with ash, SiO_2, and Al_2O_3 (Group 1 of table 18), are interpreted to be principally derived from a common source. Incorporation from randomly mixed sources (i.e., detrital, plant, and chemical) should not lead to statistically significant positive correlations.

Mineral matter is concentrated during the transformation from plants to peat to coal because of the loss of organic matter. If we accept the hypothesis that mineral matter from plants was the dominant source of the ash in the Upper Freeport coal bed, then the variations in the concentrations of the Group I elements (table 18) were caused primarily by variations within the peat-forming environment such as 1) differing plant communities, 2) variable water depth, and 3) variable peat and water chemistry. In general, the ash content of the coal of the study area, with the possible exception of A and A' facies, is too low to have resulted from a dominant detrital source.

Those elements that correlate with sulfur (Group II, table 18) are primarily of chemical and biochemical origin. The pH of the peat-forming environment affected and/or controlled bacterial degradation of the peat, the $SO_4^=$ reduction, and the resultant sulfur fixation. This conclusion is based on the positive correlations among Ca, S, Fe, micrinite, and sporinite. We believe that calcium fixation with organic acids during the peat stage of coal formation partially neutralized peat acidity (pH >5), thereby allowing $SO_4^=$ reducing bacteria to function. Micrinite is probably a product of microbial degradation, and spores are resistant to decay. Therefore, as other coal premacerals were degraded, micrinite was produced, spores were enriched, and $SO_4^=$ was reduced and fixed as FeS_2 and perhaps as organic sulfur. Arsenic, Hg, and Se were fixed in pyrite by chemical processes. Vertical and lateral variations in sulfur content were controlled primarily by variations in water and peat chemistry during the peat stage. Secondary controls are related to roof rock lithology; coal beneath a sandstone roof has a higher sulfur content than coal beneath a shale roof. Roof shales are generally organic-matter rich relative to the sandstones. Therefore, microbial activity would tend to fix available sulfur and iron as pyrite within the shales because there would not be a geochemical gradient between the shale and the underlying peat/coal. A geochemical gradient between the peat and sandstone would tend to bring about increased pyrite concentrations in the peat/coal beneath sand bodies that contained little or no organic matter. Iron and sulfur species would tend to diffuse from the sandstone into the peat/coal. Diffusion would occur in response to concentration gradients caused by pyrite formation with the peat/coal.

High concentrations of pyrite commonly observed in fusain (C facies throughout the dedicated reserves) are probably the result of favorable microchemical conditions within prefusain layers. Favorable pH conditions (pH >5) resulted from the hydrolysis of alkali and alkaline earth metal ions, which were concentrated by oxidation/carbonization during peat formation. Because of large aggregate particle size, the pyrite associated with fusain should be removable by physical coal preparation. Removal of this pyrite should also remove most of the As and Hg and much of the Se.

TECHNICAL APPLICATIONS

It is becoming increasingly important to understand the physical and chemical properties of coal as the nation develops coal as a major energy source. Prior to this investigation, no systematic effort has determined the interrelationships of important coal quality parameters such as calorific value, sulfur content, maceral composition, mineralogy, ash content, element content, etc. Although the present study is not all inclusive, it does represent a major effort by the U.S. Environmental Protection Agency and the U.S. Geological Survey to determine the geologic factors that govern the variation of more than 100 parameters that affect coal quality. The premise upon which this study is based is that if causes of variation can be understood, then such variations may be predictable or predictable within limits.

Perhaps one of the most important aspects of Phase I of this study has been the recognition of the importance of geochemical controls on mineral matter variations within a coal bed (Cecil and others, 1978; 1979; 1980a; 1980b; 1980c; 1981a; 1981b; Stanton and others, 1980; Dulong and others, 1980; Finkelman and others, 1979). This finding leads to the conclusion that exploration for low-sulfur coal should focus on stratigraphic sequences where calcareous sediments are rare. Coals in such sequences will normally have a low sulfur and low ash content and minimal variability. Ash and sulfur will be more highly variable as the calcium carbonate content of a given coal and associated rocks increases. Thus, exploration and development costs can be minimized by utilizing geologic information obtained from exploratory drilling. Minimum drilling will be required to evaluate coal quality if it can be established that the ancestral peat accumulated under acid conditions of pH 5 or less. By establishing the geologic and especially the geochemical environment of deposition from exploratory drilling, development drilling can be planned to obtain maximum information from a minimum number of bore holes. Mines can be planned and developed to minimize quality variation through blending of products from different mine faces. Furthermore, selected areas may be of such quality that coal preparation would not be necessary.

Our Phase I study and a preliminary analysis of float-sink data indicates that at least two basic size types of iron disulfide are present in the Upper Freeport coal. First, relatively small framboids and euhedral crystals are encapsulated in macerals and dispersed throughout the coal. The small framboids and crystals are not expected to be highly susceptible to removal during coal preparation. Second, megascopic occurrences are commonly associated with fusain and fractures. Although individual crystals in fusain layers may be small (i.e., cell filling), they will be amenable to removal because of their aggregate nature (layered pyrite of the C facies).

Iron disulfide microscopic data obtained from channel samples will be compared to similar data obtained from float-sink fractions collected at the same location in Phase II of our investigations. From these comparisons, the float-sink behavior will be determined for the various iron disulfide forms, associations, and sizes. The degree to which microscopic techniques (maceral analysis, vitrinite reflectance, and iron disulfide analysis) estimate float-sink characteristics of coal will be evaluated from this information. Microscopic analyses may be an effective

method in estimating and predicting the cleaning potential of coal resources and reserves. Such analyses could be conducted on coal core samples without completely destroying them and would generate data pertaining to vertical and lateral variations of sulfur and its mode of occurrence, which in turn can provide information to aid in mine planning, development, and preparation-plant operations.

Description of a coal core is commonly limited to thickness measurements and notation of parting thickness. We strongly recommend that iron disulfide occurrences also be noted because a visual estimate of the amount present may reflect the amount that can be removed by coal preparation. Furthermore, such notation may allow anomalously high sulfur values to be adjusted in cases where coring encounters anomalously pyritized zones such as pyritized/fusinized logs.

The "transition zone" of the Homer City dedicated reserves represents an area where mining passes from thick coal (>6 ft. or >2 m) to thin coal (<4 ft. or <1.3 m). Knowledge of the geologic cause of this thickness change can aid in mine planning with respect to variable roof conditions. For example, if the thickness change and parting formation were caused by a fluvial channel and crevasse splay, then mine development would probably encounter not only a change in coal thickness but also a change from shale to sandstone roof and the normal roof problems associated with such a change. However, coal facies A, A', and B developed from a peat island with clay being deposited marginal to the island in a lacustrine environment; therefore, when passing through the "transition zone", shale roof conditions can be expected. Mine development has substantiated this latter condition. Sandstone roof conditions in other areas are associated with channels which eroded the previously deposited shale.

The depositional system or systems overlying a coal govern roof rock lithology and also affect coal quality. Therefore, interpretation of the environment of deposition of the roof shale and the Mahoning sandstone interval is considered to be an essential element of Phase I and III of our study. Recognition of the Mahoning sandstone as possibly being derived from a braided stream system could lead to a better understanding of predictable mining and quality conditions. Presently it is extremely difficult if not impossible to predict changing roof conditions because detailed systematic studies have never been conducted that would relate variation of roof rock lithologies to depositional environments. Thus, a comparative analysis is not possible; however, we believe that detailed studies of depositional environments can lead to prediction of hazardous roof conditions related to roof rock lithology. It follows that quality variations in coal related to roof rock can also be predicted.

The Phase I study has demonstrated that the major, minor, and trace elements occur in the coal in expected mineral forms (the lithophile elements such as Si, Al, K, and Mg are in silicates and the chalcophile elements such as Zn, Cu, Pb, and Fe are associated with sulfides). The mineralogy of the coal was controlled primarily by diagenesis particularly where the LTA content is 20 percent or less; however, the elemental composition is a function of elements contributed from vegetal matter and geochemical conditions of the paleoenvironment. Thus, the lithophile and chalcophile elements of Group I (table 18) were primarily derived from vegetal matter, and authigenesis/diagenesis determined the mineral form observed in the coal. The element concentrations of Group II (table 18)

were primarily controlled by geochemical conditions, and authigenesis/diagenesis also controlled the mineral form. Concentrations of the elements of Group I (table 18) are related to the amount of material originally in the plants; concentrations of the elements of Group II (table 18) are primarily a function of material chemically precipitated and sulfur content was controlled by the amount of vegetal sulfur and bacterial reduction of available sulfate. The elements of Group I and II may be further concentrated by the chemical and biochemical degradation of plant tissues during the peat stage and by the loss of organic matter during coalification. Therefore, the results of the Phase I study strongly indicate that the ash content (other than pyrite and calcite) of the Upper Freeport coal is inherent (derived from vegetal matter). Thus, the concept that the inherent ash is limited to the very fine (submicron size) disseminated material is perhaps incorrect. For the purpose of coal preparation, the inherent ash concept should be expanded to include those elements and minerals of Group I. More research is needed on the various factors that control mineral concentrations and sizes.

The findings of this investigation establish 1) that the inherent ash contribution to the origin of mineral matter in the Upper Freeport coal and, perhaps, to most major coal beds is predominant, and 2) that the fixation of sulfur and iron in iron disulfides and the associated trace elements As, Hg, and Se is strongly related to the pH of the peat-forming environment. The commonly observed relationship of high sulfur coal/marine roof rock is a special case of sulfur fixation under nearby neutral pH conditions. The occurrence of moderately high to high sulfur coals (2-6%) associated with freshwater sediments (such as the Upper Freeport) can be attributed to the availability of dissolved $CaCO_3$, $SO_4^=$, and iron during the peat stage of coal formation. Iron disulfide minerals (marcasite and pyrite) formed in all phases of coal formation. As noted by other authors (Reyes-Navarro and Davis, 1976; Carruccio and others, 1977; Neavel, 1966), much of the pyrite in coal formed early in the peat stage. The genesis of the sulfur in the Upper Freeport coal bed is consistent with the latter statement.

Framboidal pyrite is particularly common in the lowermost facies and is less common to absent in other facies. The occurrence of pyrite framboids in coal has been linked to a marine environment (Kemeyz and Taylor, 1964), or a marine paleoenvironment (Reyes-Navarro and Davis, 1976), or lower delta plain environment (Caruccio and others, 1977). Other authors have pointed out that framboids can form in freshwater sediments (Vallentyne, 1963) and freshwater coals (King, 1978). Marine sediments are not associated with the Upper Freeport coal bed; however, the coal commonly overlies a once subaerially exposed freshwater limestone or limy mudstone. Apparently, a pH environment of 5 or greater was the primary controlling factor of pyrite formation and, in particular, of framboid formation.

Elements necessary to react to form pyrite are obviously iron (Fe) and sulfur (S). The source of sulfur in peat can be from 1) plant debris that organically concentrates sulfur, and/or 2) dissolved sulfate species in the water. In marine sediments, iron may be derived from detrital iron-bearing minerals (Kaplan and others, 1963; Berner, 1964) or may be adsorbed on exchange sites with clay minerals (Carroll, 1958). Neavel (1966, p. 159) states that iron is "transported into swamps adsorbed on clays or as an organic-matter-stabilized ferric oxide hydrosol." Another

possible source of some iron could be from the underclays that are leached during plant growth and peat accumulation. After burial, iron may be introduced in response to geochemical gradients across the interface between roof sediments and peat/coal.

Pyrite formation has been postulated by Neavel (1966) to occur early in coal formation. Neavel stated that all the pyrite found in coal formed syngenetically; he (1966, p. 160-161) defined syngenetic pyrite as forming "in the peat swamp in contradistinction to having formed after the peat was covered by more than a few inches of detrital sediments." He explains cleat-filling pyrite also as the result of syngenetic processes, citing examples where cleat evidently had formed very early in peat accumulation.

Of the pyrite forms reported in the current study, much of the pyrite fits into Neavel's definition of syngenetic origin. However, it is quite conceivable that the cleat pyrite is produced during diagenesis. Also, pyritic sulfur values are higher beneath sandstone channel cut and fill deposits than beneath shale roof deposits. In this study area, 6-13 meters of silt and clay were deposited above the coal before streams cut down through the deposit. The higher pyritic sulfur content results from increased availability of iron and sulfur resulting from interaction of chemical gradients across the peat/coal and sand interface. This interaction not only suggests a control of pyrite formation by the availability of iron but also suggests pyrite formation post-syngenetically. Close proximity of the sandstone to the coal increases sulfur variability.

There are layers within the coal that have little or no FeS_2 minerals. Element concentrations determine the mineral phase; thus, siderite ($FeCO_3$) occurs where iron is abundant but sulfur is in low concentration. During coalification, CH_4 and CO_2 are generated, and organically bound calcium may be liberated. If H_2S is present, pyrite formation will occur, and the calcium and CO_2 may react to form calcite.

Selenium apparently will combine with lead to form a PbSe mineral in association with sphalerite and "chalcopyrite." This mineral assemblage appears to occur when Pb, Zn, and Cu are also present. Where these elements are absent, the selenium is tied up in pyrite.

The classification of macerals into their major groupings of vitrinite, inertinite, and exinite is useful for predicting the behavior of coal upon coking or combustion; however, these groupings are not as useful when evaluating depositional or degradational differences among coal samples within an interpreted sedimentological framework. Therefore, either specific macerals or groupings of macerals, both of which are based on genetic relationships, should be used in comparisons for environmental (either depositional or degradational) interpretations.

The relation between vitrinite reflectance and low temperature ash within a vertical section of the coal bed may be very significant. This relation suggests that below 20 percent LTA, certain ash constituents may have a retarding effect on metamorphism or that submicroscopic element inclusions in vitrinite may adversely affect the reflectance measurement. Further study of this relation on more samples and samples of other coals is presently being conducted and may give insight into coalification processes as well as understanding the dependence that vitrinite reflectance may have on specific element concentrations. It may be possible and necessary to correct reflectance readings to an ash-free basis for comparisons of data within and among beds.

The 20-percent LTA value may also indicate the contribution of plant-derived elements to the coal ash. Samples whose values are greater than 20 percent LTA may have the difference contributed by detrital minerals, solution-precipitated minerals, or very high levels of decomposition that would concentrate mineral-forming elements.

SUMMARY

The primary objectives of Phase I as stated in the Introduction were to determine the geologic factors that controlled the variability of 1) the total and pyritic sulfur, 2) the forms and size range of iron disulfide minerals, 3) the concentration of major, minor, and trace elements, 4) the dominant minerals, and 5) the maceral composition and mineral matter associations in the Homer City, Pa., dedicated reserves of the Upper Freeport coal bed. The conclusions drawn from the results of the Phase I study are:

1. The primary control on total and pyritic sulfur content is the geochemistry of the ancestral peat-forming environment. The most important geochemical parameters are the pH and the availability of sulfate and iron; pH controls the activity of sulfate-reducing bacteria and total sulfur content. Roof rock conditions are a secondary control on sulfur variability. Coal, in a given coal bed, occurring beneath a sandstone roof has a relatively higher sulfur content than coal beneath a shale roof.

2. The forms and sizes of iron disulfides are also a function of complex geochemical processes. Microscopic crystals encapsulated in macerals and dispersed throughout the coal are believed to have formed mainly during the peat stage in response to geochemical and microbial conditions. Significant removal of the microscopic iron disulfides by physical coal preparation is unlikely. The two dominant megascopic forms of pyrite occur in fusain and in fractures. The pyrite in fusain formed in response to favorable chemical and physical conditions. The fracture-filling pyrite may have been derived from the organic matter during coalification. The megascopic iron disulfides are expected to be removed by physical coal preparation.

3. The concentrations of the major, minor, and trace elements (other than Fe, Ca, and S) were primarily derived from the inherent ash of the plants of the ancestral peat-forming environment. Therefore, variations may have been caused principally by variations in plant communities, variable conditions in peat chemistry, and variable degrees of peat degradation.

4. The dominant mineral species are mainly the product of authigenic processes. Variations in the concentration of mineral species are attributed to variations in the inherent ash as noted in item 3 above.

5. Variations in maceral composition and mineral-matter associations are a function of variables noted in items 1 through 4 above. Changes in water depth and chemistry controlled: 1) plant communities; 2) degree of microbial and chemical degradation and the formation of premacerals; and 3) the concentrations of the inherent ash, calcium, iron, and sulfur. The banding of the coal is a product of compaction/coalification and thus is not a primary sedimentary structure. Mineral-rich bands are often erroneously interpreted as detrital in origin when they are commonly mixtures of authigenic minerals and highly degraded coalified organic matter (macerals).

The findings of the Phase I study will be used as a basis for interpreting the data derived from the float-sink testing of Phase II. It is expected that the combined results of Phases I and II can be utilized in coal exploration and development as well as in coal preparation and utilization. The results should be pertinent to the prediction of quality in advance of mining and to quality control during coal preparation and utilization.

References Cited

American Society for Testing and Materials Cited (ASTM), 1977a, Standard method of preparing coal samples for microscopical analysis by reflected light, D2797: 1977 Annual Book of ASTM Standards, pt. 26, p. 350-354.

_____1977b, Standard method for microscopical determination of volume percent of physical components of coal, D2799: 1977 Annual Book of ASTM Standards, pt. 26, p. 359-360.

_____1977c, Standard method of microscopical determination of the reflectance of the organic components in a polished section of coal, D2798: 1977 Annual Book of ASTM Standards, pt. 26, p. 355-358.

_____1977d, Standard test method for forms of sulfur in coal, ANSI/ASTM D2492: 1977 Annual Book of ASTM Standards, pt. 26, p. 322-326.

_____1977e, Standard test methods for total sulfur in the analysis sample of coal and coke, D3177: 1977 Annual Book of ASTM Standards, pt. 26, p. 383-389.

Berner, R. A., 1964, Stability fields of iron minerals in anaerobic marine sediments: Journal of Geology, v. 72, p. 826-834.

Bostick, N. H., and Foster, J. N., 1973, Comparison of vitrinite reflectance in coal seams and in kerogen of sandstones, shales, and limestones in the same part of a sedimentary section, in Petrographie de la Matiere Organique des Sediments (B. Apern, ed.): Centre National de la Recherche Scientifique 75700 Paris, p. 13-25.

Carroll, Dorothy, 1958, The role of clay minerals in the transportation of iron: Geochim. et Cosmochim. Acta, v. 14, p. 1-27.

Caruccio, F. T., Ferm, J. C., Horne, J., Geidel, G., and Baganz, B., 1977, Paleoenvironment of coal and its relation to drainage quality: U.S. Environmental Protection Agency Report 600/7-77-067, 107 p.

Cecil, C. B., Stanton, R. W., Allshouse, S. D., and Finkelman, R. B., 1978, Geologic controls on mineral matter in the Upper Freeport coal bed: Proceedings: EPA/DOE (U.S. Environmental Protection Agency/Department of Energy) Symposium on coal cleaning to achieve energy and environmental goals, p. 110-125.

Cecil, C. B., Stanton, R. W., Allshouse, S. D., Finkelman, R. B., and Greenland, L. P., 1979, Geologic controls on elements concentration in the Upper Freeport coal [abs.]: Am. Chemical Society, Preprints of Papers, v. 24, no. 1, p. 230-235.

Cecil, C. B., Stanton, R. W., and Dulong, F. T., 1980a, Mineral matter in coal [abs.]: in Atomic and nuclear methods in fossil energy research, Dec. 1-4, 1980, Mayaguez, Puerto Rico, Am. Nuclear Soc./Am. Chemical Soc. Topical Conference.

Cecil, C. B., Stanton, R. W., Dulong, F. T., and Renton, J. J., 1980b, Geologic controls on the sulfur content in coal [abs.]: Am. Assoc. of Petroleum Geologists Book of Abstracts, 1980 Annual Meeting, Denver, Colorado, p. 38.

_____1980c, Geologic controls on mineral-matter content in coal of the Central Appalachian Basin [abs.]: Am. Assoc. of Petroleum Geologists Book of Abstracts, 1980 Annual Meeting, Denver, Colorado, p. 37-38.

_____1981a, Geologic factors that control mineral matter in coal: Proceedings of Atomic and Nuclear Methods in Fossil Energy Research, Dec. 1-4, 1980, Plenum Press (in press).

Cecil, C. B., Stanton, R. W., Dulong, F. T., and Ruppert, L. F., 1981b, Geochemical model for the origin of low ash and low sulfur coal; Mississippian-Pennsylvanian boundary in the central part of the Appalachian Basin, Guidebook to field trip no. 4, 1981 Geological Society of America Annual Meeting (in press).

Chung, F. H., 1974, Quantitative interpretation of X-ray diffraction patterns of mixtures: Matrix-flushing method for quantitative multicomponent analysis: Jour. Appl. Cyrst., v. 7, p. 519-525.

Clark, W. J., 1979, An Interfluve Model for the Upper Freeport Coal Bed in Part of Western Pennsylvania: Unpublished M.S. Thesis, U. of So. Carolina, 47 p.

Coleman, J. M., 1969, Brahmaputra River: Channel processes and sedimentation: Sedimentary Geology, v. 3, no. 2/3, p. 129-239.

Davis, J. D., Reynolds, D. A., Sprunk, G. G., Holmes, C. R., and McCartney, J. T., 1943, Carbonizing properties and petrographic composition of thick Freeport-bed coal from Harmor Mine, Harmorville, Allegheny County, Pennsylvania, and the effect of blending this coal with Pocahontas No. 3- and No. 4- bed coals: U.S. Bureau of Mines Tech. Paper 655.

Dulong, F. T., Cecil, C. B., and Stanton, R. W., 1980, X-ray mineralogy of the Upper Freeport coal [abs.]: Am. Assoc. of Petroleum Geologists, Book of Abstracts, 1980 Annual Meeting, Denver, Colorado, p. 48-49.

Edwards, A. H., Jones, J. M., and Newcombe, W., 1964, The extraction by nitric acid of pyrites from vitrains and coal samples: Fuel, v. 43, p. 55-62.

Finkelman, R. B., 1978, Determination of trace element sites in the Waynesburg Coal by SEM analysis of accessory minerals, in Scanning Election Microscopy, v. 1, (ed. O. Jaheri) SEM, Inc., AMF O'Hare, IL, p. 145-148, 52.

Finkelman, R. B., and Stanton, R. W., 1978, Identification and significance of accessory minerals from a bituminous coal: Fuel, v. 57, p. 763-768.

Finkelman, R. B., Stanton, R. W., Cecil, C. B., and Minkin, J. A., 1979, Modes of occurrence of selected trace elements in the Upper Freeport coal [abs.]: Am. Chemical Society, Preprints of Papers, v. 24, no. 1, p. 236-241.

Garrels, R. M., and Christ, C. L., 1965, Solutions, minerals and equilibria: Harper and Row, New York, 450 p.

Gibbons, J. D., 1976, Nonparametric methods for quantitative analysis: Holt, Rienehart and Winston, New York, N.Y., 463 p.

Grady, W. C., 1977, Microscopic varieties of pyrite in West Virginia coals: Transactions Society of Mining Engineers AIME, v. 262, p. 268-274.

Gray, R. J., Schapiro, N., and Coe, G. D., 1963, Distribution and forms of sulfur in a high volatile Pittsburgh Seam Coal: Transactions Society of Mining Engineers AIME, v. 226, p. 113-121.

Griffiths, J. C., 1967, Scientific methods in analysis of sediments: McGraw-Hill Book Co., New York, N.Y., 508 p.

Harris, L. A., Yust, C. S., and Crouse, R. S., 1977, Direct determination of pyritic and organic sulfur by combined coal petrography and microprobe analysis (EPMA) - a feasibility study: Fuel, v. 56, p. 456-457.

Hawks, H. E., and Webb, J. S., 1962, Geochemistry in mineral exploration: Harper and Row, New York, N.Y., 415 p.

Hoffman, E., and Jenkins, A., 1932, Die inkohlung und ihre erkemung in mikrobild: Gluckauf, v. 68, p. 81-88.

ICCP (International Committee of Coal Petrology), 1963, International handbook of coal petrology: Centre National de la Recherche Scientifique, Paris, France.

_____1971, International handbook of coal petrology, supplement to second edition: Centre National de la Recherche Scientifique, Paris, France.

Jenkins, Ronald, Haas, D. J., and Paalini, F. R., 1971, A new concept in automated powder diffractometry: Norelco Reporter, v. 18, no. 2, p. 12-27.

Kaplan, I. R., Emery, K. O., and Rittenberg, S. C., 1963, The distribution and isotopic abundance of sulphur in recent marine sediments off southern California: Geochim. et Cosmochim. Acta, v. 27, p. 297-332.

Kemeyz, Michelle, and Taylor, G. H., 1964, Occurrence and distribution of minerals in some Australian coals: Institute of Fuels, v. 37, p. 389-397.

Khawaja, I. U., 1975, Pyrite in the Springfield Coal Member (V) Petersburg Formation, Sullivan County, Indiana: Indiana Dept. of Natural Resources, Geological Survey Special Report 9, 24 p.

King, H. M., 1978, The morphology, maceral association and distribution of iron disulfide minerals in the Waynesburg coal at a surface mine: M.S. Thesis, West Virginia University, 181 p.

Koppe, E. F., 1963, Petrography of the Upper Freeport Coal-Harmor and Springdale Mines, Allegheny, and Westmoreland Counties, Pennsylvania: Pennsylvania Geological Survey Bulletin M55, 43 p.

_____1967, Petrography of coal in the Houtzdale Quadrangle, Clearfield County, Pennsylvania: Pennsylvania Geological Survey Bulletin M48, 73 p.

Lee, R. J., Huggins, F. E., and Huffman, G. P., 1978, Correlated Mossbauer, SEM studies of coal mineralogy: Scanning Electron Microscopy, v. 1, (ed O. Jahari), SEM, Inc., O'Hare, IL, p. 561-568.

Mackowsky, M-Th, 1968, Mineral matter in coal, in Murchison, D. G., and Westoll, T. S., eds., Coal and coal-bearing strata: London, Oliver and Boyd, p. 309-321.

Minkin, J. A., Chao, E. C. T., and Thompson, C. L., 1979a, Distribution of elements in coal macerals and minerals: determination by electron microprobe (abs.): American Chemical Society Preprint of Papers, v. 24, no. 1, p. 242-244.

Minkin, J. A., Finkelman, R. B., Thompson, C. L., Cecil, C. B., Stanton, R. W., and Chao, E. C. T., 1979b, Arsenic-bearing pyrite in the Upper Freeport coal, Indiana County, Pennsylvania (abs.): Ninth International Congress of Carboniferous Stratigraphy and Geology, Abstracts of Papers, p. 140-141.

Moore, C. A., 1965, The use of X-ray diffraction for the quantitative analysis of naturally occurring multicomponent mineral systems: Southeastern Geol., v. 6, p. 139-148.

_____1968, Quantitative analysis of naturally occurring multicomponent mineral systems by X-ray diffraction: Clays and Clay Min., v. 16, p. 325-336.

Neavel, R. C., 1966, Sulfur in coal: its distribution in the seam and in mine products: Ph.D. Thesis, Pennsylvania State Univ., 332 p.

Postma, D., 1977, The occurrence and chemical composition of recent Fe-rich mixed carbonates in a river bog: Journal of Sedimentary Petrology, v. 47, no. 3, p. 1089-1098.

Puglio, D. G., and Iannacchione, A. T., 1979, Geology, mining and methane content of the Freeport and Kittanning Coal beds of Indiana and surrounding Counties, Pa.: U.S. Bureau of Mines Report of Investigations 8406.

Rao, C. P., and Gluskoter, H. J., 1973, Occurrence and distribution of minerals in Illinois coals: Illinois State Geological Survey Circular 476, 56 p.

Raymond, R., Jr., and Gooley, R., 1978, A review of organic sulfur analysis in coal and a new procedure: Scanning Electron Microscopy, (O. Johare, ed.), v. I, p. 93-107.

Renton, J. J., and Hidalgo, R. U., 1975, Some geochemical considerations of coal: West Va. Geol. and Econ. Survey, Coal-Geol. Bull. no. 4, 38 p.

Reyes-Navarro, J., and Davis, Alan, 1976, Pyrite in coal: its forms and distribution as related to the environments of coal deposition in three selected coals from western Pennsylvania: Pennsylvania State University Special Research Report SR-110, 141 p.

Ruch, R. R., Gluskoter, H. J., and Shimp, N. F., 1974, Occurrence and distribution of potentially volatile trace elements in coal: a final report: Illinois State Geological Survey, Environmental Geology Notes No. 74, 96 p.

Siegel, Sidney, 1956, Nonparametric statistics: for the behavioral sciences: McGraw-Hill Book Co., New York, N.Y., 312 p.

Sinclair, A. J., 1974, Selection of threshold values in geochemical data using probability graphs: J. Geochem. Explor., v. 3, p. 129-149.

Soloman, P. R., and Manzione, A. V., 1977, New method for sulfur concentration measurements in coal and char: Fuel, v. 56, p. 393-396.

Stach, E., Mackowsky, M.-Th, Teichmuller, Marlies, Taylor, G. H., Chandra, D., and Teichmuller, Rolf, 1975, Stach's textbook of coal petrology: Gebruder Borntraeger, Berlin, 428 p.

Stanton, R. W., and Finkelman, R. B., 1979, Petrographic analysis of bituminous coal: optical and SEM identification of constituents: Scanning Electron Microscopy, v. 1, (ed) O. Jahari, SEM, Inc., O'Hare, IL, p. 465-472.

Stanton, R. W., Cecil, C. B., and Dulong, F. T., 1980, Form and association of pyrite in the Upper Freeport coal bed, Homer City, Pennsylvania [abs.]: Am. Assoc. of Petroleum Geologists Book of Abstracts, 1980 Annual Meeting, Denver, Colorado, p. 124.

Stopes, M. C., 1935, On the petrography of banded bituminous coals: Fuel in Science and Processing, v. 14, p. 4-13.

Tennant, C. B., and White, M. L., 1959, Study of the distribution of some geochemical data. Econ. Geol., v. 54, p. 1281-1290.

Thiessen, R., and Voorhees, A. W., 1922, A microscopic study of the Freeport coal bed, Pennsylvania: Carnegie Institute of Technology Bulletin 2, 75 p.

Vallentyne, J. R., 1963, Isolation of pyrite spherules from recent sediments: Oceanography and Limnology, v. 8, p. 16-30.

Ward, C. R., 1977, Mineral matter in the Springfield-Harrisburg (No. 5) coal member in the Illinois Basin: Illinois State Geological Survey, Circular 498, 35 p.

Whelan, P. F., 1954, Finely disseminated sulphur compounds in British coals: Journal of the Institute of Fuel, v. 27, p. 455-458, 464.

Williams, E. G., Bergenback, R. E., and Weber, J. N., 1968, Relationship between paleotopography and the thickness and geochemistry of a Pennsylvanian freshwater limestone: Journal of Sedimentary Petrology, v. 38, no. 2, p. 501-509.